INTERNATIONAL JOURNAL OF
IJCOE
COASTAL, OFFSHORE & ENVIRONMENTAL ENGINEERING

Volume 7 | Issue 1 | Feb 2022

www.ijcoe.org

International Journal of Coastal, Offshore and Environmental Engineering (IJCOE)

Vol. 7, Issue 1, Feb 2022

Since 2015

International Journal of Coastal, Offshore & Environmental Engineering

ISSN: 2980-8731 (online)

Volume 7 | Issue 1| Feb 2022

IJCOE

Editor-in-Chief: Prof. Hamid S.Bahai

International Journal of Coastal, Offshore & Environmental Engineering
Since 2015
ISSN: 2980-8721 (online)

In The Name of God

Message from the Editor-in-Chief

The IJCOE journal office was established in 2015,and its first issue was published in 2016. TheIJCOE covers a wide range of research in thefields of oceanography & ocean technology, aswell as marine industries & marine engineering.The editorial board of IJCOE consists of nearly130 of the greatest scientists and researchersfrom over 30 countries worldwide, and thejournal's review board comprises 1,000 membersfrom all five continents. The membership andapplication process for joining the editorial andreview boards of this journal is ongoing. IJCOE isa research-academic quarterly journal that haspublication and distribution permissions fromthe Press Organization and permission topublish scientific-research articles from theMinistry of Science, Research, and Technology(MSRT) with an "A" rating. It also holds a "Q1"rating from the ISC institute with an impactfactor (IF) of approximately 0.43 and isconsidered a "core journal" (prestigious andoutstanding journal). IJCOE is an open-accessjournal and allows the download and receipt ofaccepted articles in full text for free. It respectsand adheres to copyright and COPE regulations.The journal's office operates 24/7, providingservices to researchers. In addition to publishinga regular quarterly journal, IJCOE has 16 specialissues on specific topics in preparation. It alsoprovides conditions for publishing specializedbooks, references, and handbooks. Moreover, itis ready to cooperate with the secretariats ofreputable international conferences to publishtheir selected and outstanding articles. IJCOEevaluates, appraises, and publishes books,articles, and the scientific achievements andfindings of esteemed researchers and scientistsworldwide who are innovating and conductingin-depth research in the "important and strategicfield of the maritime technology & Oceanengineering." It welcomes any form of jointcooperation with universities, research institutes,and related research centers at the national,regional, and international levels, and extends ahand for collaboration.

Classification of Editorial Board in IJCOE

- Editor-in-Chief
- Director-in-Chief
- Deputy Editor
- Executive Managers
- English Text Editor
- Technical Editor
- International Editorial Board
- National Editorial Board
- Editorial Board Associate
- Editorial Board Assistant
- Guest Editorial Board
- Advisory Board
- Administrative Coordinator
- Honorary Board Member
- Methodology Advisor

Author Benefits

- Open Access
- Rapid Publication
- Thorough Peer-Review
- No Copyright Constraints
- Coverage by Leading Indexing Services
- Discounts On Article Processing Charges (APC)
- No Space Constraints, No restriction on the maximum length of the papers, number of figures or colors

INTERNATIONAL JOURNAL OF IJCOE COASTAL, OFFSHORE & ENVIRONMENTAL ENGINEERING

Aims of IJCOE

Hydrodynamics

Marine equipment

Structural mechanics

Ocean environmental predictions

Stochastic calculations Experimental

Automatic Control of Marine Systems

Scope of IJCOE

Marine Hazards

Ocean Acoustics

Naval Architecture

Ocean Engineering

Coastal Engineering

Marine Meteorology

Marine Earth Sciences

Underwater Technology

Marine Renewable Energy

Polar & Arctic Engineering

Marine Renewable Energy

Marine Geography & Geodesy

Marine Environmental Engineering

Automatic Control of Marine Systems

Hydro Physics & Physical Oceanography

Type of papers

- Case Studies
- Book Reviews
- Review Article
- Letters to the Editor
- Methodology Papers
- Editorials and Commentaries
- Response or Rejoinder Papers
- Perspective or Opinion Papers
- Conceptual or Theoretical Papers
- Meta-Analysis and Systematic Reviews
- Short Communications or Brief Reports
- Research Articles (Original Research Papers)

Scientific Research Journal

Ministry of Science, Research And Technology (MSRT)

Jurnal Ranking 2023: A

Ministry Of Science, Research And Technology (ISC)

Citation Impact 2022: 0.429

Quartile 2022 : Q1

Core Collection

IJCOE is a Member of

Cantact Us

Office 1 | Research Institute of Meteorology and Atmospheric Science

Address | Tehran, Shahid Kharrazi Highway, Pajoohesh Blvd, Research Institute of Meteorology and Atmospheric Science, Sand and Dust Storm International Research Center (SDS-IRC), No. 13, 1st floor.

Phone | +982144787652

Postal code | 13611-14977

website | www.rimac.ac.ir

Office 2 | Iranian National Institute for Oceanography and Atmospheric Science

Address | Tehran, Dr. Fatemi Gharbi St., Shahid Etemadzade St., No. 3, third floor.

Phone | +982166944873

Postal code | 13389 – 14118

website | www.inio.ac.ir

Email | Info@ijcoe.org

Website | www.ijcoe.org

Follow Us

www.ijcoe.org

INTERNATIONAL JOURNAL OF IJCOE COASTAL, OFFSHORE & ENVIRONMENTAL ENGINEERING

Volume & Issue:

Volume 7, Issue 1, February 2022

Number of Articles: 6

Content

INTERNATIONAL JOURNAL OF
COASTAL & OFFSHORE ENGINEERING
IJCOE Vol.7/No. 1/Winter 2022 (1-14)

Available online at: www.ijcoe.org

Rationality for Engineers:

Part IV: Misconceptions and Debiasing

Sirous F. Yasseri

Brunel University London; Sirous.Yasseri@Brunel.ac.uk.

ARTICLE INFO

Article History:
Received: 02 Jun. 2021
Accepted: 05 Dec. 2022

Keywords:
Heuristics
Intuition
Statistical Thinking
Rationality
Judgment
Biases
Debiasing
Reasoning

ABSTRACT

Humans are thought of as predictably irrational, primarily due to apparent inconsistencies in their decision-making. When presented with the same information on different occasions, the same people often draw different conclusions. There is a noise in the decision-making of individuals, whether in the same or a different environment. Humans are likened to a faulty scale; every time you weigh the same thing you get a different answer. This variation is more pronounced when we examine decisions by different decision-makers. Noise in decisions implies that humans' internal gauges are imprecise and that their dial rests on a different position when confronted with the same choice at different times. Decision errors can relate to; correlation, causal reasoning, probabilistic reasoning, thinking statistically, hypothetical thought, dubious justification, not seeing everything, and even seeing something which is not there. This part of this series of papers attempts to clarify errors in engineers' decision-making processes and describe how to avoid them.

1. Introduction

Engineers' approach to finding solutions is often to develop a model of the required system. The solution is not separate from the 'purpose' and 'objective' of the system's owner. A skill set, as well as a knowledge base, is required to solve a problem, or design and implement a system. The knowledge base is most likely to be multidisciplinary, and dependant on the type of problem. It may also need regular topping up of the skill. Design and implementation define engineering profession, and this differentiates engineering from pure science.

Engineering aims to work with available knowledge to fulfil society's needs. Good engineering practice is founded on the experience and applying existing knowledge, together with suitable heuristics, to produce 'desirable outcomes' which in turn produce new 'experience' leading to the refinement of an engineer's skill; this is the evidence-based approach to engineering [44]. An engineering knowledgebase also allows the use of routines and rules of thumb for problem-solving, which are usually denied to scientists. The knowledge gained might be in an improved heuristic, more refined approach, or how to deal with constraints. Evidence-based engineering requires; finding the evidence, understanding what it means and where it might lead, and then drawing a conclusion [44]. Engineers often rely on heuristics to simplify their work and enhance their effectiveness. Heuristics on occasions may lack accuracy or even proper justification. However, heuristics used with good engineering judgment [44] rooted in the understanding of when and where a heuristic can be applied, would afford an important tool. Here, the engineer relies on the collective experience of all the engineers who came before as well as his/her own.

To be effective, engineers need to look deeper to discover what you ae not seeing. What you see is not always all there is. Take this story- two friends were walking along a riverbank. Suddenly they saw somebody in the water drowning and calling for help. One of them jumps into the river and rescues the victim. Before he can catch his breath, he sees a second person in the river shouting for help. Without hesitation, he jumps back in the river and saves the second person. A few moments later, they hear another person calling for help. Though he is tired, he jumps again into the river and saves the third person. The friend who was just observing these events, runs upstream and returns a few hours later. His friend asks, "Where have you been? I saved two more people since you have been away, however, for the last hour, the river did not bring any more people. The friend who came from the upstream said "When I saw the river bringing the bodies downstream, I wondered what the cause could be. I went to investigate. When I reached a bridge further up, I saw a man on the bridge pushing people who were to

cross the bridge into the river. I subdued him and took him to his family in the village. That is the reason why there have been no more bodies in the river". All you see might not be all there is. Research suggests that experts who regularly work with uncertain information have better numeracy skills and a better ability to interpret events than the public [33,40]. The assumption is that the experts know better because they have seen it before. They are certain that there is more than what they see. Analysis of biases and heuristics among experts adds credence to this belief, and thus the effects of framing and biases may be enhanced due to their domain-specific training and experience which keeps them alert.

This part looks at misconception of statistics and how to avoid them. Debiasing of decision-making process is discussed in some details in this part.

2. Ergodicity

Sometimes it is assumed that the average behaviour over time is the same as the average behaviour at a point in time; this is known as ergodicity assumption [49]. Few things are precisely ergodic, but many things are reasonably close for the practical purposes. The real reason for caring about ergodicity is to decide if we can rely on predictions from past data at all. If we have a hundred-year sample of data that looks ergodic, there is no guarantee that tomorrow will not bring a surprise, nevertheless we have some confidence that it won't deviate too much from historical norms. However, if historical data is full of violent event that seem to occur irregularly, we don't have too much confidence that we can predict tomorrow.

Suppose you are looking at waves coming from the distance up on a shore. If you look from sides, you form an opinion about the distribution of heights at different locations at any given time. That is If you measure at one location, you get an impression of height distribution at that specific location over time. If you assume the process is ergodic, then by walking up and down the beach, you can judge the behaviour of waves over time and decide on a safe spot to spread your blanket as close as possible to the water's edge without risking getting wet. You would look at the maximum height you see in either direction, also, perhaps, you add a couple meters to be sure you are on the safe side. Your inference is incorrect since the wave heights are not ergodic over the relevant time scale. You may not see evidence of the tide during your observation, neither you have observed changes in sea conditions. You may also have forgotten that wave heights are affected by the height and slope of the beach at different locations.

Japanese building codes were based on the highest tsunami observed at different locations. The assumption was that the distribution of tsunami extent is ergodic, so the highest flood ever observed is a good estimate of the maximum likely extent. The Fukushima Daiichi disaster [43] proved this assumption not to be correct- there were also other errors beside assuming tsunami ergodicity.

We assume ergodicity any time we use a sample of data taken at one point in time to estimate likely future outcomes; or take samples of data over time to estimate probability distributions for the next event. An example is using a baseball player's season batting average to estimate his probability of getting a hit at his next at-bat.

One practical example is casino gambling. A roulette wheel is very close to ergodic, the distribution of numbers that have come up in the past is very close to the probability distribution of numbers on the next spin. But Blackjack is dealt from a set of cards that are not reshuffled after each hand. Therefore, the probabilities for the next hand are distinct from the outcomes earlier in the deck. Players need an Ace and a ten card to make a blackjack, and there are fixed numbers of them in the deck, so a high number of historical blackjacks means a lower probability of future blackjacks, and vice versa, all else equal. Players can exploit non-ergodicity to gain an advantage over the house.

Another example:

1. Take a coin and toss it 1 billion times and record the results.

2. Then imagine one billion people flipping a coin once and recording their results.

In Case 1: the random process (coin flipping) is taking place over "time" - sequentially flipping the same coin repeatedly. In Case 2: the random process is taking place in "space" - different coins, different people, different locations but all at the same time. If any given statistical measure that you choose gives the same results for both cases, then you can say the system is "ergodic."

Suppose a coin appears to be completely fair when given to you, but it is made of different materials on each side, and one material wears faster than the other. When you flip this coin one billion times, it is going to become less and less fair. It is not possible that this coin in one billion flips to be identical with coins that flipped by one billion people, as they do not have this problem of wear. The statistics of the two trials, i.e., your coin over time and the one billion other coins over "space", will not be the same.

To "do" statistical inference, we need to know how a system evolves over time. However, it is possible by considering the "ensemble" of all possible configurations. The idea of an "ensemble" can be helpful to understand ergodicity in general [49]. Instead of the simple coin flipping of above example, consider something more complex and perhaps more practical. Suppose you have a machine that you know will randomly make some mistakes. But you do not know exactly what the rate or distribution of mistakes is. If you can justify the idea that these mistakes will be

ergodic, then you could create an "ensemble" of 100 machines and observe them each for 100 hours of running and conclude that any statistical observations you make would be the same as observing one machine for 10,000 hours.

2. Data, Information, Knowledge, and Wisdom

Russell Rakoff's [50,51] stepped flow from data to information to knowledge to understanding to wisdom must be at the heart of any profession that relies on knowledge.

According to Russell Ackoff, the content of the human mind can be classified into five categories:

Data simply exists and has no significance beyond its existence. Its existence does not imply being usable or not. They can be on paper or in a computer database and can have any form numbers, words, pictures. For example, census takers collect data. The Bureau of the Census processes that data, converting it into information that is presented in the numerous tables published in the Statistical Abstracts [51].

Information is obtained when data is interrogated, distilled and potential can be gainfully exploited; but not necessarily are meaningful. For example, a data bases turns data to information and store it. Information is contained in descriptions, answers to questions that begin with such words as who, what, when, where, and how many[51]. "Like data, information also represents the properties of objects and events, but it does so more compactly and usefully than data. The difference between data and information is functional, not structural [51]" .

Knowledge is making sense of relevant collection of information. The aim is to make it useful. When people "memorize" information, then they believe they have the knowledge. This knowledge has meaning for them, but don't know its applicability, implementation and limitations. but it does not provide for, in and of itself, an integration such as would infer further knowledge. Even, my not help to further gaining more knowledge. Use of the acquired knowledge requires reasoning and analytical ability which in turn requires understanding of the knowledge. They are just stored 'knowledge'. Knowledge is conveyed by instructions, answers to how-to questions. Understanding is conveyed by explanations, answers to why questions [51]

Understanding is the process apply the knowledge. It is cognitive and analytical. One can use previously held knowledge and synthesis it to gain new knowledge. The difference between understanding and knowledge is the difference between "applying" and "knowing". Those who have understanding can synthesise new knowledge, or in some cases, at least new information, from what is previously known (and understood). That is, understanding can build upon currently held information.

Wisdom [52] is the ability to think and act using knowledge, experience, understanding, common sense, and insight. It is also the ability to guess where your action will take you and consequences of your decision. It calls upon all the previous experiences, and specifically upon all human values (moral, ethical codes, etc.). It is the essence of probing the likely consequence of an action. Asking question to which there is no easy answer, there may be no answer. Wisdom is, therefore, the process by which we also discern, or judge, between right and wrong, good and bad. Wisdom is a very human trait; it is what that makes a person human.

Ackoff asserts the first four categories relate to the past; they deal with what has been or what is known. Only the fifth category, wisdom, deals with the future because it incorporates vision and consciousness. With wisdom, people can create the future rather than just grasp the present and past. But achieving wisdom is not easy; one must travel successively through the other categories.

Engineers should use wisdom to create the society's future and well-being to solve problems and decide how to move forward. This is done in situations when there are no clear answers.

Peter Drucker wrote: "There is a difference between doing things right and doing the right thing." Ackoff has amended the above to this: "Doing the right thing is wisdom, effectiveness. Doing things right is efficiency. The curious thing is that the righter you do the wrong thing, more wrong you become. If you're doing the wrong thing and you make a mistake and correct it, you become even more wrong. So, it's better to do the right thing wrong, than the wrong thing right. Intelligence is the ability to increase efficiency; wisdom is the ability to increase effectiveness."

Wisdom deals with values. It involves the exercise of judgment. Evaluations of efficiency are all based on a logic that, in principle, can be programmed into a computer and automated. These evaluative principles are impersonal. We can speak of the efficiency of an act independently of the actor. Not so for effectiveness. A judgment of the value of an act is never independent of the judge, and seldom is the same for two judges [52].

Accessing information stored in our brain an accessing information stored somewhere else are just knowing; accessed fact is just the bigging of wisdom an intelligence, that is wisdom is not just accessing information but understating them and apply them effectively. It is this which marks somebody as intelligent, not the ability to regurgitate masses of information. Sometimes we are fooled to think otherwise. Knowledge alone of the content of papers and books is not an indicator of wisdom or intelligence. It is what we do with that knowledge counts.

2. Misconceptions of Chance

The French Mathematician Laplace said, "Probability is the common sense reduced to calculus", but common sense does not make better probability assessments. It enables one *to get a feel for the real world, which inevitably involves biases.* Misconceptions of the rules of probability are discussed next section.

Kahneman's idea of biases mostly revolves around the misconception of probability. This section explores the misconception of chance events.

The second of Hammurabi's laws states, "If anyone brings an accusation against a man, and the accused go to the river and leap into the river if he sinks in the river his accuser shall take possession of his house. But if the river proves that the accused is not guilty, and he escapes unhurt, then he who had brought the accusation shall be put to death, while he who leaped into the river shall take possession of the house that had belonged to his accuser." This law seems to presume that the guilty are more likely to be drowned than the innocent. Hammurabi is not alone in misunderstanding the rule of probability. This is faith-based reasoning.

The following example illustrates humans' comprehension of probabilities. Suppose you wish to know what the weather will be like next Monday, as you are planning a job which requires a dry spell or clement weather such as installing offshore facilities. You look for the weather forecast and read, "There is a 10% chance of rain." You decide to go ahead with the job, then low and behold, it rains. You get frustrated, but was the forecast wrong? No, the forecast did not say it would not rain, only that rain was not probable. The forecast would have been wrong only if a probability of zero was predicted and it subsequently rained. However, if you assemble every prediction over an extended time and ascertained that it rained on 50% of the days that the forecasted probability was 0.10, then again you could say the weather forecast is wrong. The question is when is it correct to say that the probability of rain is 0.10? According to frequency interpretation, this means that it will rain 10% of the days for which the probability of raining is forecasted at 10% rain, not 10% of the day nor 10% of places where the forecast applies.

Many people excruciatingly scrutinize a lot of statistics but suddenly leave them aside and make a snap judgment based on what their gut says. Mr. Phillips, the protagonist of John [27], is an accountant, and on the previous Friday he was made redundant, a victim of his own cost-benefit analysis. His wife and family, and his neighbours, do not know he has been sacked. His hobby is calculating the odds of everything; the percentage of Londoners who have never seen a corpse; or been on a boat on the Thames; or at what time before each lottery draw should he buy a ticket to have a probability of winning the jackpot that exceeds the probability of dying before the draw. The novel tracks Mr. Phillips roughly from 9 am to 5 pm on the first Monday of the rest of his life. He leaves home pretending to go to work. On this fatal day, he walks into his bank to check his bank balance, only to find he is stumbled into a robbery. He passes the time calculating the odds of winning the lottery (one in 13,983,816) against the odds of dying in any given minute (one in 49,200,000). He speculates as he lies face down on the floor, about "how rational bank robbers must be; how they need to think of everything. 'There must be a lot of details to think about, being a bank robber.' He muses, 'It would seem like a job for the headstrong and reckless, but there must be a great deal of planning too,". But, out of nowhere, Mr. Phillips suddenly stands up, in the middle of the drama, and says: 'I'm not doing that anymore.' It is a moment of astonishing and consummate bravery, by refusing to comply. It is the being told to lie down that Mr. Phillips is objecting to, not just (or necessarily) the robbery, nor if odds are in his favour. It is what is called a risk taken with reckless disregard for the consequences. Mistakes happen when there is a mismatch between reality and perception.

Kahneman [19] stated "*people expect that a sequence* of events generated by a random process will represent the essential characteristics of that process even when the sequence is short." In the independent trial of tossing a coin. The same probability rule applies for getting the specific sequences of HHTHT or THTHT. Since the probability of getting a tail, or head is 0.5, then the probability of both sequences is obtained by multiplying 0.5 five times, which yields 0.03125. This probability is true for both sequences – but it implies no relationship between the probability of a specific outcome at each toss. Coins, unlike people, have no sense of equality and proportion.

There is a specific variation of the misconception of chance that is known as the "Gambler's Fallacy". This fallacy implies that when you come across a local imbalance, you expect that future events will smooth it out. We will act as if every segment of the random sequence must reflect the true proportion and, we expect the imbalance to be corrected. The basis of the Gambler's Fallacy is a misconception of the laws of chance and the belief in fairness, which is believing that if the nature has done something wrong, it will correct itself and balance things out the gambler feels that the fairness of the coin toss entitles him to expect that any aberrance in one direction will soon be corrected by a corresponding aberrance in the other direction. Kahneman illustrates this with an example of the roulette wheel and our expectations when a reasonably long sequence of repetition occurs. After observing a long run of black on the roulette wheel, most people mistakenly believe that it is now the turn of red. Roulette is random, in which the chance of getting red or black will never depend on the past sequence.

A small random sample is not representative of a larger population. If you are relying on data inference, then beware of the data size; when statisticians say a large sample, they mean a very large sample. If luck has a larger share in success than skill, then you need more data to separate chance from skill. A gambler said, "if it wasn't for my bad luck, I would have won every game". Luck is not a noise that can be cancelled, but it is governed by the rules of probability. In the long run, quality of decision is a winning strategy, not good luck. History remembers those who have succeeded, not perished. The road to success is not signposted by rose petals.

For example, assume that the average IQ of a specific country is known to be 100. To assess the intelligence in a specific district, we draw a random sample of 50 people. The first person in our sample happens to have an IQ of 150. What would you expect the mean IQ to be for the whole sample? The correct answer is (100*49 + 150*1)/50 = 101. Yet without knowing the correct answer, it is tempting to say it is still 100 – the same is true for an entire country.

Some natural phenomena obey such laws, that is a deviation from a stable equilibrium produces a force that restores the equilibrium. This is only true for the problem of physics. Idioms such as "errors will cancel each other out" reflect the image of an active self-correcting phenomenon. Indeed, this may be true in thermodynamics, chemistry, and physics (every action has an equal and opposite reaction). However, these are false analogies. It is important to realize that the laws governed by chance are not guided by principles of equilibrium, and the number of random outcomes in a sequence does not have a common balance.

The skill part of a decision can be controlled and improved, but one cannot control the chance. If a drunkard decides to drive and has no accident, it does not mean that he has made a good decision. The quality of the outcome is not an indication of the quality of the decision. In the short run, the chance element may not be favourable. One needs to be careful not to confuse luck with skill.

3. Thinking in Probability

The following three simple laws are at the heart of Probability Theory; if applied correctly, they can give insight into how nature works [31]:

1. "The probability that two events will both occur can never be greater than the probability that each will occur individually.

2. If two possible events, A and B, are independent, then the probability that both A and B will occur is equal to the product of their probabilities.

3. If an event can have several different and distinct possible outcomes, A, B, C, etc., then the probability of the occurrence of either A or B is equal to the sum of the individual probabilities of occurrence of A and B. Also, the sum of the probabilities of all possible outcomes (A, B, C, and so on) is 100% (or 1)."

Navigating through the laws of probability, andomness, and statistics sometimes leads to a misunderstanding of chance. Kahneman [19] used the term "misconceptions of the chance" to describe the phenomenon when people extrapolate from small size samples to large-scale situations. For this, the random process must be ergodic. As discussed in Section 2 A random process is said to be ergodic if the time averages of the process tend to the appropriate ensemble averages. In other words, "A radon process is ergodic if its statistical properties can be deduced from a single, sufficiently long, a random sample of that process" This means if you observe a process long enough, then you will learn all the statistical properties of that process, since your observation approaches (converges) to the "true" ensemble properties of the process. Some things never repeat themselves, like the weather on Christmas Day 2022. However, if the weather were ergodic (which it is not) you could watch the weather for many days or years and then determine the probabilities of different weather conditions on Christmas Day of 2022. This means, if you live long enough, you will experience everything. Using statistical properties of an ensemble to predict the behaviour of the whole process is not possible. As such, ergodicity establishes some equivalence between multiple trials in the same period and prolonged observation of the same process over time.

Imagine that you face a tough decision between investing in the production of two different products, A and B. You are interested in knowing which product would appeal to most of the market, so you decide to conduct a customer survey. Out of the first five pilot surveys, four customers show a preference for Product A. While the sample size is quite small, given the time pressure involved, many of us would already have some confidence in concluding that the majority of customers would prefer Product A. However, a quick statistical test will show that the probability of a result just as extreme is, in fact, 3/8, assuming that there is no preference among customers at all. In simple terms, this means that if customers had no preference between Products A and B, you would still expect 3 customers out of 8 to prefer Product A). Studies of such a small size have little to no predictive validity; such results could easily be obtained from a population with no preference for one or the other product. The more random cases we examine, the more reliable and accurate are the results, and the closer we will be to obtaining the true proportion. If we want absolute certainty, we need a very large sample.

There will always be cases where a guesstimate, based on a small sample will be enough because we have other critical information guiding our decision-making

process or we simply do not need a high degree of confidence. Yet rather than assuming that the samples we come across are always perfectly representative, we must treat random selection with the suspicion it deserves.

The ease of remembering or imagining an event in our mind is taken as evidence of the degree of likelihood (beware of representative bias). Naturally, events that are frequently experienced will be easily remembered and judged to be likely. On the other hand, if it is hard to remember a particular event, then it is of rare probably and hence remote. However, if an unusual event happens, and if we witness it, or it happened to someone that we know, then there is a tendency to overestimate its probability. If we cannot even imagine how an event could happen, then we consider there is no chance for that event to occur. But according to Gumbel [14] "*improbable is bound to happen one day*." Which is the same advice given by Sherlock Holmes to Dr. Watson "*When you have eliminated the impossible, whatever remains, however improbable, must be the truth*."

When a numerical estimate of likelihood is not possible, it may be assessed in linguistic terms as negligible, moderate, high, remote. These are vague terms, but the strategy must be to use different approximate methods in parallel, to build up a better understanding of seeing through probability. Probability is an estimate, not a telephone number.

Kahneman makes a lot of emphasis on conjunctions. A "conjunction", is a sentence in the form: "…and—." For instance, the sentence: "Today is Saturday and it is raining" is a conjunction (together). When a conjunction is used as a noun, it means either term of the conjunction, whereas the verb conjunction means the act of joining or the condition of being joined. A conjunct is a statement that is part of conjunction. For example, conjuncts of the example sentence are "Today is a Sunday" and "it is raining". The probability of conjunction is never greater than the probability of its conjuncts. In other words, the probability of two things being true can never be greater than the probability of one of them being true. For example, 'the probability of seeing an alien is more likely than the probability of seeing an alien and being offered a lift in their spaceship'; For the second to be true, both seeing the spaceship AND being offered a lift must true, i.e., both conjuncts must be true which is less likely. People sometimes think that the conjunction is more probable than one of the conjuncts. This happens when the conjunction suggests a scenario that is more easily imagined than its conjuncts alone. One reason for this error may be people assume that there is an unstated conjunct that is withheld [15].

4. The Potential for Error

You see what we want to see. If there are several events taking place at the same time, then your brain cannot keep track of all of them. You can track one possibly two of concurring events. Seeing other people's intention where none is apparent, is a result of attributing the action to others of what you would do in their place.

We confuse causality for correlation, and we make more out of a coincidence than statistics should warrant.

Subjective approaches, involving probability, expert opinion, and decision theory, are employed in 'Probabilities-as-degree-of-belief' and 'Probabilities-as-revealed-by-actions'. These tools are less precise and may be a virtue provided one remembers this fact; like the economist Milton Keynes who "preferred to be approximately right than precisely wrong."

Relying on memory and imagination when judging the probability of events has served foraging humans well, but in the modern world, we are constantly exposed to vivid vicarious experiences through the media. However, common events are uninteresting, and it is the out-of-the-ordinary events that capture our imagination. There is an old saying: "When a dog *bites a man that is not news, but when a man bites a dog that is news*." Unusually, a relatively uncommon event will make the news. The media choose uncommon events as "news", and hence we mistakenly believe that such events are quite common. In my newspaper, there is a report about the CO_2 hazard to the environment and melting the ice caps, while your paper warns about shutting down power plants leading to the loss of employment; We get two different views on the use of fossil fuels.

This is the "Anecdotal Fallacy" which occurs when the perception is based on a single anecdote, leading to an unwarranted generalization. No matter how emotionally compelling a specific incident is, it is just one data point and nothing more. But, if it is based on more than one anecdote, the set of these stories is unlikely to be representative of the class. This is especially true if the anecdotes are based on news stories since journalists tend to write about unusually extreme events. What we read or hear about from the news media are the best or worst-case scenarios.

5. Cognitive Debiasing

It is difficult to completely avoid cognitive biases as they are built into the way our brain functions [1,21,23] Humans think in patterns, and it is very difficult to ignore them. Whether these patterns help to solve a problem or lead to wrong decisions depends on the context. The key is for the engineer to take advantage of the positive aspects of heuristics while mitigating the biases by being vigilant and implementing processes for mitigating their effects. Identification of the source of erroneous reasoning improves decision-making.

Mitigating biases through targeted "Debiasing" interventions can have a positive impact [9,11,28]
Debiasing techniques can appear in many forms, and they often revolve around the concept of "*Metacognition"*, which involves awareness and understanding of one's thinking process. A common debiasing technique is to simply make people aware of a certain bias and explain to them when and how they're likely to experience it.

Debiasing techniques may be categorized into different practices; namely, techniques that attempt directly to influence decision-makers and those that attempt to modify the decision-making environment, which in turn influence the decision-makers. For instance, when you make decisions by following others, you may be subject to a bias called the "*Bandwagon Effect",* which is blindly believing the wisdom of the crowd. This bias causes people to follow the crowd because they believe that others are acting rationally, or they know better. One approach could be to consider alternative options beyond those being promoted by the crowd. Conversely, one could shut out the opinion of others completely.
The decision-maker should consider the specifics of a debiasing method, i.e., if the method applies to a particular case or it is of general applicability. Then it is possible to categorize debiasing techniques into groups based on whether they are

- Universal: namely they work on most cognitive biases,
- Generic: namely they work on substantial groups of cognitive biases, or
- Specialized: namely they work only on a small number of biases.

Debiasing techniques may be also categorized based on other factors. For example, they can be categorized based on required training and skill level. Similarly, they can be categorized based on time and effort, with some techniques requiring little-to-no effort.

Cognitive biases can also be explained through the "Dual Process" theory. Under this model, biases occur for two main reasons:

- System 1 generates an erroneous intuitive judgment, and System 2 fails to correct it, either because System 2 fails to supervise System 1 properly, or because System 2 goes into action, but fails to stop System 1's hasty intervention.
- System 2 fails to engage in proper analytical reasoning.

Thus, debiasing involves one of the following:

- Train System 1 to generate better intuitions.
- Train System 2 to better supervise and stop System 1, as well as conducting a proper reasoning process.

A few debiasing techniques are described below:

Develop awareness of the bias: In some cases, simply being aware of a cognitive bias can reduce its impact. For example, consider the *illusion of transparency*[39], which is a cognitive bias that causes people to believe that their thoughts and emotions are more apparent to others than they are. This bias means that people tend to think that others can tell if they're feeling nervous or anxious, even in situations where there is no clue. Speakers who were informed of this bias before giving a public speech would appear more composed and calmer than those who were not told about it. One reason may be our own emotional experience is so strong, that it 'leaks out' [39].

Improve the way information is presented: How you present information can affect the way people process it. The same information, presented in two different ways to the same person, can lead to two very distinct outcomes. An example of this is presenting statistical information using an easy-to-understand graph instead of a numerical description.

Use simpler explanations and solutions: When it comes to information presentation in general and debiasing, simple explanations and solutions are often preferable to complex ones. For example, consider the *"Hindsight Bias"* [8], which is a cognitive bias that causes people to overestimate how predictable a past event was. Just asking people to think of ways in which a past event might have turned out differently, could reduce this bias. If you ask people to list only two ways, they will find it easier compared to asking them to list 10 ways which could result in a significant Hindsight Bias. Generally, a useful debiasing technique is using the simplest explanation, provided all things being equal.

Express beliefs without ambiguity**.** Asking people to express their beliefs more clearly can sometimes help reduce their biases.

Make the reasoning process explicit. Clearly outlining things such as what evidence is available and how it supports the conclusions that were reached.

Standardize the reasoning process. Checklists can be used to reduce cognitive load, and hence bias [7,17] (

Slow down the reasoning process**.** Many cognitive biases can be mitigated by slowing down and taking time to carefully thinking through the relevant information.

Elicit external feedback. Encourage others to react and give feedback, in an attempt to reduce certain cognitive biases. This is useful when trying to mitigate biases that influence people's perception of themselves, such as believing they are *worse-than-average*, i.e. people incorrectly believe that they are worse than others at performing certain tasks.

Reduce reliance on memory**.** Our memory of past events is subjective, malleable, and prone to various distortions. For example, there is a cognitive bias that causes people to remember past events as being more positive than they were. Another example is divorcing couples remember acrimonious days of divorce, not the many happy years they had together.

Consider alternatives**.** Considering alternative explanations for a certain phenomenon, or alternative interpretations for an event can help reduce some cognitive biases.

Create psychological self-distance**.** This means to separate yourself from your egocentric perspective when assessing events and emotions. This helps to reduce cognitive biases in some cases. For instance, the *spotlight effect* is another cognitive bias that causes people to overestimate the degree to which they are observed or noticed by others, as well as the degree to which others care about the things that they notice about them. This bias may cause people to overestimate the degree to which others are likely to notice their actions or appearance, that is believing that others are likely thinking that they are wearing something funny or saying something stupid, which may not be the case.

A list of useful debiasing techniques is given in Appendix. The focus is on relatively general debiasing techniques that can be helpful for a large range of cognitive biases. For an extended list of biases see https://thedecisionlab.com/biases/

Reasoning backward. In solving a problem, it is important to be able to reason backward. Johnny, a 3rd-grade pupil was 10 minutes late. The annoyed teacher asked him what his excuse was. Johnny answered, "I was running too fast to think of an excuse". He worked backward to come up with an excuse; not because he woke up late or started up late.

In problem-solving sometimes, it is useful to start from it being solved and work backward to what you must do to generate the solution. Another use for backward thinking is in risk management, where you assume an undesirable event has happened. The question you must ask is 'What must happen just before that to make that undesirable event occur?' Reasoning means being conscious of basic facts. It also requires making logical, sound inferences and deductions that avoid the many fallacies. It requires arguments that link cause and effects together, rather than making breath-taking leaps of faith.

Safety engineers when studying the safety requirement of a plant, create credible stories of undeniable future states (scenarios). By starting from an undesirable future, they see how they can control all triggering events that could lead to undesirable consequences and manage to prevent their happening. Engineers think ahead and generate scenarios to explore all possible outcomes, and then reason backward to investigate how to prevent the undesirable events.

Backward reasoning is a type of cause-and-effect thinking that is useful to weed out errors. When you think forward, you are looking for consequences caused by a triggering event. But there can be several triggering effects and it can be difficult to know which one will cause the future event. While probable future states may have many causes, and one can trace all of such causes. The past to the present and then to the future is often clearer than vice versa.

Although backward reasoning is a useful tool to avoid biases, it also can be used for fallacious arguments as well.

In reasoning backward, one should be aware of ambiguity or loose use of language. A puzzle known as "unexpected hanging paradox" [54]. Baggini has re-told it as a story of a pizza restaurant. The logic is the same, but the details differ [54].

"When the health inspector visited Emilio's pizzeria and immediately closed it down, none of his friends could believe he had let it happen. After all, they said, he knew that an inspection was imminent, so why didn't he clean things up?

Emilio had been told that an inspector would be making a surprise call sometime before the end of the month. Emilio reasoning was simple. It could not be on the 31st: if the inspector hadn't come before then, the inspection could only be on that day, and so it wouldn't be a surprise. If the 31st was ruled out, then so was the 30th, for the same reason. The inspection couldn't be on the 31st, so if it hadn't taken place by the 29th, that would only leave the 30th, and so it again would not be a surprise. But then if the inspection couldn't be on the 30th or the 31st then it couldn't be on the 29th either, for the same reasons. Working backwards, Emilio eventually concluded that there was no day the inspection could take place.

Ironically, having concluded no surprise inspection was possible, Emilio was very unpleasantly surprised when the inspector walked through his door one day. What was wrong with his reasoning?"

One version of this paradox is about a judge passing sentence on a death row prisoner. It is also often set up using a teacher telling his students that they will get a surprise exam the following week. Regardless of the circumstances involved, the gist of the story is the same and its logic has been widely studied.

Chow, a mathematician has published a **paper on the paradox**, which does a very thorough job of explaining the difficulties involved here. Chow first acknowledges the main paradox whereby the logic seems correct for the pizza restaurant's owner (or the prisoner in the

original version, or the students Chow uses in his chosen example), and yet the restaurant still gets inspected, and the owner is also surprised by that. Beyond this, there is also an important second paradoxical level to be aware of, which Chow describes as a "meta-paradox." He said:

"The meta-paradox consists of two seemingly incompatible facts. The first is that the surprise exam paradox seems easy to resolve. Those seeing it for the first time typically have the instinctive reaction that the flaw in the students' reasoning is obvious. Furthermore, most readers who have tried to think it through have had little difficulty resolving it to their own satisfaction. The second (astonishing) fact is that to date nearly a hundred papers on the paradox have been published, and still no consensus on its correct resolution has been reached. The paradox has even been called a "significant problem" for philosophy. How can this be? Can such a ridiculous argument really be a major unsolved mystery? If not, why does paper after paper begin by brusquely dismissing all previous work and claiming that it alone presents the long-awaited simple solution that lays the paradox to rest once and for all?"

Okay, okay. I must be delusional if I hope to follow that up by claiming a solution to the paradox, so let's make sure we understand what those "nearly one hundred papers" had to say. As Chow summarises: "In general, there are two steps involved in resolving a paradox. First, one establishes precisely what the paradoxical argument is. Any unclear terms are defined carefully, and all assumptions and logical steps are stated clearly and explicitly, possibly in a formal language of some kind. Second, one finds the fault in the argument."

Seek contradictory opinion. Paraphrasing Carl Popper [36] "*Disagreement is the engine of progress*". Give the argument some chance to take shape. You will learn more when others disagree with you, and you are forced to justify your decision. Dismissing opposing views without a good reason is falling into the abyss of irrationality.

6. Putting it all Together

To be or not be rational: The primary objective was to discuss the use of heuristics for fast decisions in the context of rationality. Heuristics are intuition and experienced-based tools, not guaranteed to produce optimal, perfect, logical, or rational results, but they have been shown to be adequate for fast decision-making, and possibly acceptable given all constraints. Heuristics always have a limited range of applicability and are affected by the environment where they are used. If their underlying assumptions are not valid or not well established or understood, they should be treated with suspicion. Statements such as "It is a fact" and "It stands to reason", are assumptions not proof.

In most branches of engineering, heuristics are commonly used and known as empirical methods, implying that they are not entirely based on the first principles. Engineers also learn them in practice, from their own experience, mentors, or colleagues. Even when rigorous analytical methods are used, heuristics are often employed as a sense-check on the credibility of the results. Heuristics are also the systematization of collective wisdom, experiences, and common sense. For example, the safety margin (or the safety factor) is a heuristic. The safety factor for strength design of aircraft is 1.2, which is adequate because of rigorous analyses, testing, quality control, operational monitoring, and strict operating regime, while the same level of safety factor is not used for bridges and buildings. We can pretend to know safety margins for common engineering constructions, but the use of a safety factor, in general, is precarious for most unexpected or unknowable hazards.

It may be rational to open a restaurant without a kitchen because you are convinced that your customers want burgers and you can source them from a nearby burger outlet, and re-brand them by adding your own secret sauce; what works is rational. Some airlines are also big hoteliers without having a single hotel, which is not considered as irrational. Rationality is also knowing what works and what is possible. A rational person is one who always has a good reason for what he/she thinks and does. Each step can be shown to be the best way towards their well-defined objectives.

Problem-solving: Rationality exists within a system with values and mechanisms to achieve them. Looking from the outside the scope of the system and its rational behaviours may be described as consistent and logical. Those who have lived their entire lives within one system, have difficulty making sense of the possibility that another set of totally different behaviours can also be "rational". Any decision or choice is only valuable in the context of the environment that it was made. For example, imagine that you go to a bank to deposit some money, but you also have a loan at the same bank. While talking to the clerk you notice that hooded men are running towards the bank. You believe that they are bank robbers, and you are certain that you are going to be robbed. Is it rational to pay your money towards your loan? Though paying back the loan is perfectly rational, insisting on paying it back under these circumstances may not be.

In engineering, some heuristics involve the use of visual representations (e.g., diagrams, and sketches), additional assumptions, forward/backward reasoning, and simplification. For example, George Polya's book, How to Solve It [35], gives this guidance:"

- If you are having difficulty understanding a problem, try drawing a sketch.

- If you cannot find a solution; assume that you have a solution and consider what you can deduct from that ("working backward" and reasoning backward (Section 3 of Part 3)
- If the problem is stated in abstract format, try to find a concrete example of it.
- Try solving a more general problem first; the more ambitious plan may have more chances of success)."

Polya [35] had mathematical problems in mind, but engineering shares 50% of its genes with mathematics.

To think rationally means adopting appropriate goals, taking the appropriate action given one's goals and beliefs, and holding beliefs about the world that are commensurate with the available evidence. Engineers need to be critical thinkers. "The ability to reason independently of prior beliefs is only one component of critical thinking. Many theorists view critical thinking as a sub-species of rational thinking, or at least closely related to rational thinking" [25].

Does the thought process during the concept generation phase of a project differ between engineers and architects? Both professions are required to create new or innovative designs, but their education in creative techniques is not the same. In engineering training, greater emphasis is placed on technical/analytical issues, and practical training is included in the form of project work with some emphasis on creativity to generate new ideas. In contrast, architects' training emphasis is not on the analytical ability, but repeated regeneration of the design concept combined with a critique process by a mentor as well as peers. In this training process, both engineers and architects develop heuristics to explore possible solutions, without constantly watching for constructability.

Ethics: Only Noah could sail without a compass; the rest of us need a compass, especially a moral one. Ethical issues are always a consideration in engineering decisions. For example, when an engineer has designed a "state-of-the-art communication system", this means that it is consistent with the best set of heuristics known to the engineering community at the time it was designed. With these definitions in place, we can now define ethical behaviour for the engineer, which is taken to mean complying with best known practices and social norm in good faith.

A car repair shop supervisor catches an employee stealing car parts. When confronted, the employee says. "Boss, I've become a compulsive thief." The thief also admits that he cannot change. Must the supervisor accept that he cannot change? The dilemma is, how to make an ethical decision and be fair. After a couple of minutes of thinking the supervisor says, "wash your hand every 15 minutes, if you are not cured in a couple of weeks could you please steal a Ferrari for me?" This is not an example of ideal behaviour but illustrates a point - whether to accept what you saw, pass on the problem to others, or rectify? but how? Such decisions normally have two main reference points - the difficulty of how to change behaviours, and the ethical implications of the situation. Naturally getting rid of the rotten apple is also an option even when there is only one.

Jean-Paul Sartre [53, 54] described a situation in a story. Here is Baggini's version [54]

"Mary, Mungo, and Midge. You stand accused of a grievous crime. What do you have to say for yourselves?

"Yes, I did it," said Mary. "But it wasn't my fault. I consulted an expert and she told me that was what I ought to do. So don't blame me, blame her."

"I too did it," said Mungo. "But it wasn't my fault. I consulted my therapist and she told me that was what I ought to do. So don't blame me, blame her."

"I won't deny I did it," said Midge. "But it wasn't my fault. I consulted an astrologer and she told me that since Neptune was in Aries, that's what I should have done. So don't blame me, blame him."

The judge sighed and issued his verdict. "Since this case is without precedent, I have had to discuss it with my senior colleagues. And I'm afraid to say that your arguments did not persuade them. I sentence you all to the maximum term. But please remember that I consulted my peers and they told me to deliver this sentence. So don't blame me, blame them."

You could say that Mary, Mungo, and Midge all agreed with someone else's opinion to justify their actions, which begs the question if they committed the confirmation bias fallacy - the tendency to favour information that confirms one's beliefs or hypotheses and to ignore information that disagrees with one's point of view. You could also say that Mary, Mungo, and Midge can claimed to be blameless because they intended to do the right thing by asking people, they trusted to be expert which brings up the question of what is reasonably required to do due diligence. You could also say Mary, Mungo, and Midge all made their own choices nobody forced them to take a course of action. there is nothing to dictate a person's course of action, and only the individual can decide what road to take. Sartre claims that people must take responsibility for their actions [53].

Substitution: Replacing a more difficult problem that you can't solve with an easier one is not uncommon. The Serenity Prayer is by the American theologian Reinhold Niebuhr (1892–1971); Wikipedia [42]. It is commonly quoted as Shapiro [39]:

"God, grant me the serenity to accept the things I cannot change,

courage to change the things I can,

and wisdom to know the difference."

The original Niebuhr's prayer is this:

"Father give us the courage to change what must be altered, serenity to accept what cannot be helped, and the insight to know the one from the other."

Niebuhr's asked for courage first, and specifically for changing things that must be changed, not things that simply can be changed. This is replacing a difficult problem with an easier one.

Accuracy: Heuristics are not meant to be accurate. However, after you have spotted all the holes, enough truths are left in the fabric to be gainfully employed. The tools in an engineers' toolboxes are there to boost the engineer's skills. Heuristics must be critically reviewed before use. Heuristics are there to shorten the response time, not to replace the engineer's analytical knowledge. This generalization is the primary problem, as one may stretch heuristics to fit the situation, rather than look for alternative heuristics.

Heuristics should not be taken as universally true. Is it as valid as it was twenty years ago? and will it be as valid twenty years from now? A heuristic may involve ethical assumptions (overt or covert) which the society now finds unacceptable - it pays to stop and think. They are just working hypotheses to use until proven wrong.

Some may believe that rational decision-making means exhaustively identifying all options, ranking them, and then selecting the best. But in time-constrained situations, few aspects of decision-making are as important as when to stop, since the most rational course of action is not always possible. Humans are faced with the complexity and messiness of real life, abandon the rational model, and follow simple heuristics. The difference between theory and practice, abstract and applied, reminds us of Yogi Berra's wisdom - in academia, there is no difference between academia and the real world; in the real world, there is.

7. Conclusion

Two types of thinking govern our decision-making process. Type 1 is fast, impulsive, and automatic and we rely on this to get by in our daily life. Type 2 is slower and deliberative. These two types do not work in collaboration, but Type 1 runs the show and does most of the decision-making. Type 1 system makes decisions using heuristics which may lead to errors if not used carefully. Heuristics draw their power from the various kinds of regularity and continuity in the world; they arise through specialization, generalization, and very often from analogy. As the world changes, a heuristic that was valid and useful may lose its validity. To decide we must search for further clues and guidance. The first part of this paper has discussed how and where we can go wrong. The last section of the paper discusses cognitive biases and how to mitigate their effects.

Exciting stories are more attractive than accurate statistics. In constructing a fabricated future, negative information is more vivid, and the brain stores it in such a way that it is easily accessible. This is a heritage from our foraging ancestors, who needed negative stories to be vigilant. As the newspaper's motto "if it bleeds it leads".

Acknowledgments

This papers greatly on the words of others; wherever they are borrowed , references are given. However, the exact words may not be quoted but paraphrased.

The authors would like to thank Chris Millyard, Sassan Rezaei, Mehrdad Rahbari, Kabir Sadeghi, and Michael Vigne, Mohsen Mirza, Giles Thompson for their counsel and feedback, who have assisted to improve the quality and integrity of these papers. I am very much indebted to Mehrdad Rahbari for his patience and help with improving successive revisions.

This research did not receive any specific grant from funding agencies in the public, commercial, or not-for-profit sectors.

8. References

[1] Aczel, B., Bago, B., Szollosi, A., Foldes, A. and B. Lukacs, (2015). "Is it time for studying real-life debiasing? Evaluation of the effectiveness of an analogical intervention technique." Front. Psychol. 6, 1120, 23 pages.

[2] Arkes, H. R. 1991. "Costs and benefits of judgment errors: Implications for debiasing." Psychol. Bull. 110 (3): 486.

[3] Arkes, H. R., D. Faust, T. J. Guilmette, and K. Hart. (1988). "Eliminating the hindsight bias." J. Appl. Psychol. 73 (2): 305.

[4] Bhargava, S., and G. Loewenstein. 2015. "Behavioral economics and public policy 102: Beyond nudging." Am. Econ. Rev. 105 (5): 396–401.

[5] Caputo, A. 2016. "Overcoming judgmental biases in negotiations: A scenario-based survey analysis on third party direct intervention." J. Bus. Res. 69 (10): 4304–4312.

[6] Dolan, P., M. Hallsworth, D. Halpern, D. King, R. Metcalfe, and I. Vlaev. 2012. "Influencing behavior: The mind space way." J. Econ. Psychol. 33 (1): 264–277.

[7] Ely, J.W.; Graber, M.L.; Croskerry, P. (2011). Checklists to Reduce Diagnostic Errors. Acad. Med., 86, 307

[8] Fischhoff, B. 1975. "Hindsight is Not Equal to Foresight: The Effect of Outcome Knowledge on Judgment Under Uncertainty." Journal of

Experimental Psychology: Human Perception and Performance 1 (3): 288–299.

[9] Fischhoff, B. (1982). Debiasing. In D. Kahneman, P. Slovic, & A. Tversky (Eds.), Judgment under uncertainty: Heuristics and biases (pp. 422–444). Cambridge, United Kingdom: Cambridge University Press.

[10] Fischhoff, B., P. Slovic, and S. Lichtenstein. 1977. "Knowing with certainty: The appropriateness of extreme confidence." J. Exp. Psychol.: Hum. Percept. Perform. 3 (4): 552.

[11] Fischhoff, B., P. Slovic, and S. Lichtenstein. (2013). "Knowing with Certainty: The Appropriateness of Extreme Confidence." Judgment and Decision Making 3 (4): 103–123.

[12] Garcia-Retamero, R., and M. K. Dhami. 2011. "Pictures speak louder than numbers: On communicating medical risks to immigrants with limited non-native language proficiency." Health Expectations 14 (Mar): 46–57.

[13] Gilovich, T., D. Griffin, and D. Kahneman. 2002. Heuristics and biases: The psychology of intuitive judgment. Cambridge, UK: Cambridge University Press.

[14] Gumbel, E.J. (1958), Statistics of Extremes, Columbia University Press DOI: https://doi.org/10.7312/gumb92958

[15] Hertwig, R., Benz, B., and Krauss, S., (2008). The conjunction fallacy and the many meanings of *and*, Cognition 108, 740–753

[16] Hirt, E. R., and K. D. Markman. 1995. "Multiple explanations: A consideration-alternative strategy for debiasing judgments." J. Personality Social Psychol. 69 (6): 1069.

[17] Hales, B.M.; Pronovost, P.J. (2006). The checklist—A tool for error management and performance improvement. J. Crit. Care 2006, 21, 231–235.

[18] Hodgkinson, G. P., N. J. Bown, A. J. Maule, K. W. Glaister, and A. D. Pearman. 1999. "Breaking the frame: An analysis of strategic cognition and decision making under uncertainty." Strategic Manage. J. 20 (10): 977–985.

[19] Kahneman, D. 2011. Thinking, fast and slow. New York: Macmillan.

[20] Kahneman, D., and G. Klein. 2009. "Conditions for intuitive expertise: A failure to disagree." Am. Psychol. 64 (6): 515.

[21] Kahneman, D., and D. Lovallo. 1993. "Timid choices and bold forecasts: A cognitive perspective on risk-taking." Manage. Sci. 39 (1): 17–31.

[22] Kahneman, D., and A. Tversky. 1973. "On the psychology of prediction." Psychol. Rev. 80 (4): 237.

[23] Kahneman, D., Lovallo, D., and Olivier Sibony, O., (2011), Before you make that big decision, Harvard Business Review June 2011, pp 51-60.

[24] Koriat, A., S. Lichtenstein, and B. Fischhoff. 1980. "Reasons for confidence." J. Exp. Psychol.: Hum. Learn. Memory 6 (2): 107. Lam, K. C., D. Wang, P. T. Lee, and Y. T. Tsang. 2007. "Modelling risk allocation decision in construction contracts." Int. J. Project Manage. 25 (5)

[25] Kuhn T.S. (2004). The Structure of Scientific Revolutions 3rd edition. Chicago: The University of Chicago Press

[26] Larrick, R. P. (2004). "Debiasing." In Blackwell handbook of judgment and decision making, 316–338. Hoboken, NJ: Wiley.

[27] Lanchester, J. (2013). Mr. Phillips, Faber & Faber

[28] Lilienfeld, S.O.; Ammirati, R.; Landfield, K. (2009). Giving Debiasing Away: Can Psychological Research on Correcting Cognitive Errors Promote Human Welfare? Perspect. Psychol. Sci. 2009, 4, 390–398.

[29] Meissner, P., and T. Wulf. 2013. "Cognitive benefits of scenario planning: Its impact on biases and decision quality." Technol. Forecasting Social Change 80 (4): 801–814.

[30] Miller, C. C., L. M. Burke, and W. H. Glick. 1998. "Cognitive diversity among upper-echelon executives: Implications for strategic decision processes." Strategic Manage. J. 19 (1): 39–58.

[31] Mlodinow, L., 2009 The Drunkard's Walk: How Randomness Rules Our Lives, Vintage; Illustrated edition.

[32] Morewedge, C. K., H. Yoon, I. Scopelliti, C. W. Symborski, J. H. Korris, and K. S. Kassam. 2015. "Debiasing decisions: Improved decision making with a single training intervention." Policy Insights Behav. Brain Sci. 2 (1): 129–140.

[33] Murphy, A. H., & Winkler, R. L. (1977). Can weather forecasters formulate reliable probability forecasts of precipitation and temperature? National Weather Digest, 2(2), 2-9.

[34] Mussweiler, T., F. Strack, and T. Pfeiffer. 2000. "Overcoming the inevitable anchoring effect: Considering the opposite compensates for selective accessibility." Personality Social Psychol. Bull. 26 (9): 1142–1150.https://doi.org/10.1177/0146167200261101 0.

[35] Polya, G, (1945). How to Solve It: A New Aspect of Mathematical Method. Newest edition 2014, Princeton Science Library.

[36] Popper, K., (2002). Conjectures and Refutations: The Growth of Scientific Knowledge, Routledge Classics, 2nd edition.

[37] Spengler, P. M., D. C. Strohmer, D. N. Dixon, and V. A. Shivy. 1995. "A scientist-practitioner model of psychological assessment: Implications for training, practice, and research." Couns. Psychol. 23 (3): 506–534.

[38] Savitsky, K., and Gilovich, T., (2003). The illusion of transparency and the alleviation of speech anxiety, Journal of Experimental Social Psychology Volume 39, Issue 6, November 2003, Pages 618-625
[39] Shapiro, F. (2008), Who wrote the Serenity Prayer? https://yalealumnimagazine.com/articles/214-who-wrote-the-serenity-prayer
[40] Stewart, T. R., Roebber, P. J., & Bosart, L. F. (1997). The importance of the task in analyzing expert judgment. Organizational Behavior and Human Decision Processes, 69, 205-219.
[41] Walters, D. J., P. M. Fernbach, C. R. Fox, and S. A. Sloman. 2016. "Known unknowns: A critical determinant of confidence and calibration" Manage. Sci. 63 (12): 4298–4307.
[42] Wikipedia "Who Wrote the Serenity Prayer?" The Chronicle of Higher Education cited from https://en.wikipedia.org/wiki/Serenity_Prayer.& https://en.wikipedia.org/wiki/Reinhold_Niebuhr
[43] Wikipedia, Fukushima Daiichi Nuclear Power Plant; https://en.wikipedia.org/wiki/Fukushima_Daiichi_Nuclear_Power_Plant
[44] Yasseri, S., (2015), Evidence-based practice in subsea engineering Underwater Technology, The International Journal of the Society for Underwater 32(4)
[45] Yasseri, S., (2017), Thinking Like an Engineer, available on ResearchGate https://www.researchgate.net/publication/319644185_Thinking_like_an_engineer
[46] Yasseri, S., (2021), Rationality for engineers, Part I, IJCOE Vol.4/No. 2/Summer 2020 (1-13)
[47] Yasseri, S., (2021), Rationality for engineers, Part II, IJCOE Vol.4/No. 2/Summer 2020 (1-13)
[48] Yasseri, S., (2021), Rationality for engineers, Part III, IJCOE Vol.4/No. 2/Summer 2020 (1-13)
[49] Yoshimi, G., (2010), Random Seas and Design of Maritime Structures World Scientific Publishing
[50] Ackoff, R. L., "From Data to Wisdom", Journal of Applies Systems Analysis, Volume 16, 1989 p 3-9.
[51] Ackoff, R. L. (1999) Ackoff's Best. New York: John Wiley & Sons, pp 170 – 172.
[52] Nikhil Sharma (2008), The Origin of Data Information Knowledge Wisdom (DIKW) Hierarchy https://www.researchgate.net/publication/292335202_The_Origin_of_Data_Information_Knowledge_Wisdom_DIKW_Hierarchy
[53] Sartre, J.P., (2009), Existentialism and Humanism. By Jean-Paul Sartre. Translation and Introduction by publications Philip Mairet. (London: Methuen. 1948. Pp. 70. Price 5s. net.). Published online by Cambridge University Press.
[54] Baggini, J. (2005), The Pig that Wants to be Eaten: And Ninety-Nine Other Thought Experiments, granta press Chow, T. (2018), The Surprise Examination or Unexpected Hanging Paradox, Pages 41-51 | https://www.tandfonline.com/doi/abs/10.1080/00029890.1998.12004847

Appendix

Biases and how to avoid them.

Bias	Description	How to avoid
Cognitive diversity [26,29,30]	This is the difference in the perceptions and expectations among individuals in a group.	Building a group with differing experience levels and beliefs can significantly enhance the creativity, performance, and comprehensiveness of strategic assessments and decisions by adding thought conflicts that require resolutions.
Cognitive mapping [18]	This approach requires individuals to map out their cognitive strategy before making decisions.	The application of this technique requires experts and stakeholders to list key variables and build a network diagram that promotes statistical reasoning during assessments.
Think of unknowns [19,41]	Like considering the opposite, this approach asks individuals to specifically evaluate uncertainty.	The approach reduces overconfidence in assessments and improves the decision-making quality by making individuals balance known and unknown information.
Consider the opposite [3,16, 24, 34]	This approach asks individuals to consider counter-evidence or decisions that go against the consensus of the group.	Each time a panel of experts or stakeholders needs to make assessments or decisions, they should be asked to evaluate counter-evidence and alternative possibilities as a dedicated step in the overall process. Considering any plausible alternative outcome for an event, not just the opposite outcome, leads participants to simulate multiple alternatives, resulting in debiased judgments.
Delayed decision-making [37]	This strategy requires individuals to adopt a more deliberate approach to making decisions by delaying the actual decision-making process to consider the information again.	This strategy is a simple, cost-free, and effective practice that requires experts to reconsider the information and brainstorm avenues for improvement, avoiding inaccurate diagnoses due to hasty decisions.
Incentive program [2,10,26]	This approach rewards optimal behaviour. It is useful in improving individual motivation to increase effort and to apply more cognitive resources.	By itself, this is an ineffective debiasing strategy because it does not educate individuals on biases in their judgment. However, when paired with other debiasing strategies, it can improve their effectiveness by enhancing motivation and effort among practitioners.
Mindspace [6]	This is a process that focuses on improving intuitive decision-making skills by adopting and applying nine interventions (messengers, incentives, norms, defaults, salience, priming, affect, commitments, and ego).	Application of the nine tools/strategies to improve behavioural impulses can be applied at different times during the risk management process. These can range from controlling how the information is presented (i.e., messenger) to managing social pressures (i.e., ego and norms).
Nudges [4,12]	Subtle nudges (e.g., visual cues, audio cues, default selections) alongside text-based and numerical-based information can improve critical reasoning skills by providing practitioners some direction and context to avoid potential cognitive pitfalls.	Nudges are a positive debiasing approach that reduces the abstractness and complexity of the situation to assist practitioners in using all the available information
Scenario planning [29]	This tool is used to hypothesize about future paths and potential outcomes. The aim is not to become fortune predictors, but rather for the decision-maker to consider all possible logical paths and outcomes to develop creative and comprehensive plans.	Scenario planning is a cost-free, simple, and effective strategy that would seamlessly integrate with each step of the risk management process, allowing practitioners to consider all logical eventualities.
Third-party direct intervention [5]	This is used during negotiations when a third party invested in the decisions enters the decision-making process to resolve disputes or improve performance.	A proxy (i.e., third party) with a deeper understanding of biases and faulty heuristics is placed in the group to resolve disputes, reframe information, and proffer counterarguments. Although resource-intensive, this approach results in more-deliberated assessments and decisions.
Training [13,32]	Training programs on heuristics and biases, normative rules, and statistical reasoning is designed to improve calibration, encourage. individuals to consider all the evidence and reduce overconfidence.	Multimedia training platforms can serve as quick and engaging interventions to educate practitioners and calibrate assessments and decisions.

INTERNATIONAL JOURNAL OF
COASTAL & OFFSHORE ENGINEERING
IJCOE Vol.7/No. 1/Winter 2022 (15-22)

Available online at: www.ijcoe.org

Experimental Study on the Stability of Concrete Block Revetment for High Waves Propagating over Submerged Geotube Breakwater

Md Khairul Hasan[1*], Md. Ataur Rahman[2], Silwati Al Womera[3]

[1*] *Sub-Divisional Engineer, Bangladesh Water Development Board, Dhaka, Bangladesh, k.hasan90@gmail.com*
[2] *Professor, Department of Water Resources Engineering, Bangladesh University of Engineering and Technology, Dhaka, Bangladesh, mataur@wre.buet.ac.bd*
[3] *Assistant Professor, Department of Water Resources Engineering, Bangladesh University of Engineering and Technology, Dhaka, Bangladesh, silwati@wre.buet.ac.bd*

ARTICLE INFO

Article History:
Received: 12 Nov. 2021
Accepted: 27 Jan. 2022

Keywords:
high waves
revetment
submerged breakwater
transmission coefficient
wave breaking

ABSTRACT

Bangladesh has a coastline of 710 km and a long sandy beach. Moderate and high waves causes erosion along the coastline. Concrete block revetment is widely used for shore protection in Bangladesh. As per Coastal Engineering Manual, concrete block revetment stability is limited to wave height of 1.5 m. Studies reveal that the significant wave heights are greater than 1.5 m in the most parts of coastline of Bangladesh. Therefore, in some places, the concrete block revetment has failed. Revetment constructed with Tetrapod, X-bloc, Core-loc etc. are recommended to use for high waves. However, those armor units are not suitable in the context of Bangladesh considering its cost, construction and placement. Moreover, any hard protection may stop the erosion and protect the shoreline, but the sandy beach may be lost. Geotube breakwater is low cost structure for dissipating wave energy to some extent. In this study, laboratory experiments have been carried out for wave height 1.76 m to 2.40 m (as prototype) with two layer protection consisting of concrete block revetment at the shore and submerged geotube breakwater at shallow water. Concrete block size has been calculated using Pilarczyk formula for prototype wave height 1.5 m and scaled down using surf coefficient for laboratory model. Seventeen laboratory runs have been conducted and analysis of the experimental results reveal that two layer protection is effect to protect the shore from high waves. An equation has been established to design the shore protection works along the coastline experienced by high waves.

1. Introduction

The importance to the economy and ecology makes the coastal zone one of the most significant areas of any country [1]. Bangladesh's coastal zone covers 47,201 square kilometers of land [2], which is around one-third of country's total land area. This area provides shelter, sustenance, and livelihood for nearly 35 million people [3]. Bangladesh's coastline measures around 710 kilometers in length [4]. The Cox's Bazar-Teknaf Marine Drive Road along the Cox's Bazar coastline was constructed to promote tourism prospects, the fishing sector, regional connectivity, and coastal resource management [5]. The project area is in a highly susceptible and hazardous environment [6]. To protect the Marine Drive Road, the Bangladesh government took shore protection work along the seaside of the road. Bangladesh Water Development Board (BWDB) was responsible for the design, and 17 ECB, Bangladesh Army was responsible for the construction of the shore protection work. [7]. Bangladesh Water development Board considered cubical shape concrete block as an armor unit of protective work. The revetment was built in 2008. But the revetment did not sustain for a long time. The revetment failed after completion of the work in 2009. It is to be noted that graded riprap or concrete bock in the shore protection revetment is not recommended for high waves (i.e. $H_s \geq 1.5$ m) [8]. But the maximum wave height was found 2.53 m along the Cox's Bazar coastline [5]. When the significant wave height is more than 1.50 m, other types of armor unit such as Tetrapod, X-bloc, Core-loc, etc. are recommended to use in the revetment [8]. When the concrete block is staggered rather than uniformly placed, the performance is determined to be good. Tetrapod outperforms concrete block and X-block in terms of performance [9].

However, in terms of cost, construction, and placement, such armor units are unsuitable in the context of Bangladesh. Furthermore, any hard protection structure like revetment may protect the shore from wave action, but the beach in front of it will be lost by wave-breaking action at the toe and slope of the revetment.

In case of breakwater, almost all waves break when the ratio of the deep-water wave height to the freeboard of the submerged breakwater is higher than one [10]. Impermeable underwater breakwaters of trapezoidal shapes have a stronger damping action than narrow, rectangular, and triangular shapes [11]. The breakwater reflects the most, when the incident wave has the same period as a standing wave on top of the breakwater and a wavelength equal to the crest width [12]. In sediment movement, the distance between the breakwater and the shoreline is critical. The distance between the breakwater and the shoreline is proportional to the significant wave height (H_s) and negatively correlated with the amount of sediment deposited into the marsh [13]. The transmission, reflection, and wave energy loss factors all affect the efficiency of the breakwater. The transmission and the reflection coefficients are inversely proportional to the relative breakwater width, while the energy loss coefficient takes the opposite trend [14]. Submerged geotube breakwaters are a low-cost solution that allows to dissipate wave energy up to a certain limit [15]. But the remaining wave energy passing over the breakwater may cause shore erosion to some extent.

Therefore, there are both advantages and limitations of concrete block revetment and submerged breakwater as a single-layer protection. To take the advantages and to eliminate the limitations of concrete block revetment and submerged breakwater as single-layer, this research aims to study the performance of two-layer protection in the places of high waves ($H_s \geq 1.50$ m) by using concrete block revetment at the shore and geotube breakwater at the shallow water depth. In this two-layer protection, the submerged geotube breakwater has to be designed in such a way that the transmitted wave height is less than the maximum recommended wave height of concrete block revetment. Subsequently, the concrete block revetment may remain stable as the transmitted wave height is less than the maximum recommended wave height for concrete block revetment. When the incident wave pass the submerged breakwater, the wave reduces its energy. The remaining energy may not hold the suspended sediment particals and the suspended sediment particls will be deposited in the area between the shoreline and the submerged breakwater. Therefore, One of the additional advantages of this two-layer protection is the automatic nourishment of the land between the revetment and the submerged breakwater. This research also aims to develop a relationship among water depth (h_w), wave height (H), and breakwater height (h_b) to help coastal designers to design two-layer shore protection in the places of high waves.

2. Materials and methods

2.1 Experimental setup:

To investigate the performance of the revetment and submerged geotube breakwater, experimental studies had been conducted in a 2D wave flume (Length of flume = 21.3 m, width of flume = 0.76 m and depth of flume = 0.74 m) at the Hydraulics and River engineering Laboratory of Bangladesh University of Engineering and Technology. In this experiment, four different relative breakwater heights as h_b/h_w= 0.3, 0.4, 0.5 and 0.6 in 50 cm still water depth and four diffirent wave periods as T = 1.7 sec, 1.8 sec, 1.9 sec and 2.0 sec were used in this experiment to evaluate the performance of two layer protection consisting concrete block revetment at the shore and submerged geotube breakwater at shallow water depth. The wave periods were generated by adjusting the wave paddle.

The wave generator was set up 200 cm downstream of the flume's commencement. The submerged geotube breakwater was placed 800 cm downstream from the wave generator. As illustrated in Figure 1, data was collected from five different positions. The incident wave parameters were investigated at two locations in front of the geotube breakwater. Three locations at the downstream of the breakwater were chosen to assess the impact of the breakwater. Additionally, during each experimental run, still images and video records were captured. Figure 1 depicts the experimental setup in detail.

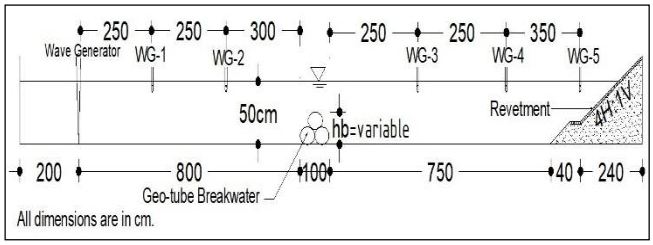

Figure 1. Detail of the experimental setup

2.2 Design of C.C. block

This experiment was carried out with a fixed bank normal slope of 1(V):4(H). All Parameters were scaled down in such a way that Surf coefficient (a dimensionless number) remain same for both prototype and laboratory data. Necessary data has been tabulated in Table 1. In the Table 1, the prototype data for significant wave height, H_s and wave period, T has been taken from previous studies [16], [17].

Table 1. **Preliminary Calculation of Parameters for both prototype and laboratory**

Prototype			Laboratory					
H_s (m)	T (sec)	Surf coefficient	Wave height, H_s		Wave period, T		Surf coefficient	Block Size (cm)
			Value (cm)	Scale	Value (sec)	Scale		
1.5	5.7	1.45	9.50	16	1.43	4.0	1.45	2.00
2.4	8.1	1.62	15.00	16	2.05	4.0	1.62	3.40

Here, significant wave height, H_s was 16 times scaled down. Wave period, T was calculated by 4.0 times scaled down from prototype. Finally the desired concrete block size was calculated by Pilarczyk formula [18] as shown in Eq.(1).

Characteristic size, $D = \frac{H_s \xi^b}{\Delta m \psi_u \, \phi_{sw} \, cos\alpha}$ (1)

2.3 Design of submerged geotube breakwater

When the width of the breakwater (B) is equal to the wave length (L), the reduction of wave height becomes optimum [19]. Because this is unlikely to be cost-effective, a narrower breakwater with a higher height was investigated subsequently, and it was found that the optimum reduction occurs when the relative breakwater width (B/L) is in the range of 0.2 to 0.4. [20].

In this research, breakwater heights of 15 cm, 20 cm, 25 cm, and 30 cm were established in a 50 cm still water depth for four different wave periods, T= 1.7 sec, 1.8 sec, 1.9 sec and 2.0 sec and corresponding wavelengths are 332 cm, 357 cm, 381 cm and 406 cm. For optimum reduction of wave height, the breakwater width was chosen as 100 cm. In this experiment, the relative breakwater width was ranged from 0.25 to 0.30 which is within the range of 0.2 to 0.4. The length of the breakwater is normally chosen to the equal length of the coastline that needs protection. The width of the 2D flume that used in this experiment is 76 cm. Therefore, in this experiment, the width of the breakwater has been selected as 76 cm.

2.4 Laboratory experimental run conditions

In this experiment, four different relative breakwater heights as h_b/h_w= 0.3, 0.4, 0.5 and 0.6 were used in still water depth of 50 cm. Therefore, the heights of the breakwater are 15 cm, 20 cm, 25 cm and 30 cm. Four wave periods were used in this experiment to evaluate the performance of submerged geotube breakwater and concrete block revetment. The wave periods that are used in this research are 1.7sec, 1.8sec, 1.9 sec and 2.0 sec. The wave periods were generated by adjusting the wave paddle. Table 2 represents the conditions of the experimental run in detail.

Table 2. Test Scenario of the experiment

Run No	Relative breakwater height ($\frac{h_b}{h_w}$)	Wave period, T (sec)	Incident Wave Height, H_i (cm)	Incident Wave Length, L_i (cm)
1	No breakwater	2.0	15	406
2	0.3	1.7	11	332
3		1.8	12	357
4		1.9	14	381
5		2.0	15	406
6	0.4	1.7	11	332
7		1.8	12	357
8		1.9	14	381
9		2.0	15	406
10	0.5	1.7	11	332
11		1.8	12	357
12		1.9	14	381
13		2.0	15	406
14	0.6	1.7	11	332
15		1.8	12	357
16		1.9	14	381
17		2.0	15	406

3. Results and Discussion

3.1 Effect of relative breakwater height on reducing wave height

The Figure 2 the demonstrate the effect of relative breakwater height (h_b/h_w, where h_b is the breakwater height and h_w is the still water depth) on wave transmission coefficient, K_t ($K_t = H_t/H_i$ (where, H_t is the wave height of transmitted wave and H_i is the wave height of incident wave) for four specific wave periods. The analysis result prevails that increases of the relative breakwater height, h_b/h_w, decreases the transmission coefficient, K_t for any specific wave period. It is also found that transmission coefficient, K_t falls as the wave period, T decreases for any particular relative breakwater height, h_b/h_w.

For relative breakwater height, h_b/h_w= 0.6 and wave period, T=2 sec, wave height drops by 40% due to breaking. For relative breakwater height, h_b/h_w= 0.5, 0.4 and 0.3 the reduction of wave height due to breaking of wave over the submerged geotube breakwater are 37%, 27% and 20% respectively for the same wave period, T= 2.0 sec. The variation in wave

height decrease follows the similar pattern for other experimental runs.

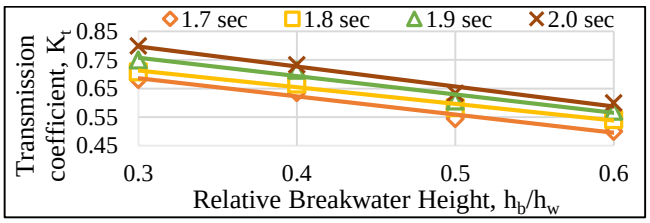

Figure 2. Effect of relative breakwater height on the reduction of wave height for different wave periods

3.2 Effect of relative breakwater width on wave height reduction

Figure 3 represents the effect of relative breakwater width, B/L (where, B = breakwater width, and L = wave length) on wave transmission coefficient, K_t for four different relative breakwater heights (h_b/h_w=0.3, 0.4, 0.5 and 0.6). For a specific relative breakwater height (h_b/h_w), with the increases of relative breakwater width (B/L), the wave height reduction increases due to wave breaking on the breakwater.

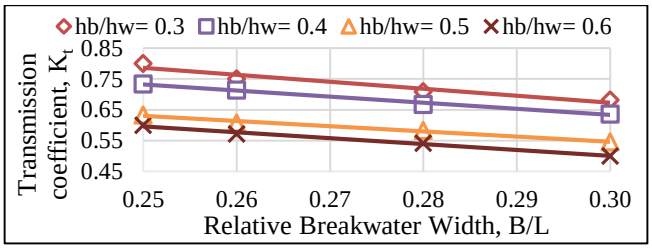

Figure 3. Effect of relative breakwater width on the reduction of wave height for different relative breakwater heights

For example, for relative breakwater height, h_b/h_w= 0.5 and relative breakwater width, B/L= 0.25, the height of wave reduces by 37% due to breaking. For relative breakwater width, B/L= 0.26, 0.28, and 0.30 the height of wave reduced by 39%, 42% and 45% respectively for relative breakwater height h_b/h_w= 0.5. The reduction of wave height follows this pattern for any specific ratio of B/L.

3.3 Dimensionless water surface profile with time

The changes of water surface profile (η) with time (t) (measured at location WG-1 and WG-4 in front and behind the breakwater respectively) is illustrated in dimensionless form (η/H_i with t/T) in the Figure 4. The location of the WG-1 and WG-4 in the laboratory flume has been shown in the Figure 1.

Figure 4(a) shows that incident wave height for wave period 1.7 sec (measured at WG-01) reduces at significant amount after passing the submerged geotube breakwater. The transmitted wave height was measured at WG-04. The figure also shows that as the relative breakwater height increases the transmitted wave height decreases for a particular wave period. For wave period, T=1.7 sec and relative breakwater height 0.6, 50% of the incident wave height is reduced. Whereas when relative breakwater heights are 0.5, 0.4 and 0.3, the incident wave height is reduced up to 45%, 36% and 32% respectively.

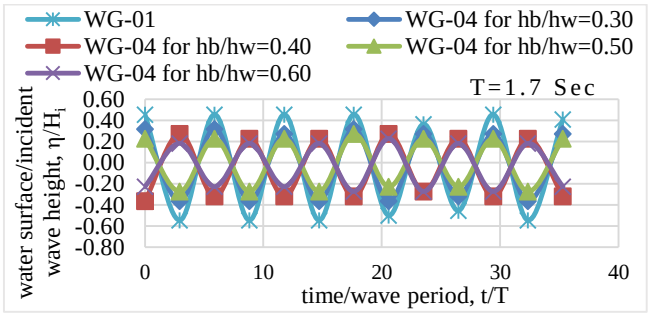

(a)

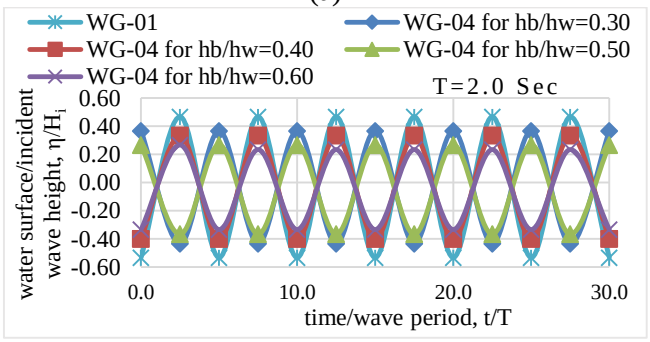

(b)

Figure 4. Variation of dimensionless water surface (η/Hi) with time (t/T)

Figure 4(b) shows that incident wave height for wave period 2.0 sec (measured at WG-01) reduces at significant amount after passing the submerged geotube breakwater. For T= 2.0 sec, when the submergence of geotube breakwater is 60%, 40% of incident wave height is reduced. 37% wave reduction occurs when relative breakwater, h_b/h_w is 0.5, whereas breakwater having relative breakwater height, h_b/h_w =0.4 reduces 27% of incident wave height. The minimum reduction (20%) occurs for 30% submergence of the geotube breakwater.

For wave period, T= 1.8 sec, When the geotube breakwater height is 30 cm, it reduces 46% of incident wave height. 42% incident wave height is reduced by geotube breakwater height of 25 cm. 20 cm geotube breakwater height, decreases incident wave height by 33%. The minimum reduction (29%) is occurred by 15 cm geotube breakwater for the same wave period of 1.8 sec.

For wave period, T= 1.9 sec, maximum reduction (43%) occurred by installing 30 cm geotube breakwater. For the same wave period, geotube breakwater having height of 25 cm reduces 39% of incident wave height, whereas geotube breakwater having height of 20 cm reduces 29% of incident wave height. The minimum wave height reduction (25%) is occurred by 15 cm geotube breakwater having relative breakwater height, h_b/h_w =0.3 for the same wave period.

3.4 Wave breaking

The main function of any breakwater is decreasing the wave energy by breaking the wave. As the breakwater height increases the breaking of the incident wave also increases. In this experiment, the incident wave height breaks on submerged geotube breakwater. Therefore, though the prototype incident wave height is higher than the maximum recommended wave height (1.5 m) for concrete block revetment, transmitted wave which breaks and reflects at the revetment is less the 1.5 m. Consequently, the concrete block revetment becomes stable as the wave height striking the revetment is less than the maximum recommended wave height. Figure 5 shows the breaking of the wave on the submerged geotube breakwater and on the revetment.

(a) Wave breaking on submerged breakwater

(b)Wave breaking on revetment

Figure 5. Wave breaking

3.5 Revetment stability

Total 17 experimental runs were performed to investigate the performance of cement concrete block revetment and submerged geotube breakwater. In the first experimental run, the prototype wave height was taken as 2.4 m [17], which is much higher than the maximum permissible limit of concrete block revetment of 1.5 m. The size of the cubical shaped concrete block has been calculated as 3.4cm x 3.4cm x 3.4cm. The size of the concrete block was calculated using Pilarczyk equation [18]. Without having any breakwater in front of the concrete block revetment (Run no. 1), the revetment failed as expected. To make the revetment stable, geotube breakwater was placed in the nearshore zone. The height of the submerged geotube breakwater had to select in such a way that the transmitted wave height become less than the maximum permissible wave height for concrete block revetment. To do this, another sixteen experimental run was performed and analyzed.

As the maximum permissible wave height for single layer revetment is 1.5m, the size of concrete block was calculated taking prototype wave height 1.5 m for other sixteen experimental runs (Run no. 2-17) [8]. The laboratory wave height was 9.5cm and the block size was 2cm x 2cm x 2cm which had been determined from Pilarczyk equation [18]. Revetment was stable for twelve experimental runs (experimental Run no: 2, 3, 6, 7, 10, 11, 12, 13, 14, 15, 16 and 17) among the sixteen experimental runs.

(a) Stable revetment (Run No: 3)

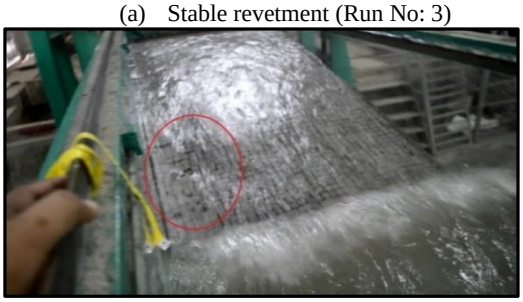

(b) Partially failed revetment (Run No: 4)

Figure 6. Revetment condition after experimental Run

The reason for the stability of those experimental runs is that the transmitted wave height of those experimental runs was equal to or less than the design wave height (9.5 cm).

Table 3. Summary of results of experimental runs

Run No	Relative breakw-ater height ($\frac{h_s}{h_w}$)	Wave period (T) sec	Incident Wave Height, H_i (cm)	Transmitted Wave Height, H_t (cm)	% of reduction of wave height ($\frac{Hi-Ht}{Hi}$)	Revetment Condition after 10 minutes experimental run
1	No breakwater	2.0	15	-	-	Failed
2	0.3	1.7	11	7.5	32	Stable
3		1.8	12	8.5	29	Stable
4		1.9	14	10.5	25	Partially Failed
5		2.0	15	12	20	Partially Failed
6	0.4	1.7	11	7	36	Stable
7		1.8	12	8	33	Stable
8		1.9	14	10	29	Stable
9		2.0	15	11	27	Partially Failed
10	0.5	1.7	11	6	45	Stable
11		1.8	12	7	42	Stable
12		1.9	14	8.5	39	Stable
13		2.0	15	9.5	37	Stable
14	0.6	1.7	11	5.5	50	Stable
15		1.8	12	6.5	46	Stable
16		1.9	14	8	43	Stable
17		2.0	15	9	40	Stable

Revetment was partially failed for three experimental runs (experimental Run no: 4, 5, and 9). The transmitted wave height of those experimental runs was higher than the design wave height (9.5 cm). Figure 6 represents the revetment condition after experimental run.

For experimental Run no.8, though the transmitted wave height (10 cm) was higher than the design wave height (9.50 cm), the revetment was stable after the experimental run. One of the reasons is that the wave height used to determine the size of concrete block by Pilarczyk equation is significant wave height. The significant wave height (H_s) is defined as the mean wave height of the highest third of the waves. Therefore, there will be higher waves than significant wave height in a wave spectrum. Another reason is the experimental run time. In this experiment, the experimental run time was 10 minutes. The revetment may fail if the experimental run time is increased. Table 3 shows the summary of results of the experimental runs.

3.6 Relationship among transmission coefficient (K_t), relative breakwater height (h_b/h_w), wave period (T) and significant wave height (H_s)

A relation among significant wave height (H_s), wave period (T), relative breakwater height (h_b/h_w) and transmission co-efficient (K_t) is required to select the economic section of geotube breakwater. Following parameters are the governing parameters associated with the performance of breakwaters considering the transmission of waves [21].

$K_t = f(H_s, T, h_w, h_b, B, D_{50}, \tan\alpha, g)$ (2)

Where, H_s = significant wave height, T = wave period, h_w = depth of water, h_b = breakwater height, B = breakwater width, D_{50} = medium size of the material, tanα = seaward slope, g = acceleration due to gravity.

To develop a relationship it is necessary to make dimensionless parameters. 'Buckingham Pi Theorem' is an established method for dimensionless analysis. In this research, the independent dimensions H_s and T were used as repeating variables. The following dimensionless groups were formed after the dimensionless analysis.

$$K_t = f\left(\frac{H_s}{h_w}, \frac{H_s}{h_b}, \frac{H_s}{B}, \frac{H_s}{D_{50}}, \frac{gT^2}{H_s}, \tan\alpha\right) \quad (3)$$

Since breakwater width (B), medium size (D_{50}), seaward angle (α) has not been changed in this experiments, $\frac{H_s}{B}, \frac{H_s}{D_{50}}, \tan\alpha$ these three dimensionless parameters have not been analyzed. Remaining two dimensionless parameters $\left(\frac{H_s}{h_w}, \frac{H_s}{h_b}\right)$ have been simplified, and a new dimensionless parameter (relative breakwater height, $\frac{h_b}{h_w}$) has been analyzed. Therefore, for this research, the transmission coefficient is a function of the following parameters.

$$K_t = f\left(\frac{h_b}{h_w}, \frac{gT^2}{H_s}\right) \quad (4)$$

Experimental results have been analyzed using Microsoft excel solver tool and the following equation has been found.

$$K_t = 1.05 - 0.67\left(\frac{h_b}{h_w}\right)^{0.83} - 2.4 \times 10^{-4}\left(\frac{gT^2}{H_s}\right) \quad (5)$$

Where,

K_t = transmission coefficient

H_s = significant wave height

T = wave period

h_w = the depth of water

h_b = the breakwater height

g = the acceleration due to gravity

The intercept of the Eq.(5) is positive (1.05) and the slope of relative breakwater height is negative (-0.67). Thus means the transmission coefficient will decrease with increase of relative breakwater height for any particular wave. In the developed relation (Eq.5) breakwater width is not considered. The relative breakwater width shall be in the range of 0.2 to 0.4 for optimal reduction of incident wave height [20].

The sum of squired residuals (SSR) of the Eq.(5) is 0.026. The sum of squired residuals is the sum of squired residuals, and residuals is the deviation of the calculated transmission coefficient by the Eq.(5) from the laboratory transmission coefficient. The mathematical expression of SSR is states below.

$$SSR = \sum_{i=1}^{n}(y_i - f(x_i))^2 \quad (6)$$

Where, y_i is the i^{th} value from laboratory experiment and f (x_i) is the i^{th} value calculated from the new developed relation.

3.7 Shore protection design along the Cox's Bazar shoreline using developed relation

The highest wave height was found 2.53 m along the Cox's Bazar shoreline [5]. The maximum permissible wave height recommended by he U.S. Army of Crops Engineers for one layer revetment is 1.50 m [8].

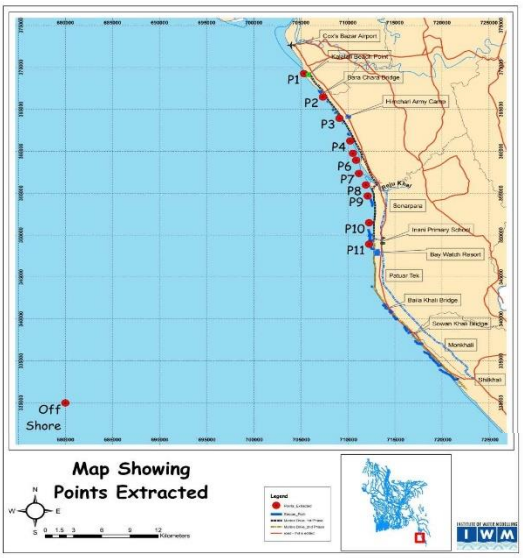

Figure 7. Nearshore locations of along Marine drive road Cox's Bazar, Bangladesh

Therefore, the breakwater height has to be selected in such a way that the transmitted wave height becomes

<= 1.50 m. Eq.(5) has been used to select the relative breakwater height. The relative breakwater height of 11 locations near the Himchari, Cox's Bazar (Figure 7) has been shown in the Table 4 in the last column. The relative breakwater width (B/L) has been taken within the range of 0.2 to 0.4 for maximum reduction of wave height [20].

Table 4. Relative breakwater height calculation

Point No. (Figure 7)	Measured data at Cox's Bazar		Max. permissible wave height for revetment	$K_t = H_t/H_s$	Relative breakwater height, h_b/h_w (using Eq. 5)
	H_s (m)	T (sec)	H_t (m)		
1	2.32	8.65	1.5	0.65	0.42
2	2.37	8.62	1.5	0.63	0.45
3	2.38	8.70	1.5	0.63	0.45
4	2.28	8.74	1.5	0.66	0.40
5	2.31	8.70	1.5	0.65	0.42
6	2.25	8.79	1.5	0.67	0.38
7	2.43	8.70	1.5	0.62	0.47
8	2.35	8.57	1.5	0.64	0.44
9	2.5	9.09	1.5	0.60	0.49
10	2.42	8.76	1.5	0.62	0.47
11	2.53	8.51	1.5	0.59	0.52

As the transmitted wave height which is the maximum permissible limit (1.5 m) for concrete block revetment has been taken as the significant wave height to calculate the concrete block size. Table 5 represents the calculated concrete block size for marine drive road having different slope. The slope of the concrete block revetment shall be finalized from geotechnical investigation.

Table 5. Concrete block size calculation for revetment

H_s (m)	T (sec)	slope	Surf coefficient	Block size (cm)
1.5	5.7	1(V):2(H)	2.90	55
1.5	5.7	1(V):3(H)	1.94	39
1.5	5.7	1(V):4(H)	1.45	32
1.5	5.7	1(V):5(H)	1.16	27

These parameters will help the coastal engineer to design two-layer shore protection at the marine drive road, Cox's Bazar considering the maximum wave height limitation of concrete block revetment.

4. Conclusions

In this study, the stability of cubical shaped concrete block shore protection revetment for high waves (wave height > 1.5 m) propagating over submerged geotube breakwater has been investigated experimentally. Results show that when the concrete block revetment is exposed to the high waves, it fails for the wave height greater than the maximum recommended wave height (1.5 m). Submerged geotube breakwater has been placed in front of the revetment to reduce the incident wave height The effectiveness of a submerged geotube breakwater in lowering wave energy is evidenced by the results of this experiment. The relative breakwater height (h_b/h_w) and relative breakwater width (B/L) are crucial characteristics for reducing incident wave height for any given wave period, according to the findings. Because of the breaking induced by the submerged breakwater, as the relative breakwater height (h_b/h_w) increases, the incident wave decreases. In addition, the reduction in wave height also increases as the relative breakwater width (B/L) increases. The incident wave breaks over the submerged geotube breakwater and its energy gets reduced. The remaining energy is transmitted to the concrete block revetment. Experimental results show that if the transmitted wave height is less than the maximum permissible wave height (1.5 m) for concrete block revetment, the revetment become stable. If the transmitted wave is greater than 1.5 m, the revetment become unstable. The relative breakwater height has to be selected in such a way that the prototype transmitted wave height becomes ≤ 1.5 m. To select sustainable and economic relative breakwater height, a relationship has been developed among transmission coefficient (K_t), relative breakwater height (h_b/h_w), wave period (T) and significant wave height (H_s), which is is $K_t = 1.05 - 0.67(\frac{h_b}{h_w})^{0.83} - 2.4 \times 10^{-4}(\frac{gT^2}{H_s})$ considering the relative breakwater width (B/L) within 0.2 to 0.4. This relationship will help the coastal designer to design two-layer protection in the places of high waves.

5. Acknowledgements

The authors gratefully acknowledge the financial support from the Committee for Advanced Studies & Research of Bangladesh University of Engineering and Technology, Bangladesh. The authors also would like to take the opportunity to acknowledge the great help and support provided by all laboratory staff of Hydraulics and River Engineering Laboratory, Department of Water Resources Engineering of Bangladesh University of Engineering and Technology, Bangladesh.

6. List of Symbols

B	Breakwater width (m)
b	Exponent related to the interaction process between waves and revetment
D	Thickness of the cover layer (m)
g	Acceleration due to gravity
H_i	Incident wave height (m)
H_s	Significant wave height (m)
H_t	Transmitted wave height (m)
h_b	Breakwater height (m)
h_w	Water depth (m)
K_t	Transmission coefficient

T_m	Average wave period (sec)
W	Weight of revetment material (kg)
ρ_s	Density of protection material (kg/m^3)
ρ_w	Density of water (kg/m^3)
Δm	Relative density of submerged material = $(\rho_s-\rho_w)/\rho_w$
α	Bank normal slope, (°)
ψ_u	System determines stability upgrading factor
φ_{sw}	Stability factor for incipient motion
ξ_z	Wave breaker similarity parameter

7. References

[1] Williams A, Rangel-Buitrago N, Pranzini E, Anfuso G., (2018) The management of coastal erosion, Ocean & Coastal Management, Vol.156, p.4–20.

[2] Kamal AMU, Rob K., (2003), Delineation of the coastal zone, Working Paper WP005, p.1–42.

[3] Ahmad H., (2019), Bangladesh coastal zone management status and future trends, Coastal Management, Vol.22, p.13-26.

[4] Islam MR, Ahmad M., (2004), Living in the Coast: Problems, Opportunities and Challenges, Development, p.1-54.

[5] Coastal Hydraulic and Morphological Study and Design of Protection Measures for Marine Drive Road, (2014) Dhaka, Bangladesh.

[6] Rahaman T, Hossain S., (2015), Marine drive protection by formation of sea forest creation utilizing by-product slag of steelmaking process on Bay of Bengal, 5th International Conference on Water & Flood Management, p.1-4.

[7] Rahaman AZ, Rahman A., (2013) Estimation of design of wave height along marine drive road from kalatali to inani at cox's bazar, 4th International Conference on Water and Flood Management, p.405-412.

[8] Fundamentals of Design, (2011), Coastal Engineering Manual, Part IV. US Army Corps of Engineers, Vol.(5), p.1-56.

[9] Hossain I., (2013), Experimental study on stability of different types of armor units used in shore protection structure experimental study on stability of different types of armor units used in shore protection structure, MSc thesis, Bangladesh University of Engineering and Technology.

[10] Liao YC, Jiang JH, Wu YP, Lee CP, (2013) Experimental study of wave breaking criteria and energy loss caused by a submerged porous breakwater on horizontal bottom, Journal of Marine Science and Technology (Taiwan), Vol.21(1),p35–41.

[11] Khader M, Rai S., (1980), A study of submerged breakwaters, Journal of Hydraulic Research, p.113–121.

[12] Milne DT, Brebner A., (1968), Solid and permeable submerged breakwaters, Coastal Engineering, p.1141–1158. (Proceedings). Availablefrom: https://doi.org/10.1061/9780872620131.072

[13] Vona I, Gray MW, Nardin W., (2020), The impact of submerged breakwaters on sediment distribution along marsh boundaries, Water (Switzerland). Vol.12(4),p.1-18.

[14] Rageh OS., (2009), Hydrodynamic efficiency of vertical thick porous breakwaters, 13th International Water Technology Conference. p.1659–1671.

[15] Shabankareh O, Ketabdari MJ, Shabankareh MA., (2017) Environmental impact of geotubes and geotextiles used in breakwaters and small breakwaters construction (case study : rigoo public breakwater in south of Geshm island - Iran). International Journal of Coastal & Offshore Engineering. Vol.5, p.9–14.

[16] Katsaprakakis D Al., (2020) Wave and Wind Energy. Salina, Italy.

[17] Liu J, Thomas E, Manuel L, Griffith D, Ruehl K, Barone M., (2018), Integrated system design for a large wind turbine supported on a moored semi-submersible platform, Journal of Marine Science and Engineering, Vol.12, p.6-9.

[18] Pilarczyk KW., (1990) Design of seawalls and dikes — including overview of revetments, Coastal Protection. Balkema, The Netherlands.

[19] Dick TM, Brebner A., (1968), Solid and permeable submerged breakwaters, 11th International Conference on Coastal Engineering, p. 1141–1158.

[20] Kawasaki K, Iwata K., (2001) Wave breaking-induced dynamic pressure due to submerged breakwater, 11th International Offshore and Polar Engineering Conference. Stavanger, Norway, p. 488–494.

[21] Rathnayaka RMDB, Rathnayaka RMJR, Pathirana KPP., (2016) Experimental investigation of transmission coefficient of reef breakwaters, Journal of the Institution of Engineers, Sri Lanka, Vol.49(1),p.31–37.

INTERNATIONAL JOURNAL OF
COASTAL & OFFSHORE ENGINEERING
IJCOE Vol.7/No. 1/Winter 2022 (23-33)

Available online at: www.ijcoe.org

Semi-active Control of an Offshore Platform Using Updated Numerical Model and Experimental Laser Doppler Vibrometer Data

Samira Mohammadyzadeh[1], Alireza Mojtahedi[2*], Javad Katebi[3], Hamid Hokmabady[4], Farhad Hosseinlou[5]

[1]School of Engineering, University of Northern British Columbia, Prince George, Canada. mohammady@unbc.ca
[2]Associated Professor, Department of Water Resources Engineering, University of Tabriz, Iran. a.mojtahed@tabrizu.ac.ir*
[3]Associated Professor, Department of Structural Engineering, University of Tabriz, Iran, jkatebi@tabrizu.ac.ir
[4]Postdoctoral Research Assistant, Department of Water Resources Engineering, University of Tabriz, Iran. h.hokmabady@tabrizu.ac.ir
[5]Assistant Professor, Faculty of civil engineering and architecture, Shahid Chamran University of Ahvaz, Iran.

ARTICLE INFO

Article History:
Received: 07 Jul. 2021
Accepted: 15 Dec. 2022

Keywords:
Numerical Model Updating
Laser Doppler Vibrometer
Offshore Structure
Semi-active Control
MR damper

ABSTRACT

In this study, a semi-active control system is assessed over a numerically updated model to achieve the most promising numerical results and to keep the performance of the numerical model as close to the prototype behavior as possible. Numerical model updating is performed based on the experimentally captured non-contact sensing data considering uncertainties. The elastic modulus of the jacket elements is specified as the calibration parameter. A mathematical function -optimized using Particle Swarm Optimization (PSO) algorithm- is also employed to reduce the structural uncertainties of the numerical model. Eight MR dampers both in X and Y directions are located in a platform numerical model. Modified Newmark-Beta method besides optimized parameters of instantaneous optimal control algorithm are utilized to predict the response of the system. The performance of the updated model is evaluated under environmental loads. The results indicate the importance of model uncertainty reduction in improving the accuracy of simulation results in a complex system. Based on the results using a non-contact sensing technology such as Laser Doppler Vibrometer (LDV) system is strongly recommended in practical cases due to great sensitivity capabilities and also no direct contact requirements.

1. Introduction

Environmental loads in offshore area may cause continuous vibrations that results in decrement of reliability, productivity, and serviceability of the structures and also increment in uncertainties and possibility of the damage and failures. However, controlling the vibrations in marine structures is challenging due to nonlinear hydrodynamic forces, uncertainties, large deformations, and highly nonlinear responses [1]. Basically, vibration control methods are classified as passive, active, semi-active, and hybrid methods, each of which is widely discussed in the literature [2-7]. Semi-active control systems show higher reliability and more efficient control effects [2]. Among different semi-active control devices, Magnetorheological (MR) damper used in this study, represented a great control performance based on previous studies [8-10]. MR fluids change from a free-flowing, linear viscous liquid into semi-solid fluid in the presence of a magnetic field. A range of researches has been performed due to the capability of MR dampers in offshore structures in the literature [11-12]. A semi-active control method might be affected by the presence of uncertainties. Simply put, many factors in experimental and numerical simulation processes in any engineering fields specifically offshore structures can cause uncertainties in which their identification are of great importance [13]. Offshore environment related uncertainties can be categorized into: aleatory (natural) uncertainties and epistemic (knowledge-based) uncertainties. Aleatory uncertainty presents a quantity natural randomness, which cannot be decreased or eliminated such as time dependent wave height variability. In the other hand, epistemic uncertainty, which is related to reducible errors that can be reduced by collecting more information about a quantity, e.g. data, statistical, model and climatic uncertainties, [14]. Uncertainty quantification in both the data and the behavior prediction of models are important and must be mathematically understood to perform correctly for calibration and validation processes [13]. Complex

engineering systems response prediction needs advanced computer simulations and experimental evidence which basically requires theoretical foundation, numerical modeling, and experimental data, all of which come with their associated errors [15]. An essential rule in validating the study results is to compare the computer model predictions results to experimental data. Uncertainty reduction method is carried out by: (i) calibrating some numerical parameters through numerical model updating used for reproducing the experimental data or (ii) by changing some experimental parameters to reproduce the numerical model [16]. An essential rule in validating the study results is to compare the computer model predictions results to experimental data [15]. Disagreements between the computer model predictions and the experiments can be categorized as three distinct factors based on the computer model: (1) Numerical uncertainty (inaccuracy in solving mathematical equations of the problem); (2) Parametric uncertainty (imprecision in model parameters' definition); and (3) Structural uncertainty (inexactness and incompleteness in engineering principles modeling). Calibrating the input parameters of a model without considering structural uncertainty might gain mathematically correct results but physically incorrect solutions [17]. However, the success of model updating procedure depends on experimental test execution. The importance of experimental data acquisition is considerably high not only due to its impact on the accuracy of updated numerical model, but also because of possible real system implementation.

In this paper, the semi-active control of a three-dimensional fixed offshore jacket platform (SPD9 located in the Persian Gulf) is studied over a numerically updated model for the first time to gain the most promising numerical results and to keep the numerical model performance close to the prototype. The experiment is performed using a shake table test and non-contact sensing Laser Doppler Vibrometry (LDV) device and utilizing a scaled hydro-elastic physical model. The updating procedure is carried out by considering both parametric and structural uncertainties within the calculation process. The elastic modulus of the platform members is defined as the calibration parameter to reduce the parametric uncertainties. A mathematical function is also utilized to reduce the structural uncertainties by using Particle Swarm Optimization (PSO) algorithm. Eight MR dampers are placed on the numerically updated model in both X and Y directions and modified Newmark-Beta method base on the instantaneous optimal control algorithm is used to estimate the response of the system. The results show the efficiency of the mentioned methodology by regarding parameter uncertainty for an infrastructural system due to the reduction in disagreement of the experimental data and numerical model in offshore industries. The results also indicate the importance of model uncertainty reduction in improving the accuracy of simulation results in a complex system.

2. Semi-active Control Process

2.1 Experimental Test

In this study, a numerical model updating approach is proposed on a controlled complex structural system. The model is built based on the prototype dimensions by ABS tubes that are welded together using argon arc welding to ensure proper load transfer and the FEM of the platform [18]. To gain 1:100 scale of the prototype, the specifications of the scaled model are considered as listed in Table 1.

Table 1. Properties of the scaled and prototype of the platform model

Properties	Prototype	Model
Height (m)	74	0.74
Low-level dimensions (m)	36×35	0.36×0.35
High-level dimensions (m)	29×16	0.26×0.16
Scale Factor	--	1:100
Material	Steel	ABS (Acrylonitrile Butadiene Styrene)
Platform weight (t)	15500	0.015

The test is implemented using a shake table and a Laser Doppler Vibrometer (LDV) as a non-contact measuring system. The LDV is well established as an efficient, fast, and also cost-effective means of analyzing and measuring device that performs without any surface contact. More details of the experimental test and models are shown in Fig.1 and Table 2.

To carry out the test, the scaled model of the structure is placed on the shake table in X direction for velocity measurement and the LDV is located and adjusted to center the measuring beam in the middle of the jacket deck. The analogue velocity output calibration can be checked employing an appropriate accelerometer in association with a charge amplifier or a standard hand-held calibrator. The calibration procedure is performed based on the optical unit user manual. A random vibration signal is also applied on the scaled model in a frequency range of 1-50Hz with duration of 20 seconds. The test is repeated 3 times to avoid any unintentional errors. The experimental measurement is considered to validate and also update the numerical model. The post-processing procedure is executed using ME'ScopeVES software package based on the captured frequency response functions (FRFs) of the scaled jacket model through the tests.

Fig. 1. Layout of the experimental test using the LDV sensing components and the scaled model.

Table 2. The LDV sensing components and shake table facility specifications

Facilities	Characteristics	Values
Laser Doppler Vibrometry (Optical Unit)	Vibration Velocity	A few μs/m to 425 mm/s
	Vibration Frequency	< 0.1 Hz to 25 kHz
	Working Distance	From 0.4m up to 25m
	Dimensions	75 × 175 × 350mm
	Temperature	+5°C to +35°C
	Relative Humidity	Up to 80%
	Weight	3.7 kg
Shake Table	Rated Frequency Range	0.5 – 1500 Hz
	Size of Table	400 × 400 mm
	Max Displacement	25 mm
	Max Load	70 kg

2.2 Numerical Model Updating

In this study, the mass and stiffness matrices of the jacket finite element (FE) model are gained employing Frame3DD software and modeling the elements and nodes coordinates of the prototype. To consider the uncertainties through the modeling a novel approach is considered. Uncertainties in computer modelling can be categorized into three various factors: (i) numerical uncertainty which is based on inaccuracy in solving method of the equations; (ii) parametric uncertainty which is defined as imprecision in parameters definition of the numerical model; and (iii) structural uncertainty which is due to incompleteness in modeling the engineering principles [19]. Through an iterative process, both structural and parametric uncertainties are considered within the calculation process of this study. In this regard, the calibration parameter for the second factor and a model form error for the third factor are determined as the solution. By proposing a relation between input and output of the modeling (y_{sim}) and the actual physical system and the experimental data ($y_{\exp}$), a formulation can be defined as follows:

$$y_{exp} = \left(y_{sim}(z_i.\theta) + \Psi(z_i)\right) + \varepsilon(z_i) \qquad i = 1.\cdots.n \tag{1}$$

where, $(z.\theta)$ is a relation between the model input and the variables z, θ, $\varepsilon(z_i)$, n, and $\Psi(z_i)$ represent control parameter, calibration variable, the experimental error, the number of experimental tests and the model form error or the discrepancy function, respectively. More details about the mentioned method for updating the numerical model can be found in [15]. The goal of model updating is to reduce the disagreement between the experimental data and numerical modeling using a discrepancy term. In the other hand, the goal is to combine parameter values and discrepancy models to reach the experimental data. Actually, the discrepancy function could be specified as any continuous and differentiable mathematical function, because of trigonometric nature of the experimental data, the model form error is defined as a combination of trigonometric and exponential functions in this paper:

$$\delta(z,\alpha) = \alpha_0 \times e^{(\alpha_1 \times sin(\alpha_2 z+\alpha_3)+\alpha_4 \times cos(\alpha_5 z+\alpha_6))} \tag{2}$$

where, α indicates the nonphysical coefficients. Basically, the aim of the proposed method is to minimize the difference between the simulation and also the experimental data utilizing an objective function and an optimization algorithm:

$$f(\alpha.\theta) = [y_{exp}(z) - \xi(z)]^2 = [y_{exp}(z) - y_{exp}(z.\theta) - \delta(z.\alpha)]^2 \tag{3}$$

$$f(\alpha.\theta) = \sum_{i=1}^{n}[y_{exp}(z_i) - y_{exp}(z_i.\theta) - \delta(z_i.\alpha)]^2 \qquad i = 1.\cdots.n \tag{4}$$

The coefficients introduced by the selected model should be trained with the available experimental data. In this study, the objective function is performed by using the PSO algorithm in which the values of swarm size, and also the social and cognitive acceleration coefficients are chosen as 30, 1.3, and 2.8, respectively. In this paper, acceleration is selected as the output of the experimental and numerical models, time is taken as the control parameter, and modulus of elasticity (E) is chosen as the calibration parameter taken in different ranges based on importance of the elements of the jacket platform. Four distinct groups are defined for the jacket elements consists of the main jacket legs, diagonal, horizontal, and also the internal members. The value of calibration parameter for each group is listed in Table 3. Unlike other structural systems, in offshore jacket platforms, the main legs are the most important structural members, then bracing, the horizontal, and finally the internal members can be considered as the most to less important members. Two main leg and bracing members have the highest effects on the first five modes (natural frequencies), while the horizontal member includes the lowest impact on modes. The final objective function of the optimization algorithm is as follows:

$$f = \sum_{i=1}^{n}[\ddot{x}_{exp}(t_i) - \ddot{x}_{sim}(t_i.E_1.E_2.E_3.E_4) - \delta(t_i.\alpha_0.\alpha_1.\alpha_2.\alpha_3.\alpha_4.\alpha_5.\alpha_6)]^2 \qquad i = 1.\cdots.n \quad (5)$$

Table 3. Group of elements lower and upper bounds (initial value is based on steel modulus of elasticity)

Bounds	Main Legs	Horizontal Elements	Diagonal Elements	Internal Elements
Lower bound	194000 MPa (-3%)	192000 MPa (-4%)	192000 MPa (-4%)	190000 MPa (-5%)
Upper bound	206000 MPa (+3%)	208000 MPa (+4%)	208000 MPa (+4%)	210000 MPa (+5%)

More details of the proposed updating algorithm are presented in Table 4. Natural frequencies of the experimental, numerical, and updated models are also presented in Table 5.

Table 4. Algorithm of model updating procedure

	Algorithm of Proposed Updating Strategy
	A) Considering an optimization algorithm. B) Defining a discrepancy model, Eq. 4. C) Defining an objective function: Eq. 5.
1:	Assume: $t_i.E_1.E_2.E_3.E_4.\alpha_0.\alpha_1.\alpha_2.\alpha_3.\alpha_4.\alpha_5,\alpha_6$;
2:	Put the assumed values of *E* into the Frame3DD input File;
2:	Compute $M_d.K_d$ as the Mass and Stiffness Matrices through Frame3DD;
	Load $\ddot{x}_{exp}$,$M_d.K_d$;
3:	Compute the $\ddot{x}_{sim}$ By solving the equation of motion using the same scaled experimental force;
4:	Compute f as the objective function considering assumed values of α for the discrepancy function;
5:	Is the objective function satisfied? Yes, Go to next Step or No go to Step 1;
6:	Stop.

Table 5. Natural frequencies of experimental, numerical, and updated models (Hz)

Natural Frequencies	Experimental Model (Scaled Model)	Numerical Model	Updated Numerical Model without Discrepancy Term	Updated Numerical Model with the Discrepancy Term
Mode 1	11.3	13.72	13.12	11.79
Mode 2	36.6	35.57	35.77	36.24
Mode 3	68	69.21	68.64	68.13

According to the results as listed in Table 5, the updated models is fitted almost poorly by utilizing the optimization process. However, as the proposed discrepancy function is defined within the updating process, higher fitness tendency could be observed. To be more specific, employing a discrepancy function or a model form error term within the numerical model updating procedure is strongly recommended. In this study, to show the importance of numerical model updating before applying the semi-active system, both numerical models (not updated) and updated model with discrepancy are compared under El Centro earthquake ground acceleration as represented in Fig. 2. Accordingly, there are obvious differences, anti-phase peaks, and amplitudes between the response of the numerical model before and after updating under an earthquake force. It is seen that achieving trustworthy numerical results not only requires a valid experimental test but also needs an efficient model updating approach before any further investigations. Displacement RMS of both numerical models are listed in Table 6.

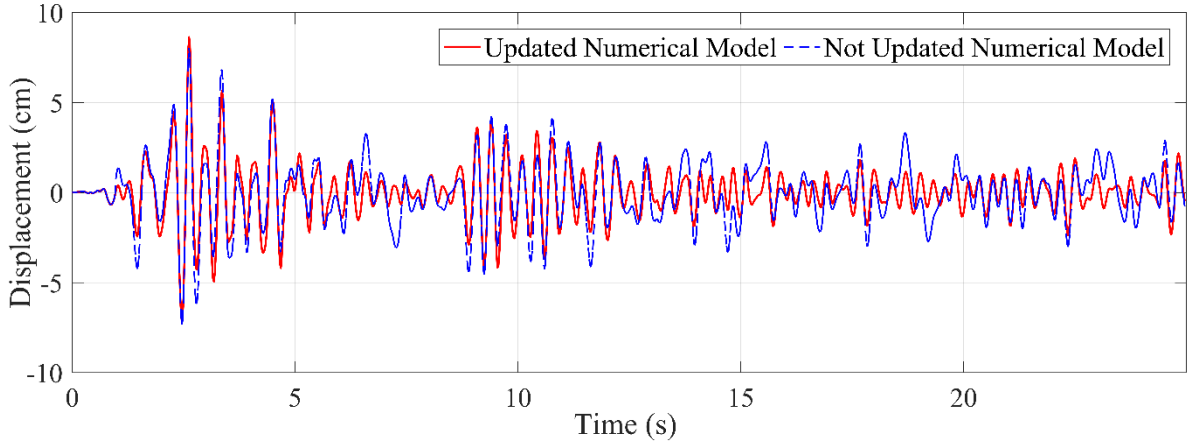

Fig. 2. Updated and Not Updated Numerical Models Comparison under El Centro Earthquake

Table 6. Displacement RMS of Updated and not Updated Numerical Models under El Centro Earthquake

Index	Numerical Model	Updated Numerical Model with the Discrepancy Term	Difference (%)
RMS	0.876	1.32	34

As seen in Table 6, the differences between the numerical models with and without updating is about 34 percent which is much higher than acceptable range. The result of Table 5 is a confirmation of model updating requirements.

2.3 Modelling MR Damper

MR dampers are one of the most promising semi-active control devices in civil engineering applications [10]. General equation of motion of the jacket platform equipped with MR damper can be expressed as follows:

$$[M^*]\cdot\{\ddot{x}\}+[C^*]\cdot\{\dot{x}\}+[K]\cdot\{x\}=\{F_W \; or \; F_E\}+[L]\cdot\{F_{MR}\} \quad (6)$$

where, F_W and F_E are n-dimensional wave loading vector and ground motion force, respectively; $\{\ddot{x}\}$, $\{\dot{x}\}$, and $\{x\}$ are vectors of acceleration, velocity and displacement, all with $n \times 1$ dimensions, respectively; $[M^*]$ and $[C^*]$ are mass and damping matrices of the jacket system considering added mass and damping, respectively, which are discussed in following; $[K]$, L and $\{F_{MR}\}$ are the jacket stiffness matrix, the matrix denoting the location of controllers, and the MR dampers force vector including f_d as each MR dampers control force, respectively. An illustration of modified Bouc-Wen model is shown in Fig. 3.

$$f_d = c_1 e + k_1(u_{MR} - x_0) \quad (7)$$

where, the evolutionary variable is known as *y* and also the variable *e* is coupled equations as follows:

$$\dot{y} = -\gamma|v_{MR}-\dot{e}|(y)|y|^{(n-1)} - \beta(v_{MR}-\dot{e})|y|^{(n)} + A_{MR}(v_{MR}-\dot{e}) \quad (8)$$

$$\dot{e} = \left\{\frac{1}{c_0+c_1}\right\}\{\sigma_0 y + c_0 v_{MR} + k_0(v_{MR}-e)\} \quad (9)$$

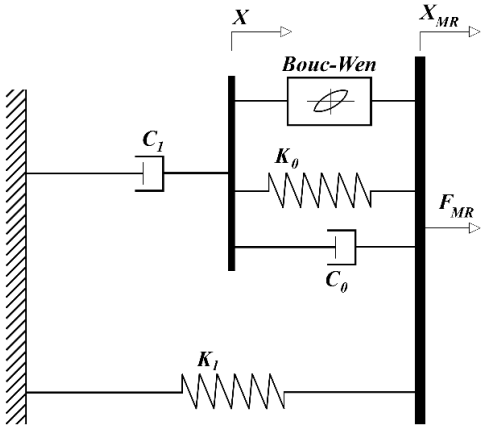

Fig. 3. Modified Bouc-Wen model

where v_{MR}, u_{MR}, k_0, and k_1 are relative velocity and displacement between connected joints in jacket members, control damper force in large velocities and accumulator stiffness respectively. The hysteresis loops shape depends on parameters A_{MR}, γ, and β. Variables c_0, c_1, and σ_0 are large velocities viscous damping coefficient, low velocities viscous damping coefficient and also evolutionary coefficient, respectively, which can be gained using the following equations based on the command voltage *u*:

$$c_0 = c_{0a} + c_{0b}u \quad (10)$$

$$c_1 = c_{1a} + c_{1b}u \quad (11)$$

$$\sigma_0 = \sigma_{0a} + \sigma_{0b}u \quad (12)$$

where, variable u is obtained within first order filter as:

$$\dot{u} = -\mu(u - v) \quad (13)$$

where variable v is control voltage, which can be determined using a control algorithm. Based on specification of MR damper and semi-active control method, choosing an appropriate algorithm not only increases the semi-active control system performance but also decreases the structure response. In this paper, the Lyapunov algorithm [8] is used as follows:

$$v = v_{max}H(-Z^T P_L B f_d) \quad (14.A)$$

where $[P_L]$ is real, symmetric, positive definite matrix, can be calculated through:

$$[A^T][P_L] + [P_L][A] = -[Q_P] \quad (14.B)$$

$$\dot{Z} = AZ + BF_d + E\ddot{x}_g \quad (14.C)$$

$$Z = \begin{bmatrix} x \\ \dot{x} \end{bmatrix}; B = \begin{bmatrix} 0 \\ -M^{-1}D \end{bmatrix}; A = \begin{bmatrix} 0 & 1 \\ M^{-1}D & -M^{-1}C \end{bmatrix}; E = \begin{bmatrix} 0 \\ r \end{bmatrix} \quad (14.D)$$

where, $H(\cdot)$ is Heaviside step function. The voltage, which should be applied to the damper, must be taken as v_{max} if the step function is higher than zero and in other cases, the command voltage must be set to zero. Variables Z, $[B]$, $[A]$, $[Q_P]$ are the state space vector with $2n \times 1$ dimensions, a state space parameter matrix, system matrix with $2n \times 2n$ dimensions, and a matrix of unity, respectively. In this paper, MR dampers are modelled within the braces (not to be replaced with braces) in upper two structural levels. Location of eight mentioned dampers are shown in Fig. 4 for both X and Y directions.

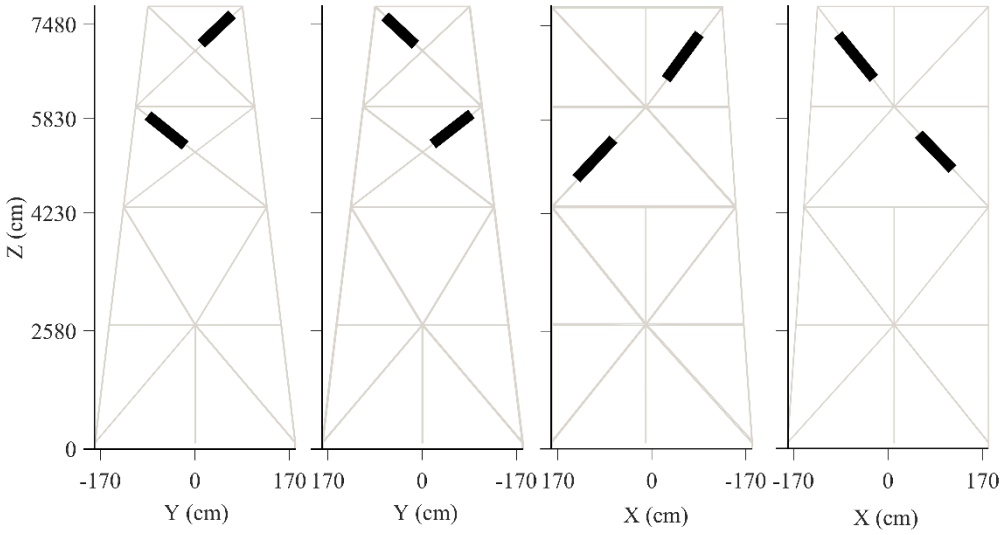

Fig. 4. Location of MR dampers: (A) X Direction; (B) Y Direction

Because of the strong nonlinear hysteretic behavior of MR dampers, the instantaneous optimal control algorithm based on Newmark's integration is used mode detail of which is available in the literature [10, 20].

2.4 Environmental Loads

The performance of the updated system is studied under environmental loads in this paper. Based on Eq. 6, the system mass and damping matrices considering added mass and damping can be derived as follows:

$$[\bar{M}] = [M] + \rho_w(C_M - 1)V \quad (15)$$

$$[\bar{C}] = [C] + \frac{1}{2}\sqrt{\frac{8}{\pi}}\rho_w C_D A \sigma_{vr} \quad (16)$$

where $[M]$ and $[C]$ are the jacket mass and damping matrices, respectively; ρ_w, V, A, C_D, C_M, and σ_{vr} are the mass density of water, displaced volume of the member, projected area normal to the member axis, drag coefficient, inertia coefficient, and the value of root mean squares of the relative velocity between the jacket and water particles, respectively. It should be noted that the Rayleigh's technique is used for the jacket damping matrix. The hydrodynamic force (chosen as wave) is calculated based on a wave theory. Wave induced forces can be calculated using the Morison Equation for a cylinder type structure as follows [21]:

$$F_W = \rho_w V C_M \ddot{q}_n + \frac{1}{2}\rho_w C_D A|\dot{q}_n - \dot{x}_n|(\dot{q}_n - \dot{x}_n) \quad (17)$$

$$F_W = \rho_w V C_M \ddot{q}_n + \frac{1}{2}\sqrt{\frac{8}{\pi}}\rho_w C_D A \sigma_{vr}(\dot{q}_n - \dot{x}_n) \quad (18)$$

where F_W is the wave force per unit length of the member; $\ddot{q}_n$, $\dot{q}_n$, $\dot{x}_n$, and $(\dot{q}_n - \dot{x}_n)$ indicate the acceleration of the fluid, velocity of the fluid, the absolute velocity, and the relative water velocity at joint *n*, respectively. In this paper, Morison equation (linearized form) is employed and the main parameters of wave height and period, are taken based on sea state of the Persian Gulf with 100 years of return period (see Table 7) [22]. The velocities and accelerations of the water particle are evaluated utilizing the Stokes second order wave theory [23]. Characteristics of the hydrodynamic force are listed in Table 8.

Table 7. Persian Gulf sea state characteristics [22]

Return period (year)	Wave height H_s (m)	Peak period T_p (s)
10	4.15	5.59
20	4.67	6.35
50	5.33	6.77
100	5.83	7.10

Table 8. Specification of hydrodynamic force

Specification	Values
Wave return period (year)	100
Wave heights (m)	5.83
Wave periods (s)	7.10
Water depth (m)	69.5
C_d	0.7
C_m	2

3. Results and discussion

In this study, a semi-active control of an offshore steel jacket platform is performed based on a truly updated numerical model. In this regard, the PSO algorithm is performed by 100 runs with detailed specification of swarm size of 30 and 150 iterations. The calibrated values of elastic modulus for all four groups and the value of the best fitness function (sum of squared errors) are listed in Table 9. Updated numerical model is used to investigate the structural response and semi active control of the jacket employing MR damper with 200kN capacity. The control force of the dampers is calculated using modified Bouc-Wen method. Time history response of one of the top nodes of the structure (Node 1) is illustrated in Fig. 5 using the same but scaled sinus force which is applied to the experimental model. The calculated acceleration in finite element model (obtained by the sinus force) is compared to the recorded acceleration of the experiment for updating the numerical model. For a better explanation, the scaled force of the experiment is applied into numerical model and used for updating the numerical model. In Fig. 5, two cases are compared in each figure as un-controlled structure (Uncontrolled) and semi-active controlled structure (Controlled). It is seen that using MR dampers effect on whole structural response to decrease. Fig. 5.B represents the control force of the damper as an important factor both in semi-active control process and MR damper device because of damper force limitations (MR damper can apply limited forces to the structure according to its specification).

Table 9. Calibrated values of Elastic Modulus for four groups of elements and related SSE

Values	Main Legs	Horizontal Elements	Diagonal Elements	Internal Elements
Optimized E (MPa)	200830	202500	196230	199410
SSE (g^2)	0.89×10^{-8}	0.89×10^{-8}	0.89×10^{-8}	0.89×10^{-8}

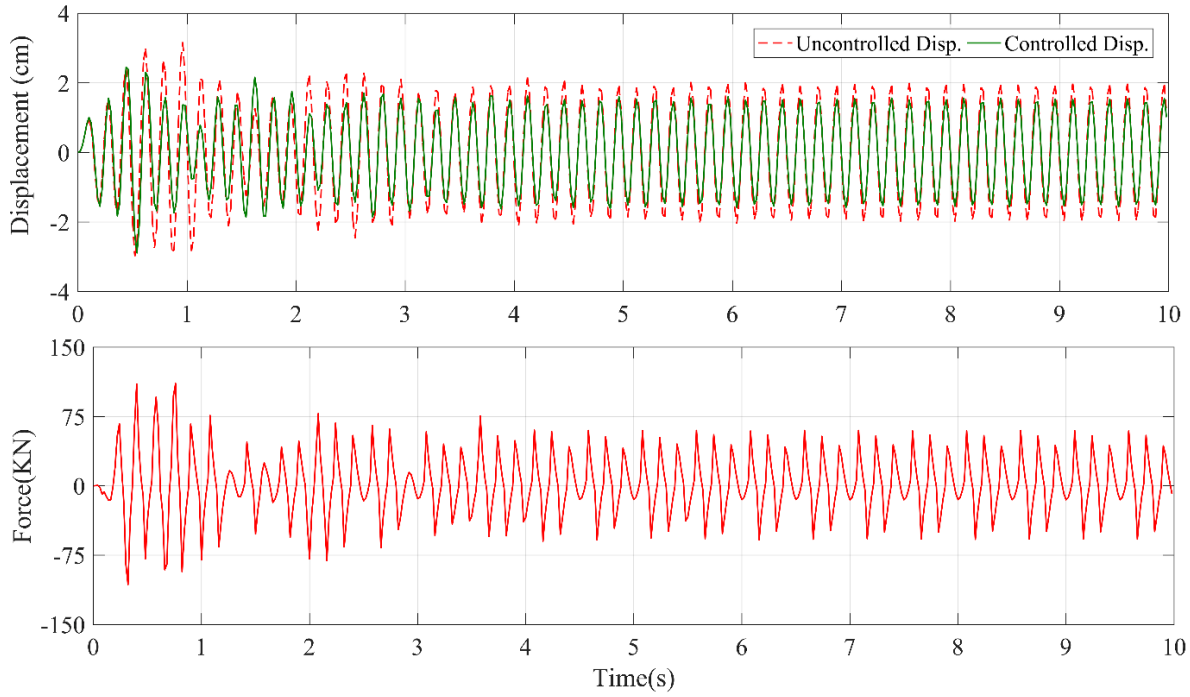

Fig. 5. Time History of Displacement and Control Force of the Jacket Platform under Sinus Force

Efficiency of the dampers are also investigated under wave and earthquake loads in this manuscript. A wave with 100 years of return period is assumed based on characteristics of Table 7 and 8. Time history of top node displacement is demonstrated under wave in Fig. 6 for uncontrolled and controlled systems. The whole system response is decreased using MR damper in both amplitude of the response and the number of the peak points which results in lower vibration in the whole system and the system lifespan improvement.

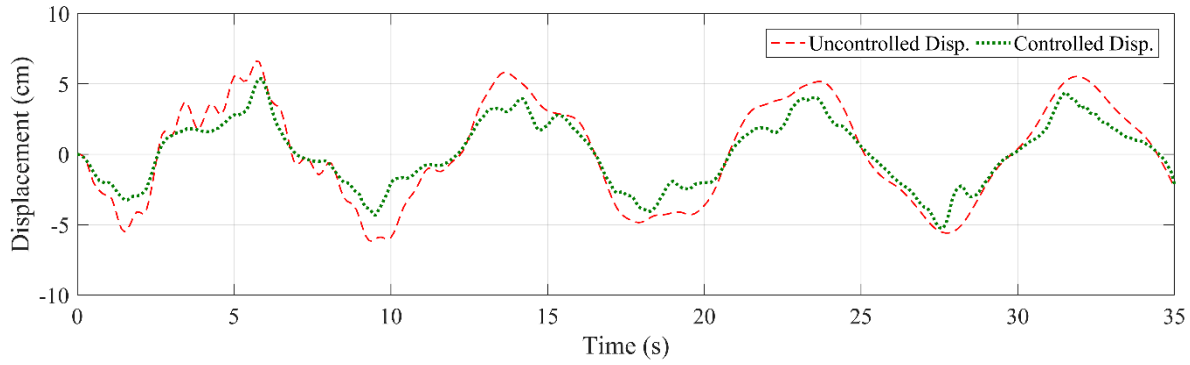

Fig. 6. Time History of Top Node Displacement under Regular Wave Load

The structural response of the jacket platform is also investigated under three major earthquake records. Proposed records are chosen as near field unidirectional ground motion records such as El-Centro, 1940, Kobe, 1995, San Fernando, 1971. Time history of top node displacement under three proposed earthquake excitations are also shown in Fig. 7. The mentioned controlled strategy results in lower vibration and the whole response reduction. The structural vibration is not only decreased through lower amplitudes but also it is reduced within lower response frequencies. Presented structural response of the jacket platform in Fig. 7 proves that using semi-active MR damper in offshore jacket platforms is an appropriate choice. Hysteresis behavior of MR damper under earthquake records is shown in Fig. 8. Nonlinear behavior of MR damper is also illustrated in hysteresis loops of Fig. 8. A summary of peak displacement and control force of top node of the jacket are listed in Table 10 for comparison.

Table 10. Summary of peak top node displacement and controlled force results under earthquake

Earthquakes	Displacement (cm)		Control force (kN)
	Uncontrolled	Controlled	
El-Centro	8.8	3.69	148
Kobe	9.8	4.82	91
San Fernando	5.8	3.71	84

4. Conclusion

Semi-active control of an offshore steel jacket platform is investigated over a numerically updated model using non-contact experimental data. The experiment is implemented using a shake table test, a non-contact LDV device, and a scaled hydro-elastic physical model of the jacket platform. The simultaneous reduction of structural and calibration parameters, which is specified as the baseline of the semi-active control system through as optimization framework, is investigated in details in this paper. The results and limitation of the study can be summarized as follows:

- The numerical model of the investigated offshore platform is updated successfully using non-contact measurements. Accordingly, utilizing an LDV sensing components is recommended because of both no direct contact requirements and also great sensitivity of non-contact sensing technology.
- Numerical updating is performed not only to achieve the most promising numerical results but also to keep the results as much close to the actual physical model behavior as possible. Therefore, updating the numerical model based on experimental data before taking a structural control strategy into account is strongly recommended.
- The results show the efficiency of the updating methodology by regarding parameter uncertainty for an infrastructural system due to the reduction in disagreement of the experimental data and numerical model in offshore industries. Based on the model updating results, which indicates the capability of the introduced model updating procedure, considering such methodology within the calculation is of great importance mostly before any further investigation on the numerical model.
- Considered trigonometric-based function, which is used for the first time as a discrepancy function in an offshore infrastructure, performed acceptably as discussed in the results.
- The proposed control devices result in lower vibration. The structural vibration is not only decreased through lower amplitudes but also it is reduced within lower response frequencies under both wave and earthquake loads. Simply put, the whole system response is decreased using MR damper in both amplitude of the response and the number of the peak points which results in lower vibration in the whole system and the system lifespan improvement.
- Definitely, it is not possible to assess all aspects of a research through a single study. Therefore, other problems are remained unsolved particularly in relation to practical cases which must be considered as the topics of the futures studies.

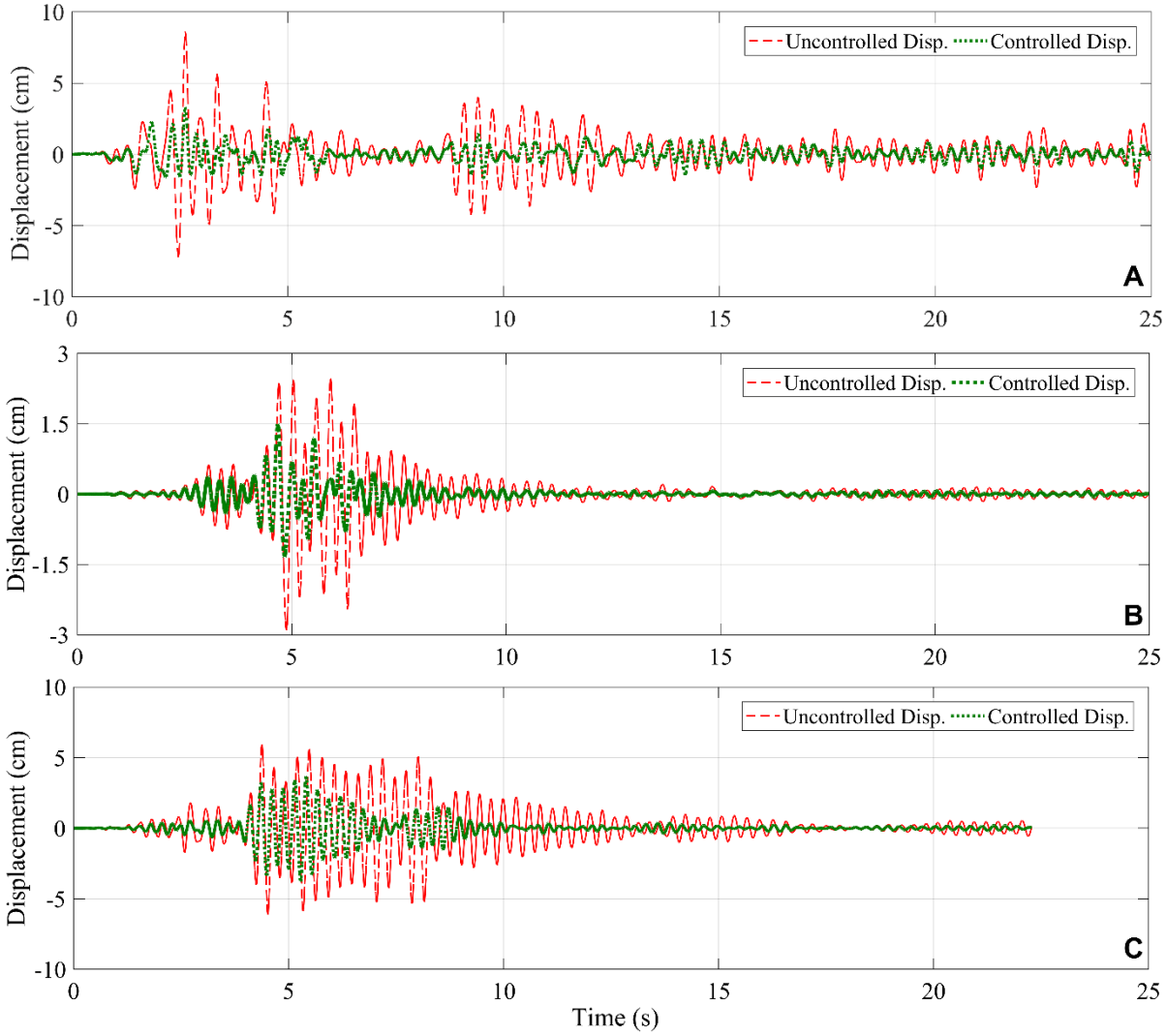

Fig. 7. Time History of Top Node Displacement under Earthquake Excitations: (A) El-Centro, (B) Kobe, (C)

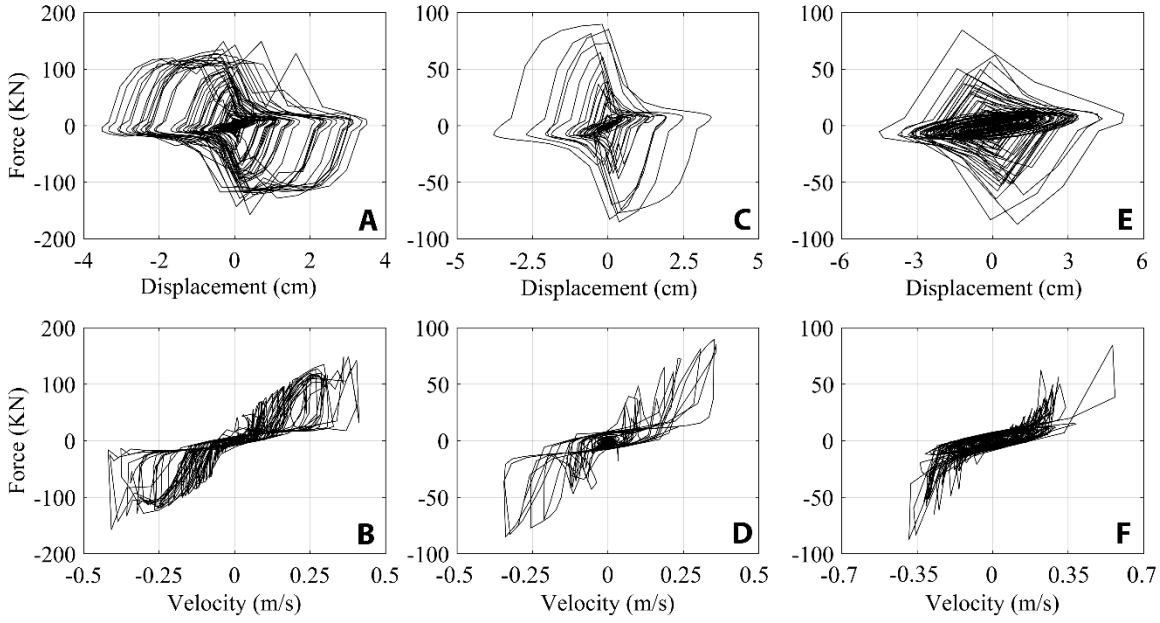

Fig. 8. Hysteresis behavior of MR damper under earthquake:
(A, B) El-Centro; (C, D) Kobe; (C, D) San Fernando

References

[1] Kandasamya R., Cuia F., Townsend N., Foo C.C., Guo J., Shenoi K., Xiong Y. (2016). A review of vibration control methods for marine offshore structures. Ocean Engineering. 127: 279–297.

[2] Som A., Das D. (2018). Seismic vibration control of offshore jacket platforms using decentralized

sliding mode algorithm. Ocean Engineering. 152:377–390.

[3] Fisco N.R., Adeli H. (2011). Smart structures: Part I - Active and semiactive control, Scientia Iranica, 18(3): 275-284.

[4] Housner G.W., Bergman L.A., Gaughey T.K., Chassiakos A.G., Claus R.O., Masri S.F., Skelton R.E., Soong T.T., Spencer B.F., and Yao J. (1997). Structural control: past, present, and future, Engineering Mechanics. 123(9): 897-971.

[5] Hokmabady H., Mohammadyzadeh S., Mojtahedi A., (2019). Suppressing structural vibration of a jacket-type platform employing a novel Magneto-Rheological Tuned Liquid Column Gas Damper (MR-TLCGD). Ocean Engineering. 180:60–70.

[6] Chen D., Huang S., Huang C., Ouyang F. (2021). Passive control of jacket–type offshore wind turbine vibrations by single and multiple tuned mass dampers, Marine Structures, 77:102938.

[7] Ghadimi, B., Taghikhani T. (2021). Dynamic response assessment of an offshore jacket platform with semi-active fuzzy-based controller: A case study, Ocean Engineering, 238:109747.

[8] Dyke S.J., Spencer B.F., Sain M.K., Carlson J.D. (1997). Phenomenological model for magnetorheological dampers, Engineering Mechanics, 123(3):230-238.

[9] Yoshioka H., Ramallo J.C., Spencer B.F. (2002). Smart base isolation strategies employing magnetorheological dampers, Engineering Mechanics. 128(5): 540-551.

[10] Katebi J., MohammadyZadeh S. (2016). Time delay study for semi-active control of coupled adjacent structures using MR damper. Structural Engineering and Mechanics. 58(6):1127-1143.

[11] Sarrafan A., Zareh S.H., Khayyat A.A., Zabihollah A. (2012). Neuro-fuzzy control strategy for an offshore steel jacket platform subjected to wave-induced forces using magnetorheological dampers. Mechanical Science Technology. 26(4): 1179–1196.

[12] Chunyan J., Menglu C., Shanshan L. (2010). Vibration control of jacket platforms with magnetorheological damper and experimental validation. High Technology Letters, 16(2):189–193.

[13] Bitner-Gregersen E.M., Ewans K.C., Johnson M.C. (2014). Some uncertainties associated with wind and wave description and their importance for engineering applications. Ocean Engineering. 86:11–25.

[14] Negro V., López-Gutiérrez J., Esteban M.D., Matutano C. (2014). Uncertainties in the design of support structures and foundations for offshore wind turbines, Renewable Energy. 63:125–132.

[15] Hokmabady H., Mojtahedi A., Lotfollahi Yaghin M.A., Farajpour I. (2019). Calibration and Bias-Correction of the Steel Offshore Jacket Platform Models Using Experimental Data, Waterway, Port Coastal and Ocean Engineering. 145(3):04019008.

[16] Wu J.R., Li Q.S. (2006). Structural parameter identification and damage detection for a steel structure using a two-stage finite element model updating method, Constructional Steel Research. 62: 231–239.

[17] Hokmabady H., Mohammadyzadeh S., Mojtahedi A. (2020). Uncertainty analysis of an offshore jacket-type platform using a developed numerical model updating technique, Ocean Engineering. 211:107608.

[18] Mojtahedi A., Hokmabady H., Yaghubzadeh A., Mohammadyzadeh S. (2020). An improved model reduction-modal based method for model updating and health monitoring of an offshore jacket-type platform, Ocean Engineering. 209:107495.

[19] Christie M.A., Glimm J., Grove J.W., Higdon D.M., Sharp D.H., Wood-Schultz M.M. (2005). Error analysis and simulations of complex phenomena. Los Alamos Science, 29:6–25.

[20] Joghataie A., Mohebbi M. (2012). Optimal control of nonlinear frames by Newmark and distributed genetic algorithms. Tall and Special Buildings. 21(2):77-95.

[21] Wilson J.F. (2003). Dynamics of offshore structures, John Wiley & Sons Inc. Hoboken, New Jersey, USA. pp. 28-29.

[22] Dastan M.A., Mohajernassab S., Seif M.S., Tabeshpour M.R., Mehdigholi H. (2014). Assessment of offshore structures under extreme wave conditions by Modified Endurance Wave Analysis, Marine Structures. 39:50-69.

[23] Chakrabarti S.K. (2005). Handbook of offshore engineering. Elsevier, Plainfield, Illinois, USA, pp. 91-93.

INTERNATIONAL JOURNAL OF
COASTAL & OFFSHORE ENGINEERING
IJCOE Vol.7/No. 1/Winter 2022 (34-42)

Available online at: www.ijcoe.org

Grain-size characteristics of seafloor sediment and transport pattern in the Caspian Sea (Nowshahr and Babolsar coasts)

Maryam Safari[1], Dariush Mansoury[2*], Seyed Ali Azarmsa[3]

[1] *Physical Oceanography, Faculty of Natural Resources and Marine Sciences, Tarbiat Modares University, maryam.safarii@gmail.com*
[2*] *Assistant Professor, Department of Marine Physics, Faculty of Natural Resources and Marine Sciences, Tarbiat Modares University, mansoury@modares.ac.ir*
[3] *Associate Professor, Department of Marine Physics, Faculty of Natural Resources and Marine Sciences, Tarbiat Modares University, azarmsaa@modares.ac.ir*

ARTICLE INFO

Article History:
Received: 29 Jun. 2021
Accepted: 1 Feb. 2022

Keywords:
Equilibrium beach profile
Sediment classification
Granulation
Caspian Sea

ABSTRACT

The aim of the current study is to determine the equilibrium beach profiles of the coasts of Babolsar and Nowshahr in the southern Caspian Sea. Using depth field data collected from two beaches in the period from 2018 to 2019, seasonal beach profiles and equilibrium beach profiles of the study area were extracted. To investigate the type and transfer of bed sediments, samples were collected from depths of 0.5, 1.5, 3 and 5 meters and were transferred to the laboratory for granulation. The results show the predominant type of sediments in Babolsar and Nowshahr are fine sand with an average of 82.39% and 82.12%, respectively. Also, the percentage of fine-grained sediments, including very fine sand and silt have increased from nearshore to offshore. In the west-east, the median diameter of sediment and the profile slope decreased, from there, the erosion and deposition rate in the two regions has changed. In the western regions, the diameter of beach sediments is more than in the eastern regions due to strong sea currents and relatively coarse-grained sediments from the rivers of western Mazandaran, as well as human activities.

1. Introduction

One of the important attempts in coastal engineering and construction of coastal and offshore structures is to understand the concept of how sediments are transported and the analysis of erosion and deposition in different regions. The shape of the beach profile is the result of natural forces that affect the structure of beach sediments. The beach profile is one of the most important parameters for beach analysis. Beach profiles are constantly changing in different parts of the world, due to factors such as waves, sea currents and water level conditions that cause the transfer and displacement of sediments [1]. These changes mainly occur in the vicinity of the beach region where the effects of breaking waves are more evident. It can be mentioned that after the breaking waves process, a lot of energy is transferred to the seabed by waves and sea currents, which cause the sediments to move and eventually lead to the deformation of the beach profile [2]. In most places, the erosion of mountains and the transfer of erosive products to the shoreline are transported to the sea by rivers, and after transfer, they are eroded and substituted by waves and sea currents. In fact, the shape and size of sedimentary grains also affect their movement and transport in the marine environment, so that a flat grain certainly behaves differently than a spherical grain in aqueous media [1]. Sediment particles are transported in two main modes: bed load and suspended load. The bed load is a part of the total load that is moving in the form of rolling and jumping in constant contact with the seabed. So, it can be concluded that accurate prediction of sediment transport rate is an important element in morphological studies of riverine, coastal and marine environments [3]. For marine environments, the sediment transport process becomes more complex due to the presence of oscillating currents, the interaction between constant and oscillating currents, as well as the effect of tides and wind-induced waves [4,5]. In addition to the factors mentioned about beach profile changes, water level is also an important factor in the process of natural activities of water basins. If there are changes in the mean sea level, then there are also changes in the beach profile. Evaluation criteria beach profile changes is the beach equilibrium profile, which is considered as an indicator. The equilibrium

profile shows the final trend of the beach profiles. In fact, in order to study the changes or relative stability of beach profiles during different periods, it is very important to study the equilibrium (average) profile [6,7]. Equilibrium profiles are also widely used to predict beach profiles in marine structures and projects [8,9]. Indeed, the equilibrium profile is the result of a balance between the constructive and destructive forces. Constructive forces appear after the storm, and move the sand the onshore. Finally, the beach profile reaches equilibrium over an average of a long period of time and in nature, it is considered as a dynamic concept, because the characteristics of waves (height, direction and period) and water levels are continuously changing and evolving [1]. The equilibrium profile is used as a model for analyzing beach profile changes over different periods of time [10,11,12]. During the study of changes in sedimentary environments, the changes in nearshore portions are greater than offshore portions. Sediments located offshore are often softer than nearshore sediments [1]. In a study conducted in 2007 in the marine regions of Noor, during sampling conducted every two months through the year, the type and percentage of bed sediments were examined. According to the obtained results, the highest amount of bed sediments was very fine sand with an average of 90.594% [13]. Also, the process of modeling sand transfer using Mike 21 in Gorgan Bay shows that nearshore sediments have changed significantly compared to offshore portion [14]. During field measurements, the results of sediment sampling from the nearshore of Miankaleh, Sorkhrood, Nattered, Anzali, Talesh and Astara, show that finer sediments appear at greater depths [15]. Due to the fact that fine-grained sediments are directed to deep zone due to sea currents, but sometimes due to the adhesion of sediments such as silt and clay, according to the Hjulstrom diagram, more force is needed to carry them by sea currents [16]. This event in some beaches reduces the percentage of fine-grained sediments at great depths. In another study in the Caspian Sea, beach profiles on some coasts of Mazandaran and Gilan, according to available measurement data (some seasons) related to 2013 have been studied. The seasonal beach profile has been compared to the equilibrium profile of some mathematical models [17]. With careful redundant and continuous studies, we can find the type of performance of these beaches in different seasons and years, and then suggest useful solutions for the proper use of these regions. In the present study, according to the investigations, the beaches of Babolsar and Nowshahr are among the tourist cities of Mazandaran province, which are located in the east and west of Mazandaran, respectively (Figure 1). They are also very prominent in terms of business activities Nowshahr and Babolsar have a high commercial position due to the construction of the port. Therefore, the study of changes in the seabed and coastlines in these regions is of particular importance, because with detailed studies and continuous analysis, it is possible to know the type of performance of these beaches in different seasons. Following that, more useful strategies for the proper exploitation of these regions can be presented and also, equilibrium beach profile is the principal concept assumed by most numerical modeling. Thus, in order to apply coastal engineering projects, the predicted profile of equilibrium should be close enough to the measured profile.

2. Materials and methods

2.1 Study area

In this study, transverse profiles of the beaches of Babolsar (36° 42' 55" *N*, 52° 40' 38" *E*) and Nowshahr (36° 39' 42" *N*, 51° 29' 40" E) in Mazandaran province located on the southern Caspian Sea coast were studied. The Caspian Sea is the largest inland water basin located in the Eurasian region. The lake is surrounded by the Caucasus Mountains in the west, the Alborz in the south, and the vast desert in the north and east [18,19]. The surface of the lake has changed frequently throughout history. In fact, geological and climatic processes are effective parameters in changing the water level of the Caspian Sea [20]. Hence, the change in river water inflow is one of the most important parameters affecting the water level fluctuations of this sea [21,22]. Beach profiles along the Mazandaran coast (Figure 1) were measured Four times per year in mild conditions during autumn, winter, spring and summer seasons so that seasonal variations could also be considered.

Figure 1. Study area on the southern coast of the Caspian Sea in Mazandaran province

2.2 The field measurement scenario

For the purpose of the present study, in order to determine the equilibrium profile in the two beaches, measurements were done in both land and sea in a cross section which was in the last month of autumn (2018), winter, spring and summer (2019), and once in each season. Initially, in the land part of the coast, the Theodolite mapping camera was utilized to capture data such as distances and heights of different points

relative to a base surface (Figure 2a). The coordinates of the desired stations were extracted from Google earth and recorded in GPS[1] (Figure 2b).The beach profiles were surveyed with a theodolite, leveling instruments, and graded stave in combination with a marine compass [23]. The beach profiles extend to a depth of 8 meters, which is approximately 1000 meters from the shoreline. As suggested by Emery (1961), a water depth gauge board was used in the initial part of the beach profiles, while a depth sounder (Figure 2c) was used in deeper waters (up to 8 m). The measurements were referenced to a fixed criterion on land (benchmark).

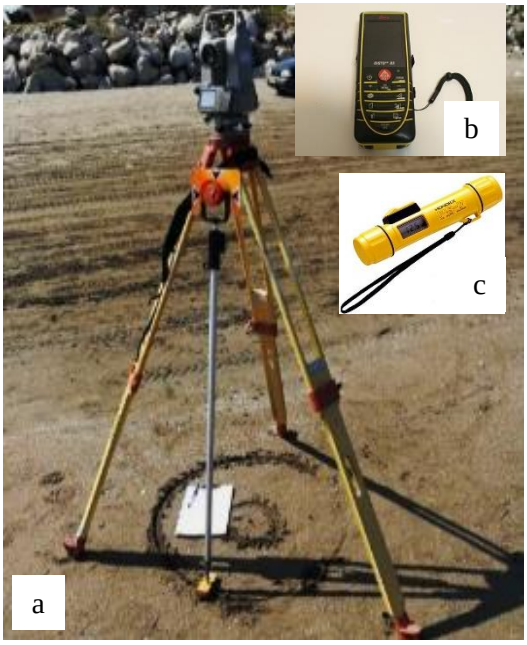

Figure 2. Theodolite mapping camera (a), GPS (b) and depth sounder (c)

The base level was considered consta nt during the measurement period in both beaches. In the sea, 19 stations in Babolsar and 17 stations in Nowshahr were considered to measure water depth (Figure 3a, b). The first and second stations were regarded at the distances of 10 and 30 meters from the shoreline, respectively. The distance between two consecutive stations in this region was 30 meters from a distance of 30 to 300 meters to the sea, and the distance between two consecutive stations was 100 meters from 300 meters to deep zone (closure depth). Based on the obtained depth measurement data, seasonal transverse profiles and mean (equilibrium) profile of Babolsar and Nowshahr beaches were plotted. In the present study, due to the seasonality of the measurements, the average seasonal data of significant wave height related to each of the cross sections of the study area was used. Therefore, in order to calculate the closure depth according to Equation (1), the significant wave height data were received from the Ports and Maritime Organization related to Babolsar and Nowshahr regions during four seasons, (www. Pmo.ir).

$$h_c = 6.75\bar{H}_s \quad (1)$$

Where $\bar{H}_s$ is the annual average of significant wave height in meters [24].

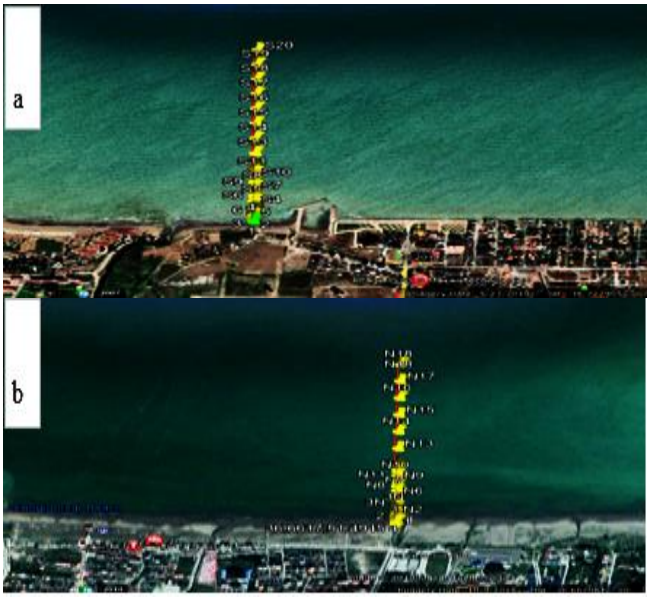

Figure 3. Beach profiles a) Babolsar, b) Nowshahr

At the same time, to investigate the type and percentage of bed sediments as well as to estimate the average diameter of the sediment, bed sediment samples were taken by Van Veen Grab at depths of about 0.5, 1.5, 3, and 5. They were transferred to the laboratory for granulation (Figure 4a, b, c, d).

Figure 4. Instruments for measuring sediments a) Van Veen Grab, b) Oven, c) Shaker and d) Laboratory Scale

First, the sediment samples were washed with oxygenated water to separate from the excess material, and then the samples were dried in an oven at 105 ° C for 24 hours. Then, Shaker was used to investigate the granulation. In this regard, sieves with mesh numbers of 30, 60, 100, 200 and 500 with diameters of 600,

[1] Global Positioning System

250, 150, 75 and 25 micrometers, respectively, were used. Sediment samples were sieved for 15 minutes by Shaker. Finally, the residual weight of sediments on each sieve was measured. Gradistat statistical software was used to calculate the type and percentage of bed sediments and also to estimate the median diameter of the sediments [25]. For this purpose, the diameter of the holes of each sieve, and the weight remaining on each sieve (in terms of grams), were given to the software as input data.

3. Results

3.1. Granulation of bed sediments

Using the output data of Gradistat statistical software, the average percentage of bed sediments during the four seasons at the desired depths were calculated (Figure 5). According to the sediment percentages in Babolsar and Nowshahr regions, from the nearshore to the deep zone, in most cases, coarse and medium sand nearshore had a higher percentage than the deep zone. In fact, with increasing depth, the percentage of fine-grained sediments, including very fine sand and clay increased, while coarse and medium sands had a decreasing trend. Because waves and sea currents play a key role in sediment transport, the motion of a particle of sand is affected by the forces acting on it. If the forces are not strong enough to push the particles out of position, then the particle will not move. In fact, ocean currents have the ability to carry sediments that are smaller in diameter than other sediment grains. Thus, smaller diameter sediments are transported away from the coast and only larger diameter sediments remain nearshore [1]. As a result, sediments in the offshore portion are often softer than nearshore sediments. According to the calculations of the type and percentage of sediments, the average percentage of sediments in autumn, winter, spring and summer is calculated in Table 1. In both east and west stations, the predominant type of bed sediments is fine sand, and the lowest percentage of bed sediments is allocated to the silt. According to obtained data related to the significant wave height (www. pmo.ir), the closure depth was calculated in Babolsar and Nowshahr (Table 2). Then, in order to investigate the changes in beach profiles in the desired stations, according to the measured data and closure depths, the mean (equilibrium) profile was extracted from different seasons.

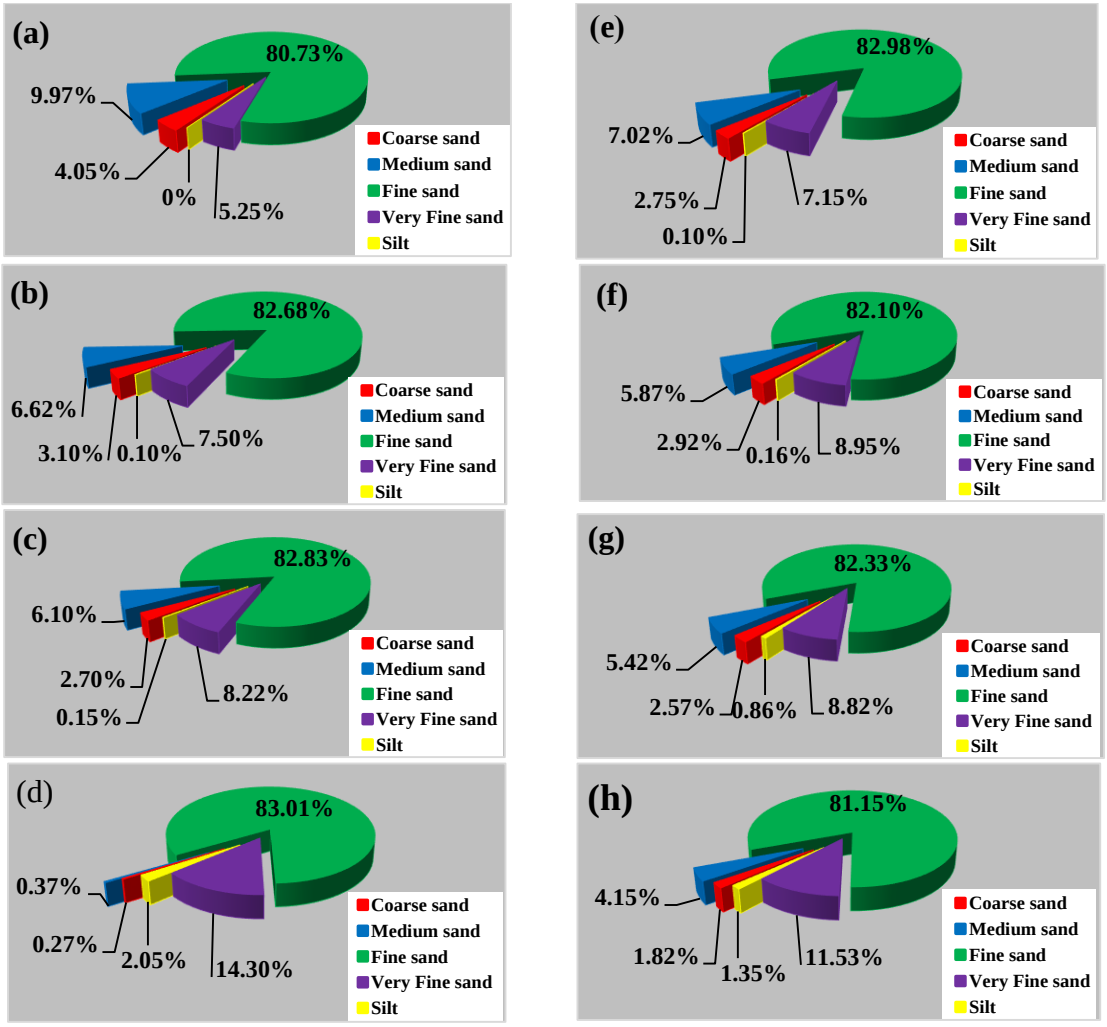

Figure 5. Comparison of the average percentage of bed sediments at depths (a: 0.5 m) (b: 1.5 m) (c: 3 m) (d: 5 m) in Babolsar and depths (e: 0.5 m) (f: 1.5) (g: 3 m) (h: 5 m) in Nowshahr.

Table 1. Average percentage of sediments in autumn, winter, spring and summer

		Average				
		Coarse sand (%)	**Medium sand** (%)	**Fine sand** (%)	**Very Fine sand** (%)	**Silt** (%)
Babolsar	Autumn	1.8	4.3	82.7	11	0.36
	Winter	2.97	3.7	83.75	9.9	1.6
	Spring	2.25	3.67	88.85	4.85	1.5
	Summer	4.1	11.4	74.27	9.35	1.7
Nowshahr	Autumn	2.55	4.75	75.47	16.22	1
	Winter	2.2	4.97	88.82	3.67	1.2
	Spring	1.65	3.05	92.75	2.15	0.5
	Summer	3.67	9.67	71.45	14.42	0.5

Table 2. Closure depth related to the beaches of Nowshahr and Babolsar in four seasons

	Nowshahr				Babolsar			
	Autumn	**Winter**	**Spring**	**Summer**	**Autumn**	**Winter**	**Spring**	**Summer**
$\bar{H}_s\,(m)$	0.791	0.760	0.741	0.707	0.859	0.771	0.681	0.743
$h_c\,(m)$	5.33	5.13	5	4.77	5.79	5.20	4.59	5.01

3.2. Babolsar beach profiles

Based on the field data, according to Figure 6, the desired profiles were drawn during the four seasons. In nearshore, from the shoreline to a distance of about 450 meters, several bars and berms are observed at different depths that have been changed during different seasons. In fact, most of the seabed changes in each season, compared to other seasons, occur in nearshore due to the direct effect of waves on the seabed. In fact, in these regions, due to the decrease in depth and the subsequent process of breaking waves and the impact of their energy on the seabed, beach sediments are eroded and transported by waves and sea currents in different directions. As a result, erosion and deposition occur more intensively nearshore, which is one of the reasons that has causes of the deformation of the seabed in different seasons. According to studies conducted to compare the two profiles of autumn and winter, the winter profile is eroded from a distance of 100 to 250 meters from the shoreline compared to the autumn due to the number of stormy days in winter. Hence the eroded sediments settled in the distance of 300 to 400 meters, and the depth has decreased compared to autumn. Because in winter, the bars and berms were eroded at a distance of 100 to 250 meters due to the process of breaking waves and turbulence, and sediments were transported to the sea (deeper zone), these sediments eventually interfered with the sediments transported to the beach and caused the formation of a wide berm with a length of 100 meters at a depth of 3.5 meters in winter. In winter, the energy owing to breaking waves increased due to more stormy days and as a result, the eroded sediments were transferred to the sea by return currents. In the surf zone, they collided with sediments that had transferred from the sea to the shore and formed bars. In the spring, the beach profile was eroded at a distance of 100 to 200 meters and also at a distance of 350 meters to deep zone, and then the eroded sediments were transported to the sea. As a result, the depth changes had an increasing trend compared to winter. In summer, due to the low height of the waves compared to spring, sediments were gradually transferred from offshore portion to nearshore, so that they settled at distances of 10 to 50 meters as well as 90 to 250 meters, and during the deposition process, depth changes have been decreasing compared to spring. In summer, due to the prevailing waves with small wave heights, sediments were gradually transferred from the offshore portion to the nearshore, and bars and berms were formed in these regions because of the energy reduction due to breaking waves. So, from a distance of 450 meters to the coast, due to the reduction of the impact of the waves on the seabed and the consequent reduction of sediment transport rate, slight changes have occurred in the beach profile. In order to investigate the variation in the profiles of different seasons compared to the mean (equilibrium) profile (Figure 6), the beach profile has a berm and bar, in autumn, at distances of 100 to 200 meters from the shoreline compared to the mean profile. In winter, the depth has decreased at a distance of 300 to 400 meters due to erosion and sediment transfer away from the beach, in spring, the beach profile was eroded at a distance of 100 to 210 meters from the mean profile. Finally, in summer, the erosion process has occurred based on the mean profile at a distance of 250 to 600 meters from the shoreline. These sediments are gradually transferred by waves to nearshore, so that the bars have been created due to the deposition of sediments transferred to these regions at the distances of 100 and 190 meters. So, most seabed changes have occurred nearshore, while in deeper zone, seasonal beach profiles have changed slightly compared to the mean profile due to reduced sediment transport. The mean profile has also

a berm at a distance of 30 to 60 meters at a depth of 0.5 meters and the profile slope equal to 0.018 at a distance of 60 to 150 meters and a bar at a distance of 200 meters.

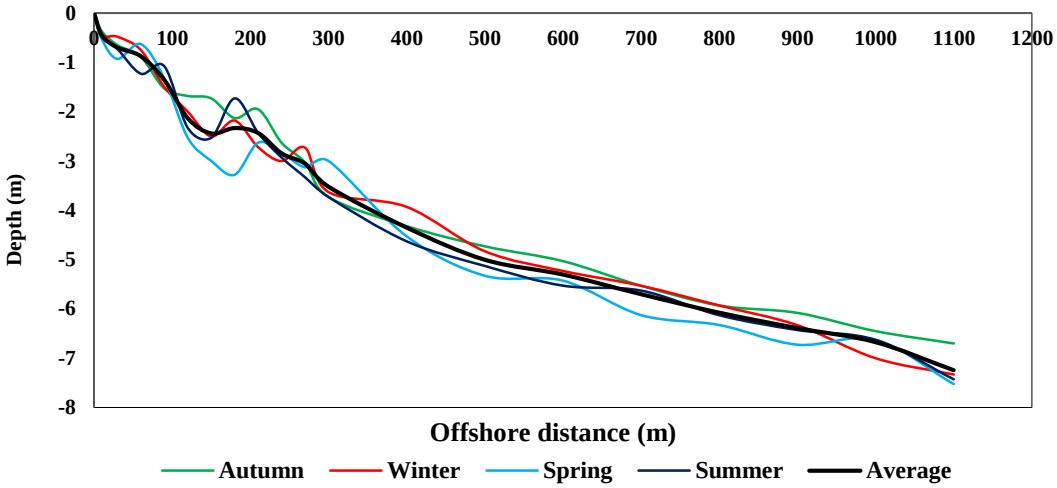

Figure 6. Babolsar beach profiles measured in four seasons (2018-2019)

3-3 Nowshahr beach profile

Based on the depth measurements performed during the study period (Figure 7), a 100-meter-wide berm was observed at a distance of 400 to 500 meters from the shoreline. Most of the seabed changes occurred in the form of bars and berm movement at a distance of 100 to 550 meters from the shoreline in the depth range of 1 to 5 meters, due to the effect of waves on the seabed in this region. In considering the changes of the bed in different seasons, in winter, the process of breaking the wave has occurred more intensively nearshore and sediments have transferred to the beach due to stormy conditions and increasing wave height. The depth increased due to the erosion of sediments compared to autumn at a distance of 180 to 250 and 390 to 510 meters. Finally, these eroded sediments settled at distances away from the beach. In spring, compared to winter, the depth has increased from the shoreline to a distance of 250 meters owing to erosion and transfer of sediments to the beach. In summer, the sediments gradually transferred from the deep zone to nearshore due to the decrease in the average significant wave height compared to spring, so that they settled from the shoreline to a distance of 170 m, and the depth changes have had decreasing trend compared to the spring. Also, a bar has been formed at a distance of 250 meters due to deposition. The profiles almost overlap from a distance of about 550 m to the deep zone during the four seasons, which indicates a reduction in the impact of the waves on the seabed and from there, a reduction in the erosion and deposition process. Then, the seabed changes were examined in relation to the mean profile, which was the result of transfer and displacement of sediments during different seasons. In autumn, the depth has decreased compared to the mean profile up to 120 meters from the shore, and also due to the bar created at a distance of 200 meters. In winter, the beach profile is eroded from a distance of 50 to 120 meters from the shoreline, compared to the mean profile, and the eroded sediments are moved to a deeper zone. However, in summer, the depth has decreased at a distance of 150 meters from the shoreline compared to the mean profile, due to the sediment transfer to nearshore. The mean profile from the shoreline to a distance of 150 meters has the profile slope of 0.014 and a berm at a distance of 190 to 210 meters from the shoreline. The mean profile slope at a distance of 290 to 400 meters is equal to 0.011. There is also a berm 150 meters long at a distance of 400 to 550 meters from the shoreline. Changes in sea level in different seasons has been another factor in changes in seabed. Measurements recorded by Theodolite mapping camera, used record shoreline changes, show shoreline movement is affected by changes in sea level. According to the results obtained in Babolsar and Nowshahr in autumn, due to the decrease in river inflows, a period of decreasing sea level was observed. In winter it remains at the same level with slight changes. Subsequently, because of the increase in the inflow of rivers including the Volga into the Caspian Sea, the increase in sea level began in early spring and has decreased in late summer. Therefore, it can be said that in addition to sea waves and currents, changes in water level have also played an important role in the movement of sediments and consequently changes in the seabed. By calculating the profile slope during the four seasons in the studied area (Figure 8), the profile slope of Babolsar (eastern areas) is less than Nowshahr (western areas). This was related to factors such as grain size and the intensity of the sea currents. As can be observed in Table 2, the median diameter of the bed sediment particles decreased from west to east, which was due to the increase in the percentage of

fine-grained sediments in the eastern regions compared to the western regions.

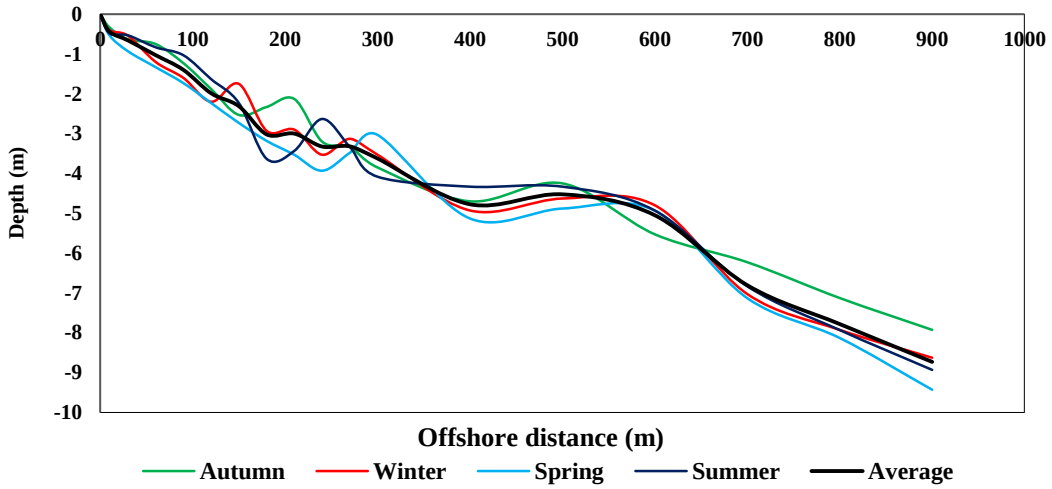

Figure 7. Nowshahr beach profiles measured in four seasons (2018-2019)

In fact, due to the weakening of sea currents in the west to east direction, finer sediments are transported by sea currents, so that their percentage has increased in the eastern regions. As a result, due to the existence of weak sea currents and fine-grained sediments, the possibility of deposition has increased in Babolsar more than Nowshahr, following which the profile slope has decreased.

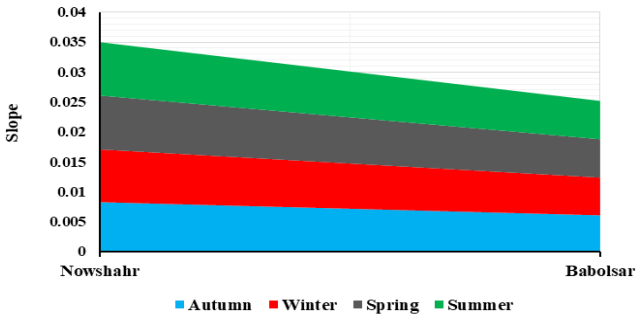

Figure 8. Bed slope changes of Babolsar and Nowshahr beaches in four seasons

4. Conclusion

Changes in beach profile shape occur as a result of changing wave conditions, which can be due to a single storm of unusual magnitude, or seasonal changes in repeated storm intensity. According to the results, the maximum change in the beach profile during different seasons have occurred in nearshore. So that the most changes in the seabed in Babolsar and Nowshahr have been observed at distances of about 450 and 550 meters from the coastline, respectively. In nearshore, following the process of breaking the waves due to the decrease in depth, the energy caused by breaking waves was transferred to the body of water, which eventually caused turbulence in these regions. Also, the process of erosion and deposition more intensely occurred during the seasons in the nearshore than in the offshore portion. In fact, most of the sediment movement and transfer takes place up to the closure depth, and the seabed, due to the minimal impact of the waves on the seabed, has not changed much from this depth to the offshore. The bed profiles of Babolsar and Nowshahr were compared with the results of other studies, including a study conducted by Ataei et al. (2014) in the Caspian Sea. Due to the topography and slope of the seabed, the beach profile had a good compatibility in the eastern regions with the Babolsar profile in the present study. Several bars and berms had been seen at a distance of about 450 meters from the shoreline, and in the depth between 0.5 to 5 meters. In fact, most of the seabed changes occurred up to a distance of about 450 meters from the shoreline, and Babolsar seabed had not changed much over years from this distance to the deep zone. But the Nowshahr beach profile was different in comparison to the Tonekabon seabed in the western regions, due to its wide berm in the bed. By studying the type and percentage of bed sediments in Babolsar and Nowshahr, fine sand has the highest amount with an average of 82.39% and 82.12%, respectively. According to the studies conducted in the two study areas, from nearshore to far offshore, the percentage of fine sediments has increased. In Babolsar (Nowshahr), at a depth of 0.5 meters, very fine sand was 5.25% (7.15%) and silt to 0% (0.10%), and with increasing depth to 5 meters, the very fine sand and silt are 14.30% (11.53%) and 2.5% (1.35%), respectively. In fact, sea currents returning to the sea are capable of carrying fine-grained sediments. Therefore, according to the results, the topography and the amount of bed changes due to the process of erosion and deposition during the seasons are different in the two study areas. This is related to various factors such as grain size and bed slope. According to studies, the median diameter

of sediments in the eastern regions has decreased compared to the western regions. This indicates the transfer of Caspian Sea sediments from west to east. In fact, in the western regions, due to strong sea currents and relatively coarse-grained sediments from the rivers of western Mazandaran, as well as human activities in those regions, the coasts have sediments with larger diameters than the eastern regions. Finally, finer sediments are transported, due to the weakening of the sea currents in the west to the east, so that their percentage has increased in the eastern regions. Also, the slope of the seabed has decreased in the eastern regions relative to the western regions due to the type and size of sedimentary grains and the effects of flow. Because of the weak flow and fine-grained sediments in the eastern regions, sediments settle and the depth decreases. As a result, the slope of the seabed has decreased in the eastern regions. The mentioned factors have caused differences in the intensity of erosion and sedimentation, followed by differences in the shape of the bed in the two beaches of Babolsar and Nowshahr during different seasons. Furthermore, considering the changes in coastal profiles during different periods, determining an equilibrium profile is important in the long-term study of beach profiles.

5. References

[1] Dean, R. G. and Dalrymple, R. A., (2004), *Coastal processes with engineering applications*, Cambridge University Press, 489p.

[2] Pan, Y., Kuang, C., Zhang, J., Chen, Y., Mao, X., Ma, Y., Zhang, Y., Yang, Y., Qiu, R., (2017), *Post nourishment evolution of beach profiles in a low-energy sandy beach with a submerged berm*, Journal of Waterway, Port, Coastal, and Ocean Engineering, 143(4): 05017001.

[3] Wilson, K. C., (1966), *Bed-load transport at high shear stress*, Journal of the Hydraulics Division, 92(6): 49-59.

[4] Watanabe, A., (1982), *Numerical models of nearshore currents and beach deformation*, Coastal Engineering in Japan, 25(1): 147-161.

[5] Van Rijn, L. C., (1993), *Principles of sediment transport in rivers, estuaries and coastal seas*, Aqua Publications, Amsterdam, 690p.

[6] Ozkan-Haller, H. T., Brundidge, S., (2007), *Equilibrium beach profile concept for Delaware beaches*, Journal of Waterway, Port, Coastal, and Ocean Engineering, 133(2): 147-160.

[7] Lopez, I., Aragones, L., Villacampa, Y., (2016), *Analysis and modelling of cross-shore profile of gravel beaches in the province of Alicante*, Ocean Engineering, 118: 173-186.

[8] Bruun, P., (1954), *Coast erosion and the development of beach profiles*, US Beach Erosion Board.

[9] Dean, R. G., (1991), *Equilibrium beach profiles: characteristics and applications*, Journal of Coastal Research, 7(1): 53-84.

[10] Mangor, K., (2001), *Shoreline Management Guidelines*, DHI-Water and Environment, 232p.

[11] Aragones, L., Serra, J. C., Villacampa, Y., Saval, J. M., Tinoco, H., (2016), *New methodology for describing the equilibrium beach profile applied to the Valencia's beaches*, Geomorphology, 259: 1-11.

[12] Lopez, I., Aragones, L., Villacampa, Y., Navarro-Gonzalez, F. J., (2018), *Gravel beaches nourishment: Modelling the equilibrium beach profile*, Science of the Total Environment, 619: 772-783.

[13] Mansoury, D., Sadrinasab, M., (2013), *Investigation of Bottom Sediment Distribution in Noor Marine Area*, Fifth National Conference on Offshore Industries, Sharif University of Technology, Tehran.

[14] Roradeh, H., Lorestani, Q., Etemadi, F., Valikhani, S., (2013), *Simulation of wave dynamics and sand transfer in the Caspian Sea coasts (Gorgan Bay)*, Quantitative geomorphological research, 2(2), p. 1-18.

[15] Khoshravan, H., Rohanizadeh, S., Malek, J., Nejadgholi, G., (2012), *Caspian Sea southern coasts zoning on the basis of sedimentary morphodynamical indicators*, Earth and Space Physics, 37(3): 1-15.

[16] Boggs, S. r., (2005), *Principles of sedimentology and stratigraphy*, Prentice Hall: New Jersey.

[17] Ataei, S., Adjami, M., Lashteh Neshaei, M. A., Haghighifar, M., (2014), *Classification of equilibrium beach profile in the Caspian Sea*, International Geoinformatics Research and Development Journal, 6: 8-18.

[18] Voropaev, G. V., (1986), *The Caspian Sea; hydrology and hydrochemistry*, Moscow, Nauka, 262p.

[19] Lahijani, H., (1997), *Riverine Sediments and stability of Iranian coast of the Caspian Sea*, PhD Thesis, Russian Academy of Science, 120 p.

[20] Rychagov, G. I., (1997), *Holocene oscillations of the Caspian Sea and forecasts based on paleogeographical reconstructions*, Quaternary International, 41(42): 167-172.

[21] Leroy, S. A. G., Marret, F., Gibert, E., Chalié, F., Reyss, J. L., Arpe, K., (2007), *River inflow and salinity changes in the Caspian Sea during the last 5500 years*. Quaternary Science Reviews, 26(25-28): 3359-3383.

[22] Zereshkian, S., and Mansoury, D., 2020. *Evaluation of ocean thermal energy for supplying the electric power of offshore oil and gas platforms*, Journal of the Earth and Space Physics, Vol. 46, No. 2, 331-345.

[23] Frihy, O.E., Iskander, M.M., Badr, A.E. and Lotfy, M. F., (2004), *Effects of shoreline and bedrock irregularities on the morphodynamics of the Alexandria coast littoral cell, Egypt*, Geo-Mar Lett .24: 195–211 DOI 10.1007.

[24] Houston, J. R., (1995), *Beach-fill volume required to produce specified dry beach width*, Coastal Engineering Technical Note, 11-32.

[25] Blott, S. J., Pye, K., (2001), *GRADISTAT: a grain size distribution and statistics package for the analysis of unconsolidated sediments*, Earth Surface Processes and Landforms, 26(11): 1237-1248.

INTERNATIONAL JOURNAL OF
COASTAL & OFFSHORE ENGINEERING
IJCOE Vol.7/No. 1/Winter 2022 (43-49)

Available online at: www.ijcoe.org

Comparison between different wave runup level prediction formulas based on the wave breaking type

Behrooz Tadayon[1], Hamid Dehghani[2], Cyrus Ershadi[3*]

[1] *M.Sc Graduate, Civil Engineering Department, Faculty of Engineering, University of Hormozgan, Hormozgan, Iran; b.tadayon.stu@hormozgan.ac.ir*
[2] *M.Sc Student, Civil Engineering Department, Faculty of Engineering, University of Hormozgan, Hormozgan, Iran; hamid.dehghani.stu@hormozgan.ac.ir*
[3*] *Assistant Professor, Civil Engineering Department, Faculty of Engineering, University of Hormozgan, Hormozgan, Iran; cyrusershadi1@yahoo.co.uk*

ARTICLE INFO

Article History:
Received: 13 Jun. 2021
Accepted: 07 Jan 2022

Keywords:
wave runup
runup level
wave breaking type
Iribarren number

ABSTRACT

In this study, the performance of some models for predicting the wave runup level is investigated. To do so, they are compared with each other over a database of 1390 field and laboratory data points. This comparison has actually two aims: The first one is to investigate the models using all data points and the second one is to consider the influence of wave breaking type on the accuracy of the formulas. The latter goal is achieved by dividing the data points based on the type of wave breaking using the Iribarren number. It is also important to mention that most of the models used here for comparison have been optimized by Power et al. in 2019 so that more accurate outcomes would be obtained by them. These models depend on certain wave and beach parameters, including wave height, wave length, wave period, and seabed slope. The results of the comparison have been demonstrated using several statistical characteristics (e.g. RMSE, R^2, etc.) so that a good understanding could be obtained from the behavior of each formula. At first, when the type of wave breaking is not considered in the comparison and all data points are used, the optimized formula derived from both studies of Holman and Atkins et al. seems to be the most accurate one with the least prediction error. Then, when the data points are divided into groups based on the wave breaking type (i.e. spilling and plunging), different outcomes are achieved. The optimized formula proposed by Poate et al. has almost the best performance in the case of spilling type and the formula of Power et al. is the most accurate one when considering the plunging type, showing that the type of wave breaking plays an important role in the accuracy of wave runup level prediction formulas.

1. Introduction

The landward propagation of waves contains several stages and wave runup is the final one. In other words, the final landward position a wave can reach before changing its movement to a seaward direction can be determined by runup. This process is actually a combination of swash and wave generated setup [1]. Therefore, the runup region is considered as an important area due to the fact that several processes such as coastal erosion, sediment exchange near shorelines and overtopping from coastal structures are directly affected by the runup level.

In order to express the runup level (i.e. the maximum elevation of water-surface measured from the still-water level (SWL) in a vertical manner [2]), several statistical measures exist in the literature [3]. The most common ones are R_{max} (which indicates the maximum elevation achieved by a single runup level during a specific period of time) and $R_{2\%}$ (which indicates an elevation exceeded by 2% of all runup events during a specific period of time) [4].

During the previous decades, several empirical models have been proposed for predicting the wave runup level [4]. These models are based on similar parameters related to wave and beach conditions such as wave height, wave length, wave period, and seabed slope. Moreover, wave breaking conditions are among the factors that have influence on the complexity of wave runup [5]. There exists a parameter by which the type of breaking waves (e.g. spilling, plunging, etc.) can be determined. This parameter is called the surf similarity

parameter [6] (also known as the Iribarren number) and is denoted by ξ_o, which is:

$$\xi_o = \frac{\tan\beta}{\sqrt{H_o/L_o}} \quad (1)$$

where, $\tan\beta$ indicates the seafloor slope, H_o denotes the offshore wave height and L_o is the offshore wave length. It is worthwhile to mention here that when waves break, a significant amount of energy is released which affects the runup level [5].

In this paper, it is tried to investigate the accuracy of some wave runup level prediction models using a large field and laboratory wave database. These models have been mentioned as accurate ones for predicting $R_{2\%}$ in the literature and most of them have been optimized by Power et al. in 2019 [4] so that their accuracy would be increased further. The database used here has been divided based on the type of wave breaking and comparisons are carried out between the results of different prediction models using all data points as well as data points related to certain breaking types, so that the accuracy of these formulas in predicting wave runup level based on the breaking type has also been examined.

2. Materials and methods

The wave runup prediction models that have been investigated here are among the most accurate ones compared to other formulas, according to the literature [4]. These models have been obtained by different researchers, including Holman [1], Vousdoukas et al. [7], Poate et al. [8], Atkinson et al. [3], Power et al. [4] and Van der Meer and Stam [9]. It should be mentioned that in the study of Power et al. [4], along with proposing a new model for predicting wave runup level, some other relationships (which are also used in this paper) have been modified with optimized parameters to improve their accuracy. In Table 1, all of the relationships that are used in this study are provided.

Table 1: Empirical wave runup level prediction relationships based on the optimized parameters (except for the formula proposed by Van der Meer and Stam [9]) proposed in Ref. [4]

Authors	Relationships
Holman (1986) [1] / Atkinson et al. (2017) [3]	$0.50\tan\beta\sqrt{H_s L_p} + 0.70 H_s$
Van der Meer and Stam [9]	$0.96 H_s \xi_o \cdots$ for $\xi_o \le 1.5$ $1.17 H_s (\xi_o)^{0.46} \cdots$ for $\xi_o > 1.5$
Vousdoukas et al. (2014) [7]	$0.005\beta\sqrt{H_s L_p} + 4.563\tan\beta H_s + 0.458$
Poate et al. (2016) [8]	$0.309\tan\beta^{0.48} T_p H_s$
Power et al. (2019) [4]	See the Appendix

As seen in Table 1, the models depend on different parameters, which are $\tan\beta$ (seabed slope), H_s (wave height), L_p (peak wave length), T_p (peak wave period) and r (hydraulic roughness length). It should be noted that the wave length considered here is actually the offshore wave length and it can be obtained using the Airy theory, in which the relation for calculating the offshore wave length is $gT_p/2\pi$, where g denotes the gravitational constant. There are also other wave runup level prediction formulas that use further parameters, such as D_{50} (grain size), but they are not investigated in this study. The hydraulic roughness length can be obtained using the grain size for the field data and there are some standard tables to find the value of this parameter when investigating the laboratory data (more information is available in Ref. [4]). Moreover, after carrying out the optimization process by Power et al. [4] and modifying the models, the formulas proposed by Holman [1] and Atkinson et al. [3] have become a single formula with optimized constants, as shown in this Table 1.

The wave runup data base used in in this study contains 1390 field and laboratory data points (Refs. [3, 8, 10-14]). These data points were gathered from different studies, which are given in Table 2, along with the range of the desired parameters in each study.

Table 2: The available compiled field and laboratory data

Dataset	H_s(m)	$\tan\beta$	T_p(s)	Data points
Field				
Stockdon et al. (2006) [10]	0.350-4.080	0.009-0.160	3.70-17.00	491
Poate et al. (2016) [8]	1.040-7.170	0.088-0.290	4.80-23.70	663
Atkinson et al. (2017) [3]	0.550-1.190	0.051-0.190	6.40-9.30	71
Nicolae Lerma et al. (2017) [11]	3.090-6.070	0.060-0.081	13.30-16.30	17
Laboratory				
Mase (1989) [12]	0.026-0.110	0.033-0.200	0.81-2.50	120
Baldock and Huntley (2002) [13]	0.019-0.066	0.100	1.03-1.98	16
Howe (2016) [14]	0.820-0.910	0.167	9.80-13.70	12

In order to divide the data points based on the wave breaking type, the criterion proposed by Battjes [6] has been applied. This criterion is based on the Iribarren number and using this number, the breaking type can be categorized as spilling, plunging, surging, or collapsing. In the following equation, different ranges of the Iribarren number for each wave breaking type are given:

$$\begin{cases} \text{spilling} & \text{if } \xi_o \le 0.5 \\ \text{plunging} & \text{if } 0.5 < \xi_o \le 3.3 \\ \text{surging/collapsing} & \text{if } \xi_o > 3.3 \end{cases} \quad (2)$$

In order to investigate the accuracy of different models shown in Table 1 in predicting the wave runup level, the calculated level ($R_{2\%(c)}$) is compared with the observed one ($R_{2\%(o)}$) based on the dataset shown in Table 2. The statistical characteristics shown in Table 3 are used for examining the results of this comparison. For more information about these characteristics and their concept, the interested reader may refer to Ref. [15]. It should be noted that in this table, $\bar{R}$ refers to the average value.

Table 3: The statistical characteristics used for comparing the results of this study

Characteristics	Relationships
Root mean square error (RMSE)	$\sqrt{\frac{\sum_{i=1}^{N}\left(R_{2\%(c),i}-R_{2\%(o),i}\right)^2}{N}}$
Coefficient of determination (R^2)	$\left[\frac{\sum_{i=1}^{N}\left(R_{2\%(c),i}-\bar{R}_{2\%(c)}\right)\left(R_{2\%(o),i}-\bar{R}_{2\%(o)}\right)}{\sqrt{\sum_{i=1}^{N}\left(R_{2\%(c),i}-\bar{R}_{2\%(c)}\right)^2}\sqrt{\sum_{i=1}^{N}\left(R_{2\%(o),i}-\bar{R}_{2\%(o)}\right)^2}}\right]^2$
Bias (B)	$\frac{\sum_{i=1}^{N}R_{2\%(c),i}-R_{2\%(o),i}}{N}$
Percentage relative error (E_{rel})	$\left\lvert\frac{\bar{R}_{2\%(c)}-\bar{R}_{2\%(o)}}{\bar{R}_{2\%(c)}}\right\rvert\times 100$
Absolute error (E)	$\left\lvert\bar{R}_{2\%(c)}-\bar{R}_{2\%(o)}\right\rvert$
Scatter index (SI)	$\frac{\text{RMSE}}{\frac{1}{N}\sum_{i=1}^{N}R_{2\%(b),i}}\times 100$

3. Results and discussion

In Tables 4-6, the results of comparing different wave runup prediction models (i.e. the ones optimized by Power et al. [4] as well as the model proposed in their study) in three cases of using all, spilling and plunging data points are provided. As it is understood from Table 4, the optimized formula derived from both studies of Holman [1] and Atkinson et al. [3] seems to be the most accurate one (RMSE=0.854m, B=0.005m, R^2=0.769, E_{rel}=0.233%, E=0.005m and SI=36.838%) when the type of wave breaking is ignored in the comparison and all data points are considered for the comparison. However, the results are different when considering the breaking type. In other words, for the case of spilling breaking type, the optimized formula of Poate et al. [8] seems to have the least error and almost acceptable performance (RMSE=0.585m, B=0.064m, R^2=0.665, E_{rel}=10.101%, E=0.064m and SI=101.965%) compared to the other formulas and when considering the plunging breaking type, the formula proposed by Power et al. [4] has the best performance (RMSE=0.779m, B=0.014m, R^2=0.804, E_{rel}=0.544%, E=0.014m and SI=31.184%). Therefore, it seems that the performance of these accurate models changes when the data points relating to specific breaking type are investigated, rather than a general group of data points in which the type of breaking is ignored. This issue complies with the concept of wave breaking as well. In other words, a significant amount of energy is released along with the wave breaking phenomena. Apart from several other factors, this amount is related to the type of breaking as well. Therefore, the runup level, which is influenced by the amount of the released energy, can be affected by the type of breaking waves. In order to show a better picture of the performance of the models when predicting the wave runup level, the scatter diagram of the observed vs. calculated value of the runup level of all models for the three cases (all, spilling, and plunging data points) are shown in Figures 1-3.

4. Conclusions

The level of wave runup plays a major role in many coastal issues (e.g. sediment transport, overtopping form structures, erosion, etc.) and being able to predict its value as accurate as possible is of significant importance. In this study, the performance of several wave runup level prediction models that have been optimized by other researchers and are considered as accurate formulas in this regard have been investigated. A database containing 1390 different field and laboratory data points was used here to apply a comparison between the models. In this comparison, two questions have been investigated; one, what is the general performance of each model when considering the whole database? and two, what is the effect of wave breaking type on the accuracy of each model? As for the answer of the first question, the optimized formula derived from the studies of Holman and Atkinson et al. was the most accurate one with the least error.

However, when the data points were divided based on the wave breaking type, different models became the almost most accurate ones (i.e. the optimized formula of Poate et al. for the case of spilling breaking type and the formula of Power et al. for the case of plunging one). Therefore, it is clear that the type of wave breaking has a direct influence on the accuracy of wave runup level prediction models and proposing different formulas based on the type of wave breaking seems to be a reasonable idea.

Table 4: Comparison between the calculated runup level and the observed one for all data points

Formula	$\bar{R}_{2\%(o)}$ **(m)**	$\bar{R}_{2\%(c)}$ **(m)**	RMSE **(m)**	B **(m)**	R^2	E_{rel} **(%)**	E **(m)**	SI **(%)**
Holman [1] / Atkinson et al. [3]	2.319	2.324	0.854	0.005	0.769	0.233	0.005	36.838
Van der Meer and Stam [9]	2.319	1.791	1.154	-0.528	0.700	29.475	0.528	49.746
Vousdoukas et al. [7]	2.319	1.574	1.341	-0.745	0.686	47.327	0.745	57.843
Poate et al. [8]	2.319	2.178	1.098	-0.141	0.719	6.483	0.141	47.360
Power et al. [4]	2.319	2.347	0.755	0.029	0.820	1.214	0.029	32.545

Table 5: Comparison between the calculated runup level and the observed one for spilling data points

Formula	$\bar{R}_{2\%(o)}$ **(m)**	$\bar{R}_{2\%(c)}$ **(m)**	RMSE **(m)**	B **(m)**	R^2	E_{rel} **(%)**	E **(m)**	SI **(%)**
Holman [1] / Atkinson et al. [3]	0.574	0.947	0.700	0.372	0.774	39.354	0.372	122.032
Van der Meer and Stam [9]	0.574	0.328	0.423	-0.246	0.721	75.092	0.246	73.750
Vousdoukas et al. [7]	0.574	0.681	0.419	0.107	0.665	15.762	0.107	73.072
Poate et al. [8]	0.574	0.639	0.585	0.064	0.665	10.101	0.064	101.965
Power et al. [4]	0.574	0.747	0.454	0.173	0.797	23.138	0.173	79.019

Table 6: Comparison between the calculated runup level and the observed one for plunging data points

Formula	$\bar{R}_{2\%(o)}$ **(m)**	$\bar{R}_{2\%(c)}$ **(m)**	RMSE **(m)**	B **(m)**	R^2	E_{rel} **(%)**	E **(m)**	SI **(%)**
Holman [1] / Atkinson et al. [3]	2.497	2.465	0.868	-0.032	0.757	1.314	0.032	34.7621
Van der Meer and Stam [9]	2.497	1.941	1.203	-0.557	0.634	28.674	0.557	48.187
Vousdoukas et al. [7]	2.497	1.665	1.402	-0.832	0.658	49.980	0.832	56.127
Poate et al. [8]	2.497	2.335	1.138	-0.162	0.704	6.956	0.162	45.550
Power et al. [4]	2.497	2.511	0.779	0.014	0.804	0.544	0.014	31.184

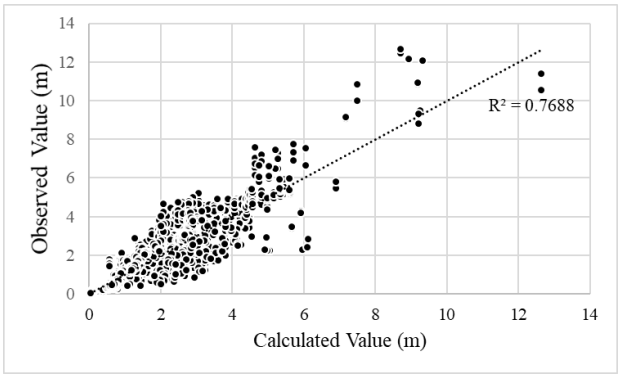

(a)

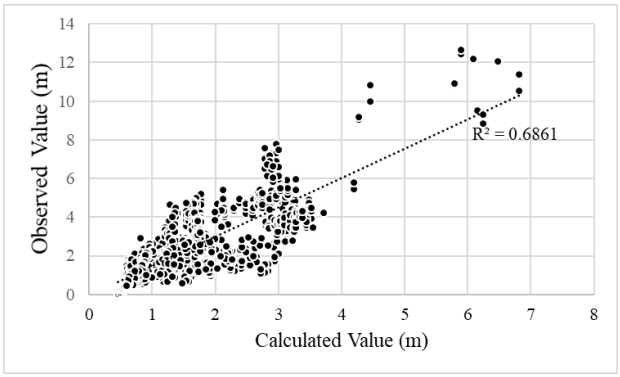

(b)

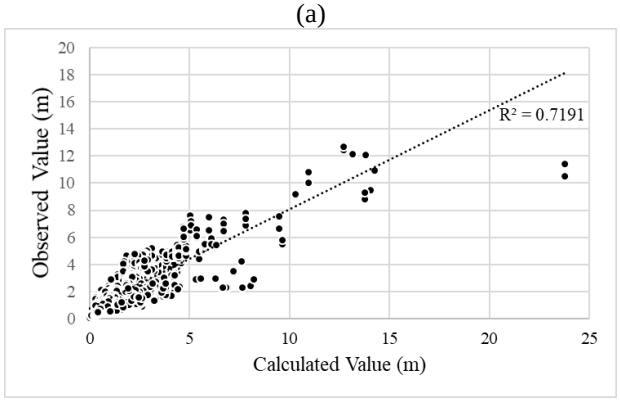

(c)

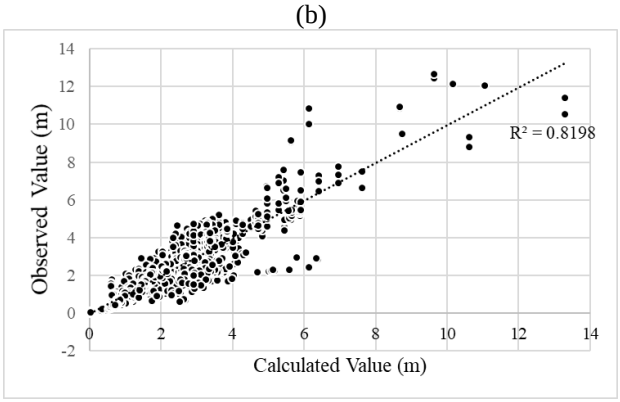

(d)

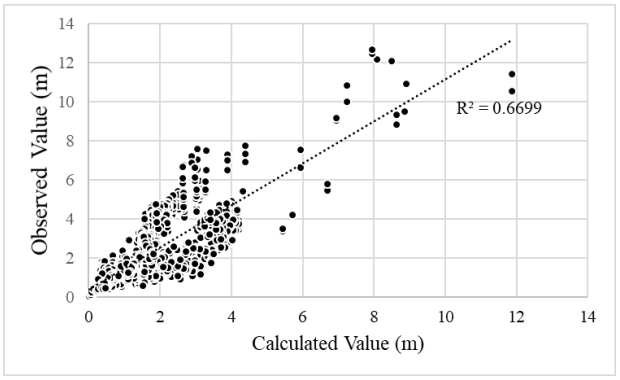

(e)

Figure 1. The scatter diagram of (a) Holman / Atkinson et al. formula (b) Vousdoukas et al. formula (c) Poate et al. formula (d) Power et al. formula (e) Van der Meer and Stam formula for all data points

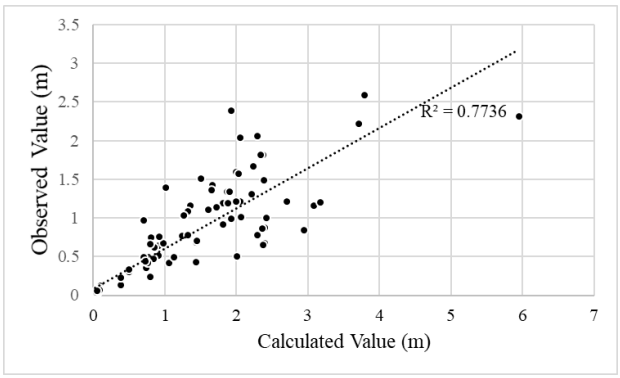

(a)

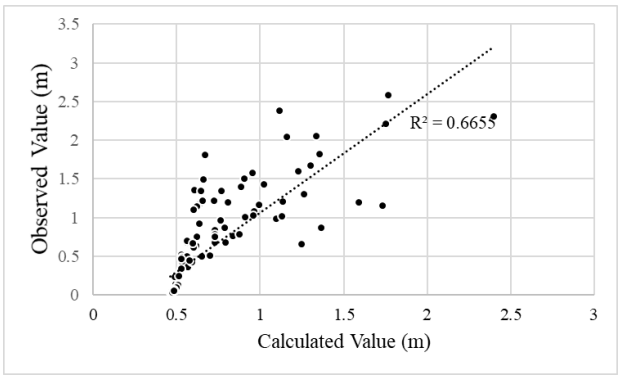

(b)

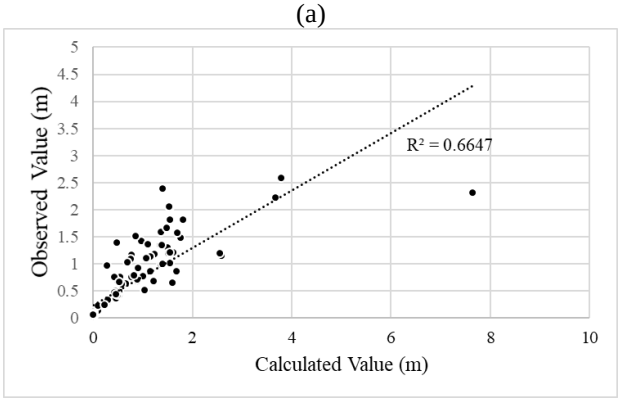

(c)

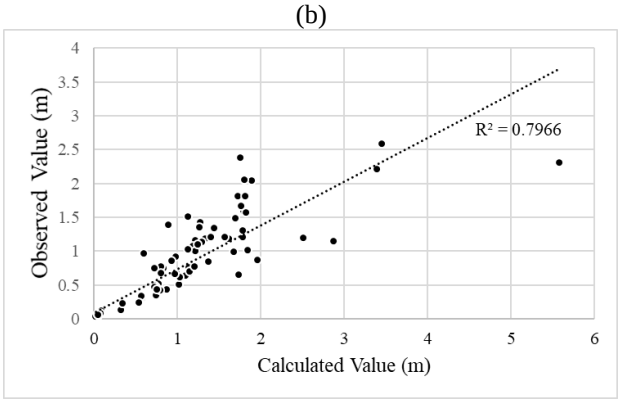

(d)

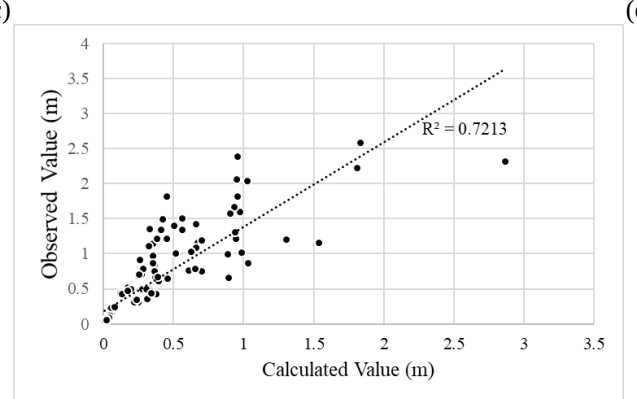

(e)

Figure 2. The scatter diagram of (a) Holman / Atkinson et al. formula (b) Vousdoukas et al. formula (c) Poate et al. formula (d) Power et al. formula (e) Van der Meer and Stam for spilling data points

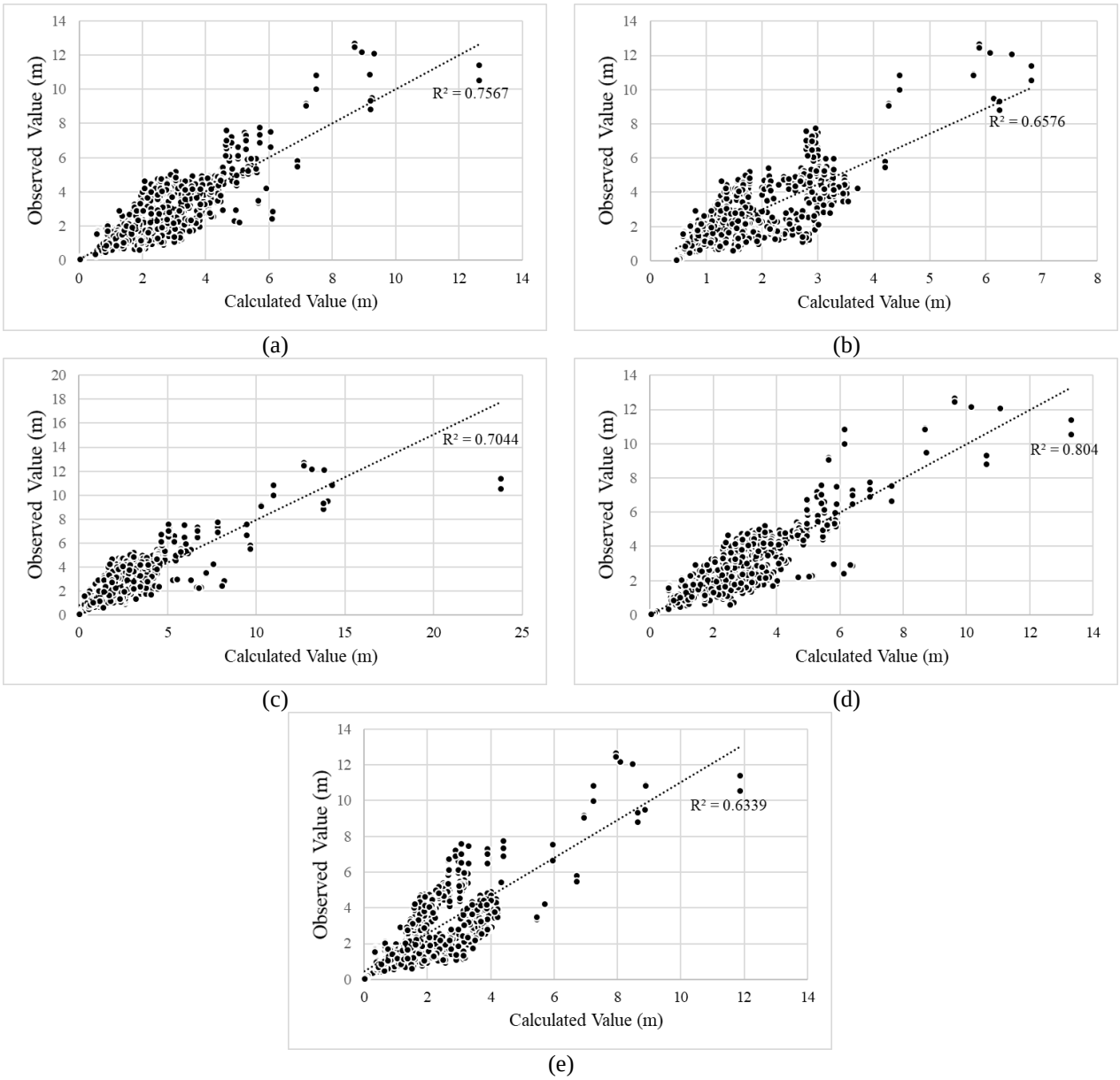

Figure 3. The scatter diagram of (a) Holman / Atkinson et al. formula (b) Vousdoukas et al. formula (c) Poate et al. formula (d) Power et al. formula (e) Van der Meer and Stam for plunging data points

5. Acknowledgment

The authors would like to appreciate Power et al. [4] for providing the necessary datasets for this study to be carried out.

6. References

[1] Holman, R.A., (1986), Extreme value statistics for wave run-up on a natural beach, Coastal Engineering, Vol.9(6), p.527-544.

[2] Burcharth, H.F., Hughes A.S., (2003), Fundamentals of Design, In Coastal Engineering Manual, Coastal Engineering Research Center, Vol.6, p.VI-5-i - VI-5-316.

[3] Atkinson, A.L., Power, H.E., Moura, T., Hammond, T., Callaghan, D.P., Baldock, T.E., (2017) Assessment of runup predictions by empirical models on non-truncated beaches on the south-east Australian coast, Coastal Engineering, Vol.119, p.15-31.

[4] Power, H.E., Gharabaghi, B., Bonakdari, H., Robertson, B., Atkinson, A.L., Baldock, T.E., (2019), Prediction of wave runup on beaches using Gene-Expression Programming and empirical relationships, Coastal Engineering, Vol.144, p.47-61.

[5] Khoury, A., Jarno, A., Marin, F., (2019), Experimental study of runup for sandy beaches under waves and tide, Coastal Engineering, Vol.144, p.33-46.

[6] Battjes, J., (1974), Surf similarity, Proceedings of the 14th International Conference on Coastal Engineering (Copenhagen, Denmark, ASCE), p. 1050–1061.

[7] Vousdoukas, M.I., Wziatek, D., Almeida, L.P., (2012), Coastal vulnerability assessment based on video wave run-up observations at a mesotidal, steep-sloped beach, Ocean Dynamics, Vol.62(1), p.123-137.

[8] Poate, T.G., McCall, R.T., Masselink, G., (2016), *A new parameterisation for runup on gravel beaches*, Coastal Engineering, Vol.117, p.176-190.

[9] Van der Meer, J.W., Stam, C.J., (1992) *Wave runup on smooth and rock slopes of coastal structures*, Journal of Waterway, Port, Coastal, and Ocean Engineering, Vol.118(5), p.534-550.

[10] Stockdon, H.F., Holman, R.A., Howd, P.A., Sallenger Jr, A.H., (2006), *Empirical parameterization of setup, swash, and runup*, Coastal engineering, Vol.53(7), p.573-588.

[11] Lerma, A.N., Pedreros, R., Robinet, A., Sénéchal, N., (2017), *Simulating wave setup and runup during storm conditions on a complex barred beach*, Coastal Engineering, Vol.123, p.29-41.

[12] Mase, H., (1989) *Random wave runup height on gentle slope*, Journal of Waterway, Port, Coastal, and Ocean Engineering, Vol.115(5), p.649-661.

[13] Baldock, T.E., Huntley, D.A., (2002), *Long–wave forcing by the breaking of random gravity waves on a beach*, Proceedings of the Royal Society of London. Series A: Mathematical, Physical and Engineering Sciences, Vol.458(2025), p.2177-2201.

[14] Howe, D., (2016), *Bed shear stress under wave runup on steep slopes*, Doctoral dissertation, Ph. D. Thesis, University of New South Wales, Sydney, Australia.

[15] Tadayon, B., Dehghani, H., Ershadi, C., (2019), *Recent Wave Breaking Prediction Formulas Evaluation Based On Compiled Laboratory Data*, International Journal of Coastal and Offshore Engineering, Vol.3(1), p.41-6.

Appendix

The wave runup level prediction model proposed by Power et al. [4] has been developed using gene expression programming (GEP). The relationship of this model is given below:

$R_{2\%} / H_s$ = (x2+(((x3.*3)/exp(-5)).*((3.*x3).*x3))) + ((((x1+x3)-2)-(x3-x2))+((x2-x1)-x3)) + (((x3.^x1)-(x3.^(1.0/3.0)))-(exp(x2).^(x1.*3))) + sqrt((((x3+x1)-x2)-(x2+log10(x3)))) + ((((x2.^2)./(x1.^(1.0/3.0))).^(x1.^(1.0/3.0)))-sqrt(x3)) + ((x2+((x3./x1).^(1.0/3.0)))+(log(2)-(1./(1+exp(-(x2+x3)))))) + ((sqrt(x3)-(((3.^2)+3).*(x2.^2))).^2) + ((((x3.*-5).^2).^2)+(((x3+x3).*x1)./(x2.^2))) + log((sqrt(((x2.^2)+(x3.^(1.0/3.0))))+((x2+3).^(1.0/3.0)))) + ((((x1./x3).*(-5.^2)).*(x3.^2))-log10((1./(1+exp(-(x2+x3)))))) + (x1.^x3) + exp(-((((x3./x1).^exp(4))+(exp(x3).^3)).^2))+ exp((log((x2-x3))-log(exp(-((-1+x1).^2))))) + ((sqrt(4).*(((x3./x2)-x2)-(0-x1))).^2) + (2.*((((-5.*x3)+x1).*(2-x3))-2)) + ((sqrt(4).*(((x3./x2)-x2)-(0-x1))).^2) + ((((-5+x1)-x2).*(x2-x3)).*((x1-x2)-(-4.^-5)))+ (exp(-((x2+(-5-x1)).^2))+((x2--5).*(x3.^2))) + sqrt(1./(1+exp(-((exp(x1)-exp(-((x3+x3).^2)))+((x1.^x3)-(x3.*4)))))) + ((exp(-((((exp(-(((sqrt(x3).*4)+(1./(1+exp(-(x2+2))))).^2))).^2)+x1).^2))).^3) (A.1)

where, x_1, x_2, and x_3 represent H_s / L_p, $\tan\beta$ and r / H_s, respectively.

INTERNATIONAL JOURNAL OF
COASTAL & OFFSHORE ENGINEERING
IJCOE Vol.7/No. 1/Winter 2022 (50-62)

Available online at: www.ijcoe.org

Probabilistic Seismic Assessment and Fragility Curves for Fixed Pile-Founded Offshore Platforms

Samira Babaei[1*], Rouhollah Amirabadi[2], Mahdi Sharifi[3]

[1] PhD Candidate, Department of Civil Engineering, University of Qom, Qom, Iran, S.Babaei@stu.qom.ac.ir*
2 Assistant Professor, Department of Civil Engineering, University of Qom, Qom, Iran, R.Amirabadi@qom.ac.ir
3 Assistant Professor, Department of Civil Engineering, University of Qom, Qom, Iran, M.Sharifi@qom.ac.ir

ARTICLE INFO

Article History:
Received: 15 Apr. 2021
Accepted: 01 Dec. 2022

Keywords:
Probabilistic Seismic Demand Model
Probabilistic Seismic Demand Analysis
Incremental Dynamic Analysis
Fragility Curve
Fixed Pile-founded Offshore Platform

ABSTRACT

Fixed pile-founded offshore platforms installed in the seismic-prone areas are exposed to the risk of earthquake-induced disastrous failure and costly operation interruption. Accordingly, the development of applied seismic evaluation methodologies for these infrastructures is a matter of utmost importance. In the context of performance-based earthquake engineering (PBEE), probabilistic seismic assessments of fixed pile-founded offshore platforms have been investigated, here. A three-dimensional (3D) finite element model of a recently installed platform located in the South Pars Oil and Gas field of the Persian Gulf has been made. Soil-pile-structure interaction, as well as dynamic site response effects, has been considered. Probabilistic seismic demand modeling (PSDM) has been employed to manifest the efficient and sufficient ground motion intensity measures (IMs) which can rigorously predict the structural engineering demand parameters (EDPs). Derived from probabilistic seismic demand analysis (PSDA), the superb results have been also evaluated by means of the predominantly used method of incremental dynamic analysis (IDA). On the other hand, the drawn findings contributed to representing the fragility curves of the fixed pile-founded offshore platforms. The demonstrated results are highly recommended to be considered in related research.

1. Introduction

With the development of the world's economy, the exploitation of marine resources has been paid more and more attention to. For this to be accomplished the offshore platform is considered as the main facility and its safety and serviceability are pivotal. The earthquake-induced responses and vibrations are categorized as one of the inevitable factors which threaten the platforms crew casualty, environmental disasters, production shutdown, and equipment damage. On the other hand, the earthquake unpredictability has made it much more difficult for the engineers to exactly estimate the seismic behavior of the complex structural systems.

Accordingly, seismic evaluations of offshore platforms have been the subject of research in many conducted studies [1-9]. Moreover, Jafari et al. presented evaluation of dynamic effects in the response of offshore wind turbines using incremental wind-wave analysis [10-13].

For a more precise and reliable result, the fragility analysis should be considered to the seismic evaluation of these structures. The fragility analysis is an operational and comparatively mature method [14-16], which is commonly utilized in conventional structures, such as steel moment-resisting frames [17-19], bridges [20–24], storage tanks [25], pile-supported wharves [26], dams [27], transmission towers [28] and gantry cranes [29] to combine the seismic uncertainties and structural uncertainties into the seismic assessment.

Yasseri and Ossei [30], presented the limit states associated with the fixed pile-founded offshore platforms and fragility curves generating six synthetic earthquakes. In 2017, The seismic vulnerability of a fixed offshore platform through development of fragility curves capturing the effects of ageing and corrosion deterioration has been assessed by Jahanitabar and Bargi [31]. Ajamy et al., worked on an analytical approach to develop seismic fragility curves for an existing fixed offshore platform located in Persian Gulf [32]. The sensitivity of a fixed offshore platform considering the uncertainty of various structural parameters under near-fault ground

motions have been studied by Zarrin et al. [33]. Furthermore, the effects of ground motions sample size on seismic fragility analysis of offshore jacket platforms using Genetic Algorithm have been evaluated by Abyani et al. [34]. However, the latter ones [31-34] have used limit states based on FEMA [35-37] and ASCE [38] considerations which reflect the ordinary building structures requisitions. Besides, they conducted IDA [39] to generate fragility curves.

Surmounting the drawbacks, generate the motivation to investigate and develop the fragility curves for fixed pile-founded offshore platforms based on the limit states which reflect the specific considerations of these kind of structures. As the objective, this paper aims to propose a methodology based on an analytical method using numerical simulations to develop seismic fragility curves for this type of structures. To illustrate the methodology, a recently installed fixed pile-founded offshore platform located in the South Pars Oil and Gas Field has been selected. Probabilistic seismic assessments of the platform have been studied. As a regard, the ideal ground motion intensity measure which can well predict the structural seismic demand measures have been achieved. To obtain the damage measures, nonlinear dynamic analyses of the selected platform under seismic excitations have been performed. Furthermore, the simultaneous effects of model and ground motions uncertainties in both soil and structure parameters as well as the effects of SPSI have been thoroughly considered.

2. Fixed Pile-founded Offshore Platform Seismic Assessments Area of Study

2.1. Probabilistic Seismic Demand Model (PSDM)

Performance-Based Earthquake Engineering (PBEE) describes the quantitative means for achieving predetermined performance levels in specific earthquake intensities by developing a probabilistic framework. One of the basic components of this framework is PSDM [39]. PSDM is based upon a representative relation between IMs and EDPs and provided based on PSDA [40] or IDA [41].

The basic formulation for probabilistic assessment of structural demands, in which the conditional seismic demand is modeled, employing a lognormal distribution, has been addressed by Cornell et al. [38]:

$$P[EDP \geq edp|IM] = 1 - \Phi\left(\frac{\ln(edp) - \ln(\eta_{EDP|IM})}{\beta_{EDP|IM}}\right) \quad (1)$$

In Eq. (2), $\Phi(\cdot)$ is the standard normal cumulative distribution function, *edp* is the peak or residual demand, $\eta_{EDP|IM}$ is the median value of the demand in terms of an IM, and $\beta_{EDP|IM}$ is the logarithmic standard deviation, or dispersion, of the demand conditioned on the IM. The relationship between median structural demand, $\eta_{EDP|IM}$, and IM can be estimated by a power model expressed in Eq.(3):

$$\eta_{EDP|IM} = a\, IM^b \quad (2)$$

Where, constants *a* and *b* are regression parameters.

Data for the regression analysis are developed by performing non-linear time history analyses with analytical fixed pile-founded offshore platform models representative of a typical offshore platform class using a suite of *N* ground motions. Peak demands (edp_i) are then plotted against the ground motion intensity for estimating the regression parameters, as well as the dispersion term ($\beta_{EDP|IM}$). The conditional standard deviation of the regression used to estimate the dispersion, where edp_i is the *i*th realization of the demands from the non-linear time history analyses, can be shown as:

$$\beta_{EDP|IM} \approx \sqrt{\frac{\sum_1^N (\ln(edp_i) - (\ln(a\, IM^b))^2}{N - (m+1)}} \quad (5)$$

The smaller the $\beta_{EDP|IM}$ is, the more efficient the IM is. Besides, the selected IM should be sufficient. A sufficient IM, quantified by the *p*-value [43-45], is conditionally statistically independent of the ground motion characteristics, such as magnitude (M_w) and source distance (*R*). The null hypothesis rejecting probability in an analysis of variance is described by *p*-value, where the null hypothesis refers to that the slope coefficient of linear regression is zero. Among widely used levels of significance this study adopts the significance level of 5% (*p*-value = 0.05) for the threshold. For *p*-values< 0.05, evidence for rejecting the null hypothesis is strengthening, and consequently, the IM which leads to *p*-values< 0.05, is considered as an insufficient IM. Therefore, an IM is sufficient in which the conditional probability distribution of EDP, given IM, is independent of ground motion parameters such as M_w, *R*, and T_p [46]. Consequently, the optimal IM-EDP pair, is the one in which the IM can appropriately predict the structural behavior observed quantifiably based on the output of the corresponding non-linear dynamic analysis.

Ground motion records selection is considered as one of the most challenging issues in analytical models of seismic performance assessments. For the purposes of this paper, a suite of 80 ground motion records is taken from the PEER strong motion database to be used in PSDA [47]. The records are selected from the studies of Babaei et al. [48-51] and based on the following criteria: (1) The site is classified as site class D according to NEHRP seismic provisions [52], (2) The earthquake magnitudes are between 6 and 8,

and (3) The source-to-site distances are between 20 km and 80 km (which are not near fault records).
It has been tried to expand the variety of IMs and EDPs to cover the main considerations of fixed pile-founded offshore platforms seismic assessments.

2.2. Fragility Curves Development

According to the performance-based earthquake engineering advancement, the site-specific deterministic design criteria are transitioning towards fragility curves as a means of describing the performance at different levels of ground motion intensity measures [23]. Thus, seismic fragility curves can provide understanding of seismic performance of offshore platforms at different limit states. Fragility is a versatile term employed throughout earthquake engineering to describe the susceptibility of a structure (or part of a structure) to seismic damage. Its estimation can be based on a variety of empirical [53], numerical [54], or expert opinion data [55], hybrid [56] and their combinations, using various methodologies that range from pure statistical processing of existing data to computational static and dynamic procedures that generate new data from scratch [57].
The fragility or conditional probability can be expressed as [58]:

$$P(D > d \,|\, IM = x) = 1 - \Phi\left(\frac{Lnx - \mu}{\beta}\right) \quad (3)$$

where *Lnx* is the median estimate of the demand as a function of IM, μ is median value of the structural capacity or the limit state, β is the standard deviation and $\varphi(.)$ is the standard normal cumulative distribution function(CDF). Since the lognormal appropriately matches a variety of structural [59,60], as well as nonstructural component failure data [61,62], it has been employed here having strong precedent in seismic risk analysis.
However, when the model includes lots of parameters -such that their probability density functions are highly nonlinear- achieving a closed form analytic solution is usually impossible. Therefore, in this paper optimal parameters are found using numerical non-linear optimization algorithms to maximize the log-likelihood functions.

3. Data and Method

3.1. Model Platform Characteristics

Recently installed in the 13th Phase, South Pars Oil and Gas Field of the Persian Gulf in (-57.2) meter water depth, the studied model is a X brace four leg battered fixed pile-founded platform with four main piles. The pile foundations penetrate 109 meters below the mudmat. To obtain the accurate results, three dimensional (3D) model of the platform has been taken into consideration and subjected to ground motion excitations in both X and Y directions. The key characteristics of the studied model (SPD 13 jacket) are presented in the Figure 1.

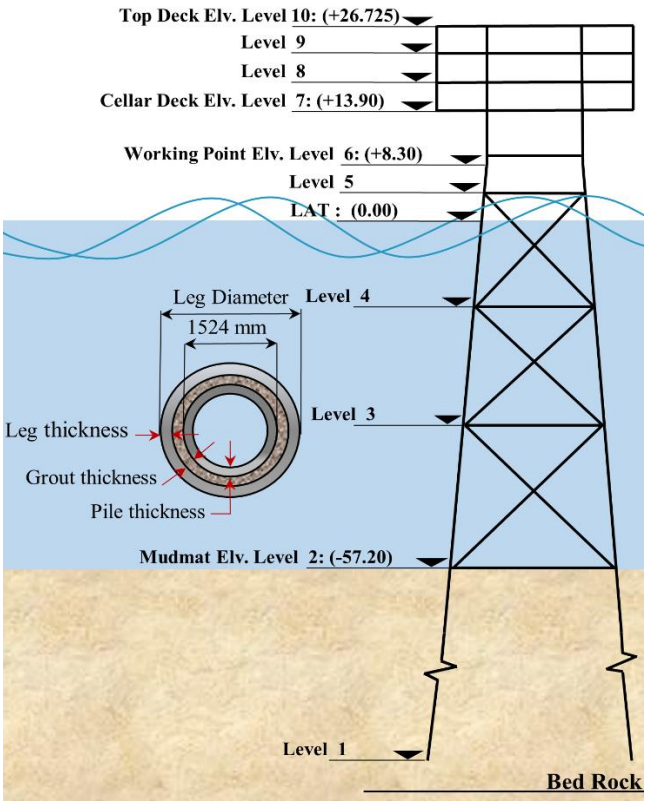

Figure 1. A schematic 2D view of SPD 13 platform illustrating the key characteristics

Aforementioned platforms generally consist of the following main parts: 1. A superstructure providing deck space for supporting operational appurtenances and other loads. 2. Completely braced welded tubular space frame, extends from an elevation at or near the sea bed to above the water surface, which is designed to serve as the main structural element of the platform, transmitting lateral and vertical forces to the foundation (jacket). 3. Foundation elements such as piles, that permanently anchor the platform to the ocean floor, and carry both lateral and vertical loads.
The Morison equation has been also used, estimating the hydrodynamic forces acting on the cylindrical platform members when the platform body moves relative to the flow in the inline direction as may occur confronting the platform to seismic-induced loadings based on equation (2):

$$F = \frac{1}{2}\rho C_D D(\dot{u} - \dot{u}_b)|\dot{u} - \dot{u}_b| + \rho C_M A(\ddot{u} - \ddot{u}_b) + \rho C_M \ddot{u} - M\ddot{u}_g \quad (4)$$

In which the first term reflects the drag force, the second and third ones refer to the hydrodynamic mass and Froude-Krylov forces, respectively [63], while the forth term is attributed to external (seismic) loading. Besides, $\dot{u}$, $\ddot{u}, \dot{u}_b$, and $\ddot{u}_b$denote the fluid velocity, acceleration and the body velocity and acceleration,

respectively. M and $\ddot{u}_g$ indicate the structure's mass and the input ground motion acceleration. Not considering the effect of simultaneous seismic and wave loading based on API RP2A-WSD [64], the equation of motion for the platform experiencing seismic-induced vibrations in still fluid will be as represented below:

$$F = M\ddot{u}_b + C\,\dot{u}_b + Ku_b \tag{5}$$

In Equation (3), C and K indicate the structural damping and elastic stiffness, and u_b reflect the platform displacement. Combining Equation (2) and Equation (3) will result in the following equation, where $\acute{M}$ is the hydrodynamic mass per unit span that equals to $\rho.C_m.A$.

$$(M+\acute{M})\ddot{u}_b + \frac{1}{2}\rho C_D D(\dot{u}_b)|\dot{u}_b| + C\,\dot{u}_b + Ku_b = -M\ddot{u}_g \tag{6}$$

3.2 Modeling of piles and the pile surrounded soil

According to the field and laboratory investigation, the stratum encountered at the borehole performed at the platform location was very soft calcareous becoming carbonate clay (CH) overlying medium dense becoming loose clayey siliceous carbonate sand (SC) at 10.60m followed by very stiff clay, and hard clay in deeper layers. All the structural elements and joints are checked in compliance with the technical considerations of API-RP-2A WSD [64]. In order to simulate the mass of the platform components in the dynamic analyses, lumped mass method has been employed. Entrapped water of flooded members and added mass for all the members below the sea level besides the mass of marine growth have been also assigned to the corresponding member joints. Moreover, the secondary and nonstructural items masses have been lumped to the nearest platform structural nodes. Since structural behavior of offshore platform in the nonlinear range depends primarily on the soil–pile–structure interaction (SPSI), the Beam on Nonlinear Winkler Foundation (BNWF) model, has been of a major concern and utilized in this study, often referred to as the *p-y* method [65]. The lateral soil stiffness is modelled using the *p–y* approach [66,67]. Sap 2000 [68] multi-linear plastic type link element is employed in the numerical model proposed in this paper reflecting the nonlinear lateral relation between the soil and the pile. In that link element, the nonlinear link stiffness for the axial degree of freedom is defined according to the *p–y* curve. Then the *p–y* curve is redefined as a force–deformation relationship in which *p* is the total force acting along the tributary length of a pile joint. In order to represent the lateral soil nonlinear behavior, a lateral link is defined for each joint along each unit pile segment. Chosen from the SAP2000 library, a multi-linear kinematic plasticity property type used for uniaxial deformation. The selected property models the hysteresis of the non-gapping soil behavior. Besides lateral loads, the pile foundation is exposed to the static and cyclic axial loads. Nonlinear axial load-deformation behavior along the shaft of driven tubular pile can be modelled using *t-z* data, recommended by API RP 2A-WSD [69]. Similarly, *q-z* curves model the elastic and plastic soil deformations around the pile tip reflecting the relationship between mobilized end bearing resistance and axial tip deflection. The schematic configuration of the proposed model in SAP2000 is illustrated in Figure 2.

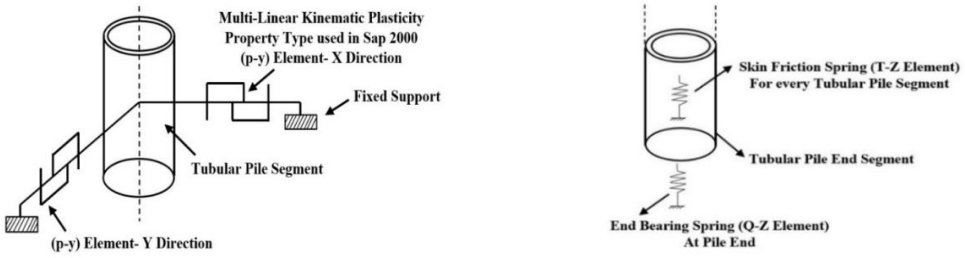

(a). *p-y* Elements **(b).** *t-z* and *q-z* Elements

Figure 2. Schematic configuration of pile segments and (a) *p-y* elements, (b) *t-z* & *q-z* elements

It is worth noticing that, incorporating soil nonlinearity in any site response analysis, is essential. Each soil layer is characterized by its thickness, mass density, shear wave velocity, and nonlinear soil properties including nonlinear modulus reduction and damping curves which effect on the selected ground motion records. In fact, the results of site response display seismic performance assessment of nonlinear ground response analysis within the soil profile, while they can reflect in the input ground motions determination uncertainties, the site velocity profile characterization and the nonlinear properties specification as well as analysis technique selection [70]. The computer program DEEPSOIL is employed to perform site response simulations based on the soil layer characteristics and selected ground motion records [71] using outcropping motions in the time domain and the layered soil column as a multiple-degree-of-freedom lumped mass system. Figure 3

shows the multi-degree-of-freedom lumped parameter model for layered soil. The displacement time history from nonlinear site response analysis are reflected, as well.

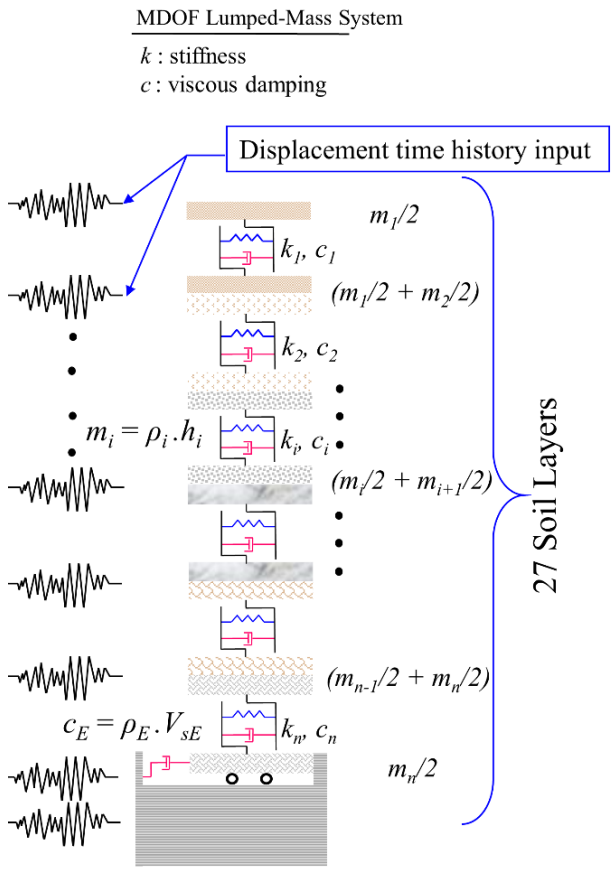

Figure 3: Seismic Site Response Considerations

3.4 Analysis Routine

The dynamic model of fixed pile-founded offshore platforms should reflect the key analytical parameters of mass, damping, and stiffness. The three dimensional (3D) model has been created employing Sap 2000, drag and inertia forces were exerted and Morison Equation has been employed calculating hydrodynamic loads. Each analysis routine includes a modal analysis to determine natural frequency as well as mode shape information, static pushover analysis (SPO) to represent yield values, and nonlinear dynamic time-history analysis (NTH) to determine demand measures. Numerous quantities were monitored in order to extract maximum and residual dynamic quantities, such as axial force, moment, horizontal and vertical displacements and so on. Access to response quantities extracted from the model is provided by post-processing. The periods of the first three vibration modes for the studied platform is listed in Table 1. Evident from the table, Sap 2000 results match well with the characteristics obtained from the initial model of the installed platform analyzed via Structural Analysis Computer System (SACS) software.

Table 1. Verification of the First Three Periods

	Period	Sap 2000(s)	SACS(s)
SPD 13, 3D Model, Modal Analysis	1st Mode	2.26	2.38
	2nd Mode	1.96	2.03
	3rd Mode	1.51	1.43

4. Result and Discussion

4.1 Optimal PSDM Determination

The structural behavior, natural period and mode shapes of the platforms have shown that these structures are flexible structures which are much more similar to high-rise buildings [48-51]. Due to this harmony in behavior, the considerations associated with these specific type of structures should be taken into account. While *PGA* exerts the greatest influence on the seismic response of the structures with higher frequencies (periods of less than 0.5 s), structures with lower frequencies (periods of more than o.5 s) are more sensitive to *PGV*. Tall long-period buildings studies indicated that due to their response frequency range which is much wider than low-rise or mid-rise buildings, IMs such as spectral values ($S_a(T_1)$) represent only specific points in frequency content of the response spectrum [72-74]. For that reason, the intensity measures comprising a wider range of frequency content of response spectra (e.g. Housner Intensity (*HI*) [75]) are more appropriate for the case of structures with periods more than 0.5 second (such as high-rise buildings and fixed pile-founded offshore platforms).

Accordingly, for the purposes of this study PSDM assessment for a large variety of IMs and EDPs has been conducted employing PSDA. Detailed evaluations have been presented in the study of Babaei et al. [48-51]. Their drawn findings indicated that PSDMs conditioned by *PGV* and the platform ductility (μ_{Global}) as well as the one provided by *HI* and the platform drift ration (θ_{Global}) are optimal based on the results presented in Table 2.

Table 2. PSDM assessments[48-51]

PSDM	Efficiency (dispersion)	Sufficiency(*p*-value)	
		w.r.t. M_w	w.r.t. R
PGV-μ_{Global}	0.28	0.249	0.164
HI-θ_{Global}	0.21	0.076	0.461

For the purposes of this study and based on the introduced damage measures, the appropriate PSDM will be used, the IM will be scaled and IDA will be performed. Accordingly, a suite of 15 ground motion

records which lead to equivalent results have been chosen, as listed in Table 3.

Table 3. Selected Records

#	Ground Motion Records	M_w	R(km)
1	Kobe, Japan, Kakogawa-1995	6.9	22.5
2	Jiroft, Bam, Iran,2003	6.6	69.28
3	Landers, Barstow, 1992	7.28	34.86
4	Trinidad, Rio Dell Overpass-FF, 1995	7.2	76.06
5	Imperial Valley-06, Coachella Canal #4, 1979	6.53	49.1
6	Big Bear-01, Featherly Park – Maint, 1992	6.46	78.81
7	Hector Mine, Amboy, 1999	7.13	41.81
8	Landers, Fort Irwin, 1992	7.28	62.98
9	Morgan Hill, Capitola, 1984	6.19	39.08
10	Borrego, El Centro, 1942	6.5	55.88
11	Duzce, Turkey, 1999	7.14	34.3
12	Manjil, Iran, Abhar, 1990	7.37	75.58
13	Superstition Hills, Imperial Valley Wildlife, 1987	6.54	23.85
14	Hector Mine, NorthPalm, 1999	7.13	61.86
15	Denali, Alaska, R109, 2002	7.9	42.99

4.2 Performing Incremental Dynamic Analyses

Recently emerged to offer a comprehensive evaluation of the structures seismic performance, Incremental Dynamic Analysis (IDA) [39] is justifiably claimed as a powerful computer-intensive method that has been used within the framework of PBEE. Using numerous nonlinear dynamic analyses under a suite of multiply-scaled ground motion records, IDA allows the detailed assessment of the seismic performance of structures for a wide range of limit states, ranging from elasticity to dynamic instability and eventual collapse.

The hunt & fill algorithm has been chosen to perform the actual dynamic analysis required for IDA in a fast and automated way. This ensures that the record scaling levels are appropriately selected and minimize the computational efforts, accordingly. Analyses are performed at rapidly increasing levels of IMs until numerical non-convergence is encountered, while additional analyses are running at intermediate IM levels to sufficiently bracket the global collapse and increase the accuracy at lower IMs [31].

Seismic assessments of SPD13-A have been conducted utilizing IDA. The results of probabilistic assessment which are represented through the following illustrations vary dramatically at different levels (indicated in Figure 5) of the studied platform.

In order to provide a better understanding of the illustrated result, the IDA curves for different levels based on their drastic differences have been split into two parts (a and b) in Figure 5. As can be seen, while the platform behavior for levels 3, 4, 5, 9 and 10 follows a similar trend subjecting to various scales of ground motion IMs, this is not complied in other levels. The inter-story drift ratios in these levels meet striking rises in higher IM values. Furthermore, the hardening and softening cases can be also seen.

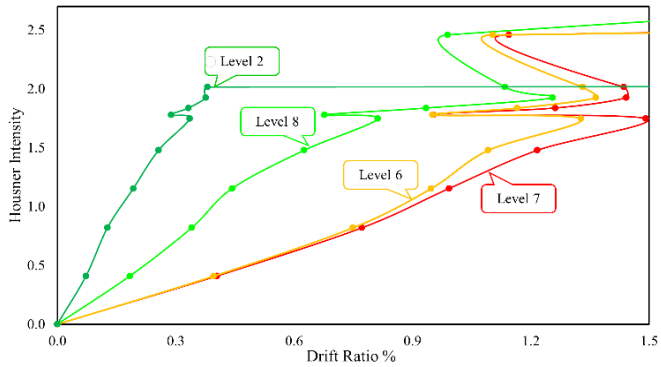

a. Inter-story Drift Ratio for Levels 2, 6,7 and 8

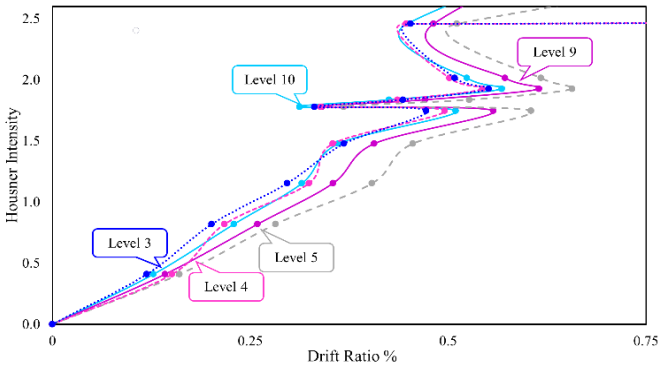

b. Inter-story Drift Ratio for Levels 3, 4,5,9 and 10

Figure 5: IDA Curves for Different Platform Levels Subjected to Record No. 8

On the other hand, the structural responses of the incremental dynamic analysis for different IM scales through the platform various levels are reflected in Figure 6, a and b. Severe increase in the inter-story drift ratios of levels 2 and 7 experienced in higher IM values, has been drawn.

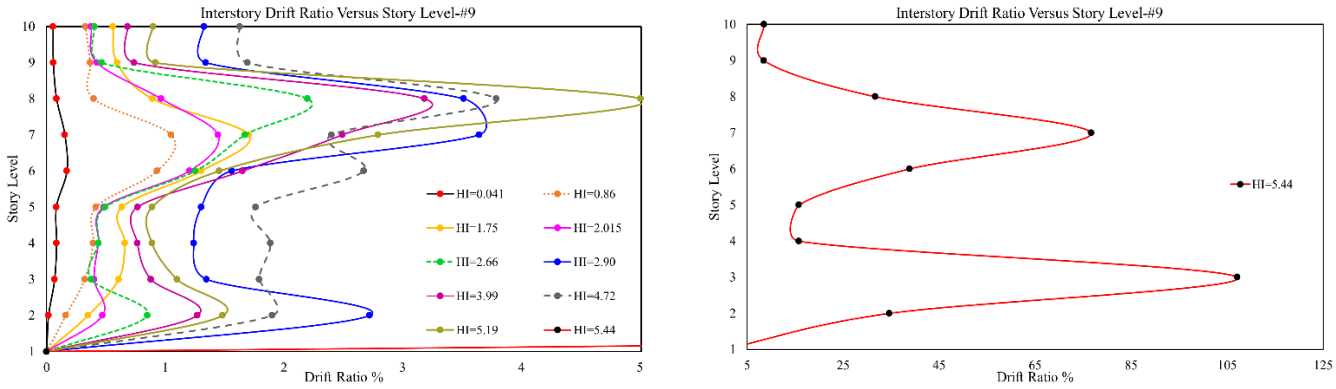

Figure 6: Inter-story Drift Ratios for Different Platform Levels according to Various IM Scales (Subjected to Record No.9)

Besides the single-record IDA curves, the multi-record IDA curves have been also prepared and represented in Figures 7 and 8, reflecting the platform global drift ratio as well as ductility, respectively. Consequently, the summary of the platform responses IDA results of 16%, 50% and 84% have been calculated which can be utilized in fragility investigations of fixed pile-founded offshore platforms.

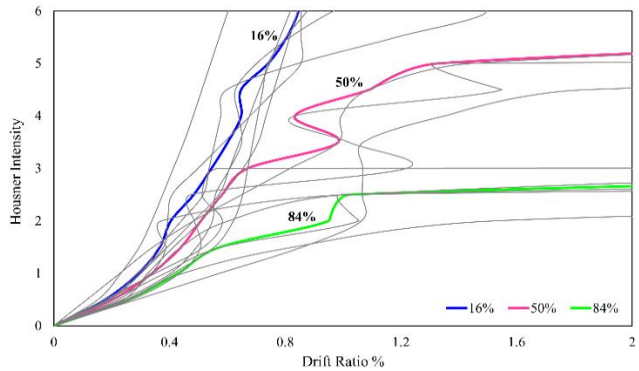

a. Multi-Record IDA Curves (Raw Curves)

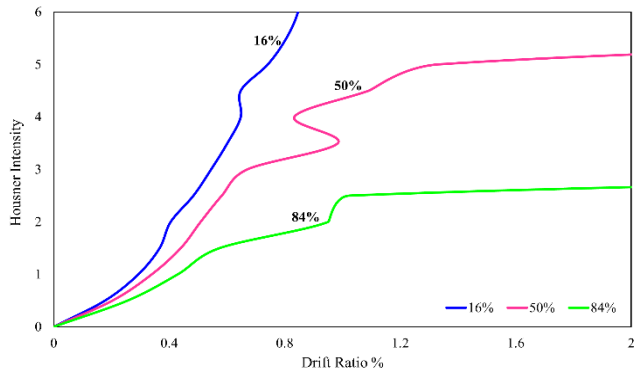

b. Summarized IDA Curves (16%, 50% & 84%)

Figure 7. Multi-record IDA Curves for *HI-*θ_{Global}

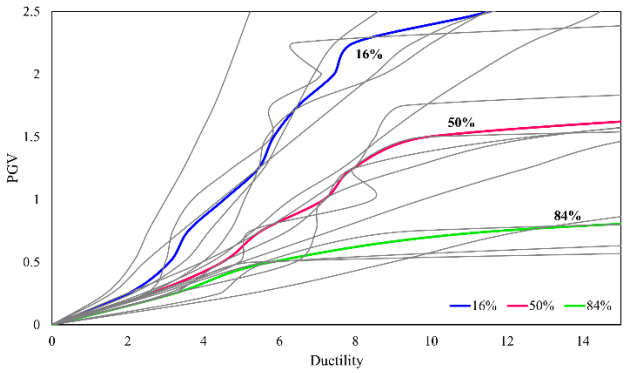

a. Multi-Record IDA Curves (Raw Curves)

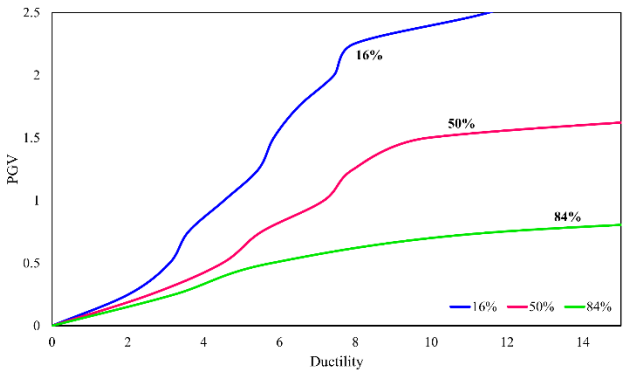

b. Summarized IDA Curves (16%, 50% & 84%)

Figure 8. Multi-Record IDA Curves for *PGV-*μ_{Global}

4.3 Fixed Pile-Founded Offshore Platforms Fragility Analysis

As a graphical illustration of structural seismic vulnerability, fragility curves can be generated by the lognormal cumulative distribution function (CDF), which represents the probability of exceedance as a function of ground motion IMs. Since in the conventional design of fixed pile-founded offshore platforms, a linear elastic behavior is assumed, no yield or buckling is allowable. Furthermore, the platform collapse can be expressed due to the first member failure occurrence. It is worth noticing that, the fragility analysis of fixed pile-founded offshore platform is in its initial stage and presenting appropriate limit states (LSs) is a challenging subject area. Recently, different structural LSs have been suggested and employed in some limited studies referring to different guidelines to address structural behaviors. These LSs have been thoroughly studied and a summary of them has been presented as listed in Tables 4 and 5.

Table 4. Previously Employed LSs

IM-EDP	LS	Code	Reference
$S_a(T_1,5\%)$-θ_{max}	**IO**: θ_{max}=1%, **CP**: θ_{max}={6% or 20% of the elastic slope}	FEMA 350	Jahanitabar and Bargi[31]
	Collapse **L**imit **S**tate: θ_{max}=2%	ASCE 41-06, FEMA 350	Ajamy et al. [32]
	CP: θ_{max}={10% or 20% of the elastic slope}	FEMA 351	Zarrin et al. [33]
	Collapse **L**imit **S**tate: IMs related to points the IDA curves flatten		Abyani et al. [34]

Table 5. LSs Represented by Yasseri and Ossei [30]

IM-EDP	LS	Damage Description
PGA-μ	μ=1	**Negligible**: Minor repairs, no disrupting
	μ=2	**Slight**: Repairable damage, some replacement required
	μ=4	**Moderate**: serious disruption
	μ=6	**Extensive**: beyond repair
	μ=7.5	**Near collapse**

As drawn from Tables 4 and 5, the only appropriate LSs for fixed pile-founded offshore platforms has been assumed to be those reflected in the study of Yasseri and Ossei [30], while other studies referred their chosen LSs to the ordinary building ones derived from the related codes. Consequently, Table 6 represent the values of the summarized 16%, 50% and 84% of demand measures (DMs) for the ductility-based LSs based on Yasseri and Ossei [27].

Table 6. Summary of the Results

	IM: PGV(m/s)			**EDP:** μ
	$IM_{16\%}$	$IM_{50\%}$	$IM_{84\%}$	
Negligable	0.124	0.096	0.078	1
Slight	0.248	0.193	0.155	2
Moderate	0.857	0.435	0.326	4
Extensive	1.558	0.823	0.509	6
Near Collapse	2.030	1.448	0.572	7.5

In fragility analysis of fixed pile-founded platforms investigated here, the platform responses, obtained from the IDA has been utilized, and the lognormal fragility function in each LSs has been defined via two parameters, the IM median value (at which the platform reaches the LS threshold) as well as the logarithmic standard deviation or dispersion. These parameters represent the IM corresponding to 50% probability of exceeding a certain LS and the dispersion in the results due to record-to-record variability, respectively. The results for five various LSs have been obtained and illustrated in Figure 9. For the purposes of this study the widely used method of Porter has been employed [74]. For each LSs, the IM values which have led to 25%, 50% and 75% probability of exceeding are obtained and shown in the illustrations.

Moreover, as shown in Table 7, the medians and the logarithmic standard deviations have been also computed and represented.

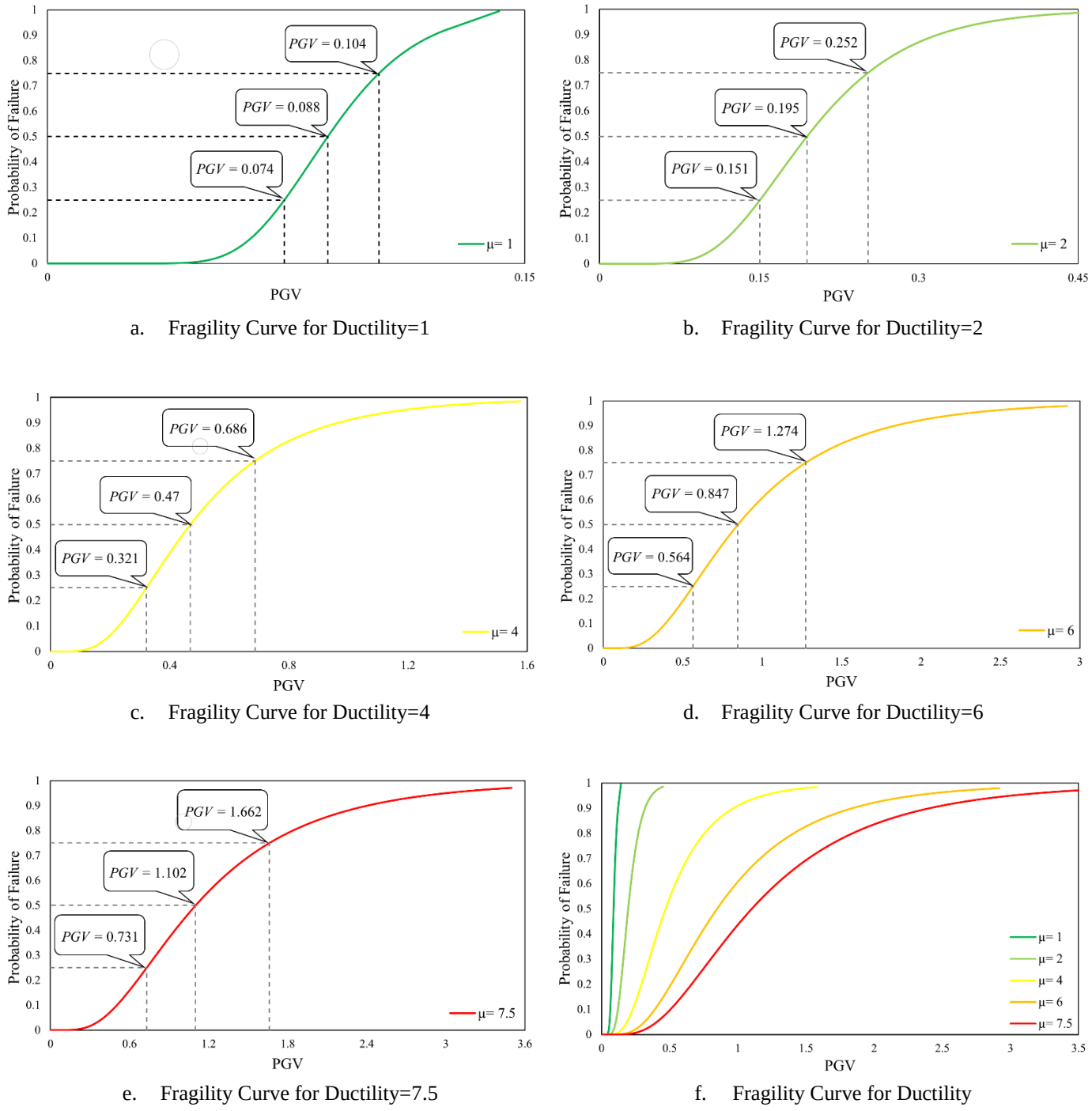

a. Fragility Curve for Ductility=1

b. Fragility Curve for Ductility=2

c. Fragility Curve for Ductility=4

d. Fragility Curve for Ductility=6

e. Fragility Curve for Ductility=7.5

f. Fragility Curve for Ductility

Figure 9. Fragility Curves for Fixed Pile-Founded Offshore Platforms

Table 7. Summary of the Results, median and standard deviation

performance Levels	Negligible	Slight	Moderate	Extensive	Near Collapse
median	0.09	0.2	0.47	0.85	1.10
standard deviation	0.258	0.396	0.583	0.626	0.631

5. Conclusion

As a general objective, this study aims to represent the results of probabilistic seismic assessment of fixed pile-founded offshore platforms. A 3D model of the platform, considering the effects of soil-pile-structure interactions and seismic site responses has been made. Accordingly, the drawn findings of PSDM evaluations obtained from PSDA for a recently installed typical fixed pile-founded offshore platforms of the Persian Gulf, has been exhibited. For the introduced PSDMs, incremental dynamic analysis (IDA) has been also performed and the significantly various results for different IM scales as well as the platform levels have been established. Since the fragility analysis of fixed pile-founded offshore platforms is presumed to be in the initial development levels, the limited studies have been explored. Among these investigations, the limit states represented by Yasseri and Ossei [30] have been considered as appropriate and employed to produce seismic fragility curves for the studied platform. The results of this paper is proposed to be utilized for the seismic assessments and fragility analysis of the similar platforms. Proposed for future studies, it is suggested to extract fragility curves for other kind of offshore platforms such as offshore wind turbines.

6. References

[1] Bea, R.G., Puskar, F.J., Smith, C., Spencer, J.S., (1988), Development of AIM (assessment, inspection, maintenance) programs for fixed and mobile platforms. In: Proceedings of the offshore technology conference. Paper OTC 5703.

[2] Yasseri, S. and Ossei, R., (2004), Seismic Fragility Analysis of Pile-founded Offshore Platforms, Proceeding of the Fourteenth International Offshore and Polar Engineering Conference, Toulon, France, Paper Number: ISOPE-I-04-028

[3] Asgarian, B., Aghakouchak, A. A., Alanjari, P. and Assareh, M. A., (2008), Incremental Dynamic Analysis of Jacket Type Offshore Platforms Considering Soil-Pile Interaction, 14th World Conference on Earthquake Engineering, Beijing China.

[4] Park, M., Koo, W., Kawano, K., (2011), Dynamic response analysis of an offshore platform due to seismic motions, Eng. Struct., Vol. 33 (5), p. 1607–1616.

[5] El-Din, M. N. and Kim, J., (2014), Seismic performance evaluation and retrofit of fixed jacket offshore platform structures, J. Performance of Constructed Facilities.

[6] Sharifian, H., Bargi, K., Zarrin, M., (2015), Ultimate strength of fixed offshore platforms subjected to near-fault earthquake ground vibration. Shock Vib., P. 1–19.

[7] Elsayed, T., El-Shaib, M., Gbr, k., (2014), Reliability of fixed offshore jacket platform against earthquake collapse, J. Ships Offshore Struct., Vol.11 (2), p. 167–181.

[8] Babaei, S., Amirabadi, R., Taghikhany, T., (2016), Assessment of Semi-Active Tunes Mass Damper Application in Suppressing Seismic-Induced Vibration of an Existing Jacket Platform, International Journal of Maritime Technology, Vol. 6, p. 1-10.

[9] Konstandakopoulou, F.D., Evangelinosb, K.I., Nikolaouc, I.E., Papagiannopoulosd, G.A., Pnevmatikose, N.G., (2019), Seismic analysis of offshore platforms subjected to pulse-type ground motions compatible with European Standards, Soil Dynamics and Earthquake Engineering, https://doi.org/10.1016/j.soildyn.2019.105713

[10] Jafari, A., & Dezvareh, R. (2021). Evaluation of dynamic effects in the response of offshore wind turbines using incremental wind-wave analysis. Research in Marine Sciences, 6(1), 860-868.

[11] Jafari, A., & Dezvareh, R. (2020). Performance based assessment of offshore wind turbine platform using the constrained new wave method. Journal of Oceanography, 11(43), 71-80.

[12] Jafari, A., & Dezvareh, R. (2021). Determination of collapse prevention (CP) of offshore wind turbine with jacket platform. Iranian Journal of Marine Science and Technology, 24(96), 35-43.

[13] Dezvareh, R. (2019). Providing a new approach for estimation of wave set-up in Iran coasts. Research in marine sciences, 4(1), 438-448.

[14] Lupoi, G.; Franchin, P.; Lupoi, A.; Pinto, P.E., (2006), Seismic fragility analysis of structural systems, J. Eng. Mech., Vol. 132, p. 385–395.

[15] Rosowsky, D.V.; Ellingwood, B.R., (2002), Performance-based engineering of wood frame housing: Fragility analysis methodology. J. Struct. Eng., Vol. 128, p. 32–38.

[16] Jia, H.; Zhao, J.; Li, X., (2018), Probabilistic pounding analysis of high-pier continuous rigid frame bridge with actual site conditions, Earthquakes Struct., Vol. 15, p. 193–202.

[17] Asgarian, B.; Sadrinezhad, A.; Alanjari, P. Seismic performance evaluation of steel moment resisting frames through incremental dynamic analysis. J. Constr. Steel Res. 2010, 66, 178–190.

[18] Fattahi, F.; Gholizadeh, S. Seismic fragility assessment of optimally designed steel moment frames. Eng. Struct. 2019, 179, 37–51.

[19] Bakalis K. and Vamvatsikos D., (2018), Seismic Fragility Functions via Nonlinear Response History Analysis, Journal of Structural Engineering, ASCE, 144(10): 04018181 DOI: 10.1061/(ASCE)ST.1943-541X.0002141

[20] Mander, J.B.; Dhakal, R.P.; Mashiko, N.; Solberg, K.M., (2007), Incremental dynamic analysis applied to seismic financial risk

assessment of bridges. Eng. Struct., Vol. 29, p. 2662–2672.

[21] Jia, H.; Lan, X.; Luo, N.; Yang, J.; Zheng, S.; Zhang, C., (2019), Nonlinear Pounding Analysis of Multispan and Simply Supported Beam Bridges Subjected to Strong Ground Motions. Shock Vib.

[22] Jia, H.; Lan, X.; Zheng, S., (2019), Assessment on required separation length between adjacent bridge segments to avoid pounding. Soil Dyn. Earthq. Eng., Vol. 120, p. 398–407.

[23] Mackie, K., and Stojadinovic, B., (2004), Fragility curves for reinforced concrete highway overpass bridges, 13th World Conference on Earthquake Engineering Vancouver, B.C., Canada

[24] Muntasir Billah, A.H.M., & Shahria Alam, M., (2014), Seismic fragility assessment of highway bridges: a state-of-the-art review, Structure and Infrastructure Engineering: Maintenance, management, Life-Cycle Design and Performance, DOI: 10.1080/15732479.2014.912243

[25] Berahman, F., Behnamfar, F., (2007), Seismic fragility curves for un-anchored on-grade steel storage tanks: bayesian approach, J. Earthquake Eng. Vol.11(2), p. 166–92.

[26] Heidary-Torkamani, H., Bargi, Kh., Amirabadi, R., and McCllough, N.J., (2014) Fragility estimation and sensitivity analysis of an idealized pile-supported wharf with batter piles, Soil Dynamics and Earthquake Engineering, Elsevier, Vol.61-62 p. 92–106, http://dx.doi.org/10.1016/j.soildyn.2014.01.024

[27] Hariri-Ardebili, M.A., and Saouma, V.E., (2016), Probabilistic seismic demand model and optimal intensity measure for concrete dams, Structural Safety, Elsevier, Vol. 59 p. 67–85, http://dx.doi.org/10.1016/j.strusafe.2015.12.001

[28] Tian, L.; Pan, H.; Ma, R., (2019), Probabilistic seismic demand model and fragility analysis of transmission tower subjected to near-field ground motions, J. Constr. Steel Res., 156, 266–275.

[29] Peng, O., Cheng, W., Jia, H., and Guo, P., (2020), Fragility Analysis of Gantry Crane Subjected to Near-field Ground Motions, Appl. Sci., Vol. 10, 4219; doi:10.3390/app10124219

[30] Yasseri, S., Ossei, R., (2004), Seismic Fragility Analysis for Pile-founded Offshore Platforms, Proceeding of the 14th International Offshore and Polar Engineering Conference, Toulon, France, ISOPE-I-04-028.

[31] Jahanitabar AA, Bargi Kh., (2017) Time-dependent seismic fragility curves for aging jackettype offshore platforms subjected to earthquake ground motions, J Struct Infrastruct Eng Mainten, Manage, Life-cycle Des Perform, Vol. 14(2):192–202.https://doi.org/10.1080/15732479.2017.1343360

[32] Ajamy, A., Asgarian, B., Ventura, C.E., Zolfaghari, M.R., (2018), Seismic fragility analysis of jacket type offshore platforms considering soil-pile-structure interaction, Journal of Engineering Structures 174 (1), 198–211.

[33] Zarrin, M., Asgarian, B., & Abyani, M., (2019), Probabilistic Seismic Collapse Analysis of Jacket Offshore Platforms, Journal of Offshore Mechanics and Arctic Engineering, Vol. 140, DOI: 10.1115/1.4038581

[34] Abyani, M., Bahaari, M.R., Zarrin, M., and Nasseri, M., (2019), Effects of sample size of ground motions on seismic fragility analysis of offshore jacket platforms using Genetic Algorithm, Ocean Engineering Vol. 189, 106326, https://doi.org/10.1016/j.oceaneng.2019.106326

[35] ASCE, FEMA 356, (2000) Prestandard and commentary for the seismic rehabilitation of buildings, Publication No. 356, Washington (DC): Federal Emergency Management Agency.

[36] FEMA 350, (2000a), Recommended seismic design criteria for new steel moment-frame buildings. SAC Joint Venture, Federal Emergency Management Agency, Washington DC.

[37] FEMA 351, (2000b), Recommended seismic evaluation and upgrade criteria for existing welded steel moment-frame buildings. SAC Joint Venture, Federal Emergency Management Agency, Washington DC.

[38] American Society of Civil Engineers (ASCE), (2007), Seismic rehabilitation of existing buildings. ASCE/SEI 41-06, American Society of Civil Engineers/Structural Engineering Institute, Reston, VA.

[39] Shome, N., (1999), Probabilistic Seismic Demand Analysis of Nonlinear Structures. PhD. Thesis, Dep. Civil and Envir. Eng. Stanford University, Stanford, CA.

[40] Shome, N., Cornell, C.A., Bazzurro, P., & Caraballo, J.E., (1998), Earthquakes, records, and nonlinear responses. Earthquake Spectra, 14(3), 467–500.

[41] Vamvatsikos D., (2002), Seismic performance, capacity and reliability of structures as seen through incremental dynamic analysis. PhD Dissertation, Department of Civil and Environmental Engineering, Stanford University.

[42] Cornell, CA., Jalayer, F., Hamburger, RO., Foutch, DA., (2002), Probabilistic basis for 2000 SAC/FEMA steel moment frame guidelines, J Struct Eng Vol. 128(4) p. 526–533. https://doi:10. 1061/(ASCE)0733-9445

[43] Fisher, RA., (1925), Statistical Methods for Research Workers, Edinburgh, UK: Oliver and Boyd

[44] Tang, WH., Ang, A., (2007), Probability concepts in engineering: Emphasis on applications to civil and environmental engineering, 2nd edn. Wiley, Hoboken, ISBN: 978-0-471-72064-5

[45] Altman, N., Krzywinski, M., (2016), Points of significance: p values and the search for significance, Nat Methods 14:3–4. https://doi:10.1038/nmeth.4120

[46] Tothong P, Luco N (2007) Probabilistic seismic demand analysis using advanced ground motion intensity measures. Earthquake Eng Struct Dyn. https://doi.org/10.1002/eqe.696

[47] Pacific earthquake engineering research center (2006) PEER NGA Database. Berkeley: University of California. http://peer.berkeley.edu/nga/

[48] Babaei, S., Amirabadi, R., Sharifi, M., (2021), Evaluation of Optimal IM-EDP pairs for Typical South Pars Fixed Pile-Founded Offshore Platforms, International Journal of Maritime Technology, Vol. 15:29-49, http://ijmt.ir/article-1-740-en.html

[49] Babaei, S., Amirabadi, R., Sharifi, M., Ventura, C., (2021), Optimal probabilistic seismic demand model for fixed pile-founded offshore platforms considering soil-pile-structure interaction, Structures, Vol.33: 4330-4343, https://doi.org/10.1016/j.istruc.2021.07.040

[50] Babaei, S., Amirabadi, R., Taghikhany, T., Sharifi, M., (2021), Optimal ground motion intensity measure selection for probabilistic seismic demand modeling of fixed pile-founded offshore platforms, Journal of Ocean Engineering, Vol. 242, https://doi.org/10.1016/j.oceaneng.2021.110116

[51] Babaei, S., Amirabadi, R., Sharifi, M., (2021), Sufficiency assessments of ground motion intensity measures employing kullback-leibler theory (applied for typical south pars offshore platforms), Numerical Methods in Civil Engineering Journal, Vol. 5(4). http://nmce.kntu.ac.ir/article-1-340-en.htm

[52] NEHRP (2001) NEHRP recommended provisions for seismic regulations for new buildings and other structures. Washington, DC, USA: Building Seismic Safety Council

[53] Rossetto, T., Ioannou, I., Grant, D., and Maqsood, T., (2014), Guidelines for empirical vulnerability assessment, GEM Technical Rep. 2014-08 V1.0.0. Pavia, Itally: GEM Foundation.

[54] D'Ayala, D., A. Meslem, D. Vamvatsikos, K. Porter, and T. Rossetto. (2015), Guidelines for analytical vulnerability assessment of low/mid-rise buildings, Pavia, Italy: Vulnerability Global Component Project.

[55] Jaiswal, K., Wald, D., and D'Ayala, D., (2011) Developing empirical collapse fragility functions for global building types, Earthquake Spectra 27 (3): 775–795. https://doi.org/10.1193/1.3606398.

[56] Kappos, A.J., Stylianidis, K.C., & Pitilakis, K. (1998). Development of seismic risk scenarios based on a hybrid method of vulnerability assessment. Natural Hazards, Vol.17, p.177–192.

[57] Shinozuka, M., Feng, M.Q., Lee, J., and Naganuma, T., (2000), Statistical analysis of fragility curves, J. Eng. Mech. Vol. 126 (12), p. 1224–1231. https://doi.org/10.1061/(ASCE)0733-9399(2000)126:12(1224).

[58] Baker, J.W., (2015), Efficient analytical fragility function fitting using dynamic structural analysis, Earthquake Spectra, Vol.31(1), p. 579–99.

[59] Aslani, H., 2005. Probabilistic Earthquake Loss Estimation and Loss Disaggregation In Buildings, Doctoral Thesis, Stanford University, Stanford CA, 355 pp.

[60] Pagni, C.A. and L.N. Lowes, 2006. Fragility functions for older reinforced concrete beam-column joints. Earthquake Spectra, 22 (1), Feb 2006

[61] Badillo-Almaraz, H., A.S. Whittaker, A.M. Reinhorn, and G.P. Cimellaro, (2006) Seismic Fragility of Suspended Ceiling Systems, Technical Report MCEER-06-0001, Multidisciplinary Center for Earthquake Engineering Research, Buffalo, NY, 225 pp.

[62] Porter, K.A., and A.S. Kiremidjian, (2001), Assembly-Based Vulnerability and its Uses in Seismic Performance Evaluation and Risk-Management Decision-Making, Report No. 139, John A. Blume Earthquake Engineering Center, Stanford, CA, 214 pp., http://keithp.caltech.edu/publications.htm

[63] Mutlu, B., Fredsoe, J., (1997), Hydrodynamics Around Cylindrical Structures, Advanced Series on Ocean Engineering, vol. 26. Technical university of Denmark, Denmark

[64] API, (2000), Recommended Practice for Planning, Design and Constructing Fixed Offshore Platforms—Working Stress Design. American Petroleum Institute, Washington, DC.

[65] Matlock, H., (1970), Correlations for Design of Laterally Loaded Piles in Soft Clay, Second Annual Offshore Technology Conference, Houston, Vol.1204, p. 557 - 594.

[66] Reese, L. C., & Cox, W. R., (1975), Field Testing and Analysis of Laterally Loaded Piles in Stiff Clay, Offshore Technology Conference, OTC 2312.

[67] O'Neill, M. W., & Murchinson, J. M., (1983), An Evaluation of p-y Relationships in Sands, A Report to the American Petroleum Institute.

[68] Sap 2000, (2005), Structural Analysis Program, Analysis Reference Manual, Computers and structures, Inc., Berkeley, California, USA.

[69] American Petroleum Institute, (2008), Recommended Practice for Planning, Designing and Constructing Fixed Offshore Platforms - Working Stress Design, API recommended practice (RP-2A-WSD), 21st Edition, Errata and Supplement.

[70] Rathje EM, Kottke RA, Trent WL., (2010), Influence of input motion and site property variabilities on seismic site response analysis, J Geotech. Geoenviron. Eng. ASCE, Vol. 136(4).

[71] Hashash, Y., Groholski, D., Phillips, C., Park, D., & Musgrove M., (2012), DEEPSOIL 5.1. User Manual and Tutorial.

[72] Shome, N., Cornell, CA., (1999), Probabilistic seismic demand analysis of nonlinear structures, RMS Program, Stanford University, Report No. RMS35. https://blume.stanford.edu/rms-reports. Accessed 2 June 2014

[73] Luco, N., Cornell, CA., (2007), Structure-specific scalar intensity measures for near-source and ordinary earthquake ground motions, Earthq Spectra Vol. 23 p.357–392. http://doi:10.1193/1.2723158

[74] Mackie, K., Stojadinović, B., (2003), Seismic demands for performance-based design of bridges, PEER 312

[75] Housner, GW., (1959), Behavior of structures during earthquakes, J Eng Mech Div Vol. 85 p.109–130

[76] Porter, K., Kennedy, R., and Bachman, R., (2007), Creating Fragility Functions for Performance-Based Earthquake Engineering, Earthquake Spectra, Vol. 23(2), p. 471-489.

List of Abbreviation

Abbreviation	Definition
PSDM	Probabilistic Seismic Demand Modeling
PSDA	Probabilistic Seismic Demand Analysis
IM	Intensity Measure
EDP	Engineering Demand Parameter
IDA	Incremental Dynamic Analysis
SPSI	Soil-Pile-Structure Interaction
PBEE	Performance-Based Earthquake Engineering